86-05042/

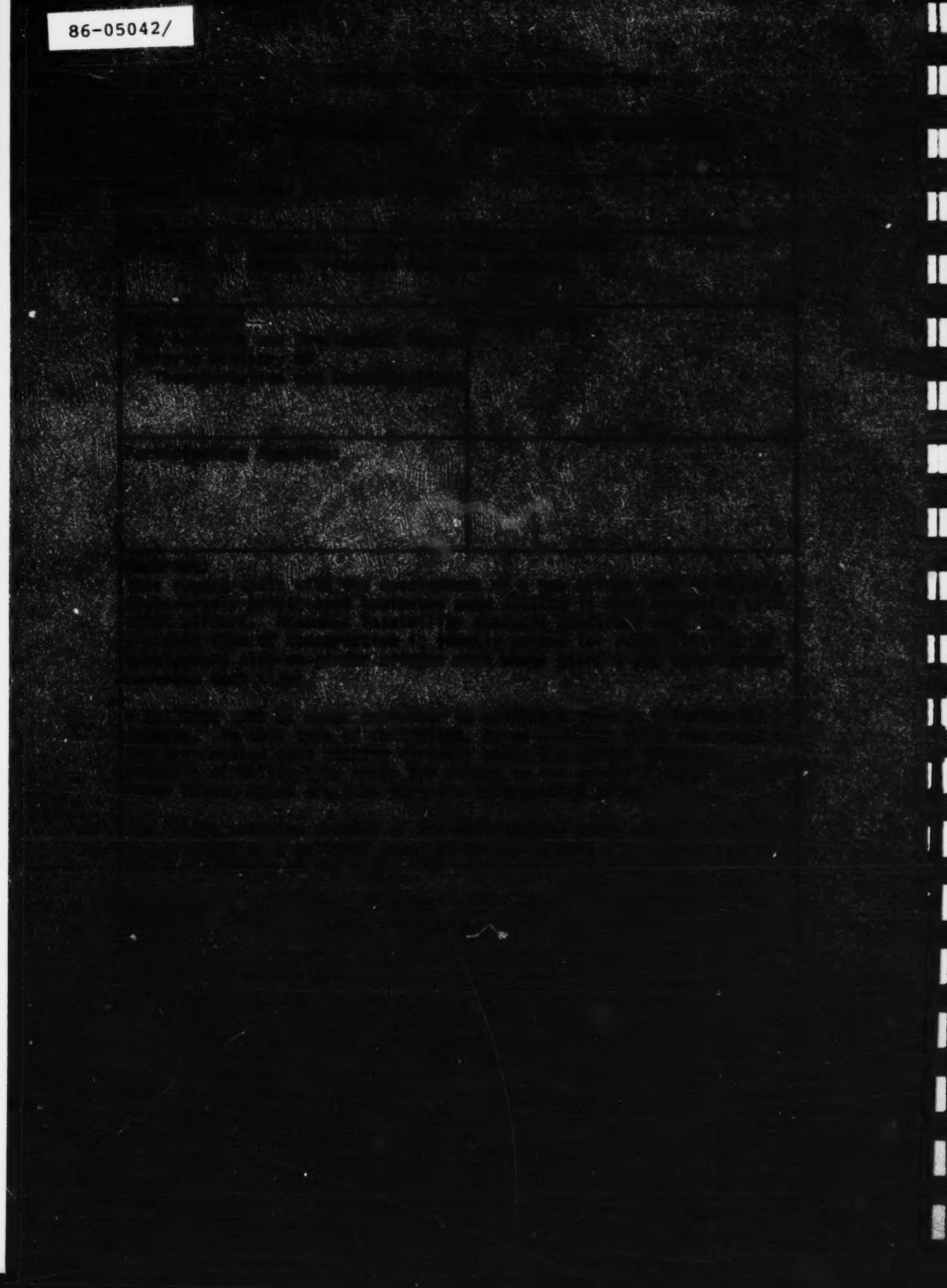

SRR-86-03

Steel-Wood Composite Bridges

T. Thanabalan
Associate Research Engineer

B. Bakht
Principal Research Engineer

Published by
The Research and Development Branch
Ontario Ministry of Transportation and Communications
Honourable Ed Fulton, Minister
D.G. Hobbs, Deputy Minister

Published without prejudice as to the application of the findings.
Crown copyright reserved; however, this document may be reproduced for non-commercial purposes with attribution to the Ministry.

For additional copies, contact:
The Editor, Technical Publications
Room 320, Central Building
1201 Wilson Avenue
Downsview, Ontario
Canada M3M 1J8

Telephone: (416) 248-7226
CNCP Electronic Mail: 21:MIN006

July 1986

TABLE OF CONTENTS

PAGE

ACKNOWLEDGEMENTS iii

SUMMARY iv

1/ INTRODUCTION 1

2/ ECONOMIC FEASIBILITY OF THE CONCEPT 5

3/ SPECIMEN PREPARATION, INSTRUMENTATION AND TESTING 10
3.1/ Preliminary Tests 10
3.2/ Shear Connectors 14
3.3/ Composite Beams 18
3.4/ Model Composite Bridge 23

4/ PRELIMINARY TESTS 30
4.1/ Static Load Tests 30
4.2/ Fatigue Tests 35

5/ BULKHEAD SHEAR CONNECTOR 41
5.1/ Shear Strength 41

6/ COMPOSITE BEAMS 51
6.1/ Load-Deformation Characteristics 51
6.2/ Load-Slip Characteristics 56
6.3/ Stress Distribution 58
6.4/ Ultimate Strength 62
6.5/ Fatigue Tests 63

7/ COMPOSITE BRIDGE 68
7.1/ Timber Deck 68
7.2/ Steel-Wood Model Bridge 68
7.3/ Grillage Analysis 71
7.4/ Cyclic Load Test on the Model Bridge 87

REFERENCES 90

APPENDIX A

APPENDIX B

ACKNOWLEDGEMENTS

J. Klubal, Technician, Research and Development Branch, worked single-handedly to fabricate the various test specimens, organize the test set-up, and conduct various tests during the course of this program. His contribution to the research is gratefully acknowledged.

Nelson Stud Welding Company Canada Ltd. supplied and welded the studs required for this study and their co-operation is acknowledged.

B. Kwok, L. Pena and R. Rigglesworth, of the Transportation Technology and Energy Branch, are acknowledged for their assistance with the instrumentation and recording of data.

SUMMARY

Economic Feasibility

The report deals with the development of a new bridge type in which a transversely prestressed laminated wood decking, with laminates running in the longitudinal direction, is made composite with steel girders. For new construction, this type of structure becomes an economic alternative to composite steel-concrete bridges only when the span exceeds about 50 m. The proposed system is very economical and ideally suited, however, for rehabilitating substandard slab-on-steel girder bridges of all spans.

Shear Connectors

Of the several types of devices for providing a mechanical connection between the wood decking and steel girders, the most suitable was found to be the concrete bulkhead type. In this type of shear connection, large diameter holes are cored in the prestressed wood decking directly above the girder flanges. Clusters of Nelson-type studs are welded to the girder flanges through these holes, which are then filled with expansive grout.

Strengths of Shear Connectors

Through direct shear tests, it was established that the strength of a bulkhead-type shear connector depends more on the number and diameter of studs than on the bulkhead diameter. Connections with machine welded Nelson type studs performed satisfactorily under cyclic loads.

Performance of Shear Connectors in Beams

It was confirmed that the forces exerted on the shear connectors in a beam are smaller than those obtained analytically. Under cyclic loading,

transverse cracks developed in the bulkheads after only 1 x 10^5 cycles. When the bulkheads were reinforced with chicken wire mesh, the beam could be subjected to 2 x 10^6 cycles without any apparent sign of distress.

Half-Scale Bridge Model

Static and dynamic tests of the half-scale steel-wood composite bridge model confirmed that the bridge has adequate strength against both static and dynamic loads.

1/ INTRODUCTION

Bridges with steel girders and decking, consisting of wood laminates nailed together, are not uncommon in Ontario. A typical bridge is shown in Figure 1.1. These bridges suffer from two major disadvantages:

1/ The decking is used solely for transmitting loads to the steel girders. It does not actively participate in sustaining the longitudinal moment, and

2/ The nail connections between the laminates become loose after a few years of service, leading to deterioration of the riding surface.

In the past, the loosening of nail connections was observed in both transverse laminated and longitudinal laminated wood decks and confirmed to be the cause of reduced load capacity of bridges and/or deteriorated riding surfaces [1]. In Ontario, the introduction of post-tensioning technique, to prevent the problem of loosening nail connections, helped to rehabilitate many bridges and to design new bridges with increased service life [2,3]. These experiences have been instrumental in formulating the specifications to design post-tensioned bridge decks which are incorporated in the new Ontario Highway Bridge Design Code (OHBDC) [4].

Although timber is a widely used structural material, inherent to many products of nature, the strength and elastic modulus values vary widely. Assuming rhombic symmetry for timber with the orthogonal axes corresponding to the longitudinal direction of the tree trunk and the radial and tangential direction of the growth ring pattern of the cross-section, the macro elastic properties of timber can be described by nine elastic constants [5,6]. These are: three moduli of elasticity, E_L, E_R, and E_T; three shear moduli, G_{LR}, G_{LT} and G_{TR}; and three Poisson's ratios, ν_{LR}, ν_{LT} and ν_{RT} with these directions identified in Figure 1.2. The longitudinal modulus of elasticity, E_L, however, is known to have the highest value amongst the various moduli [6]. The elastic modulus E_T is generally about 1/20 of the E_L value and the other elastic and shear modulus values are negligibly small. It is also known that the

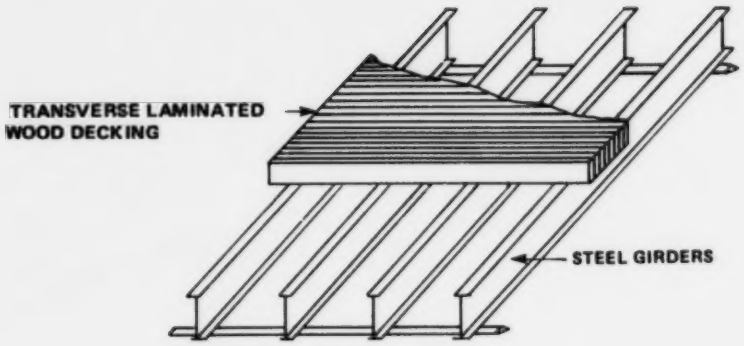

A BRIDGE USING TRANSVERSE WOOD DECKING AND STEEL GIRDERS

Figure 1.1/ Bridge With Transverse Wood Decking and Steel Girders

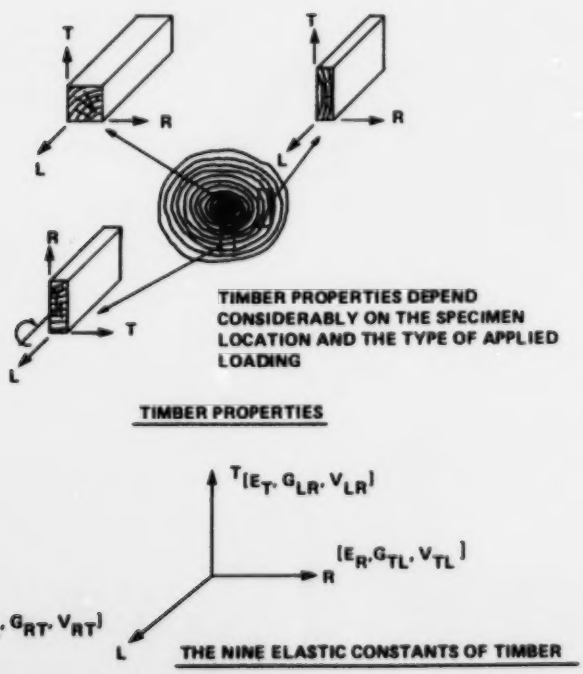

Figure 1.2/ Timber Properties

compression resistance (F_C) of timber parallel to the grain is approximately 2.0 to 6.0 times greater than that perpendicular to the grain.

Obviously the transverse laminated wood decking cannot share a large portion of the longitudinal moments carried by the steel beams because of the low E_T and F_C value of the timber decking. However, reorienting the decking so that the laminates are parallel to the steel beams and developing composite action between the deck and steel girder helps to utilize efficiently the dominant elastic rigidity $E_L I$ of the decking and higher compressive resistance of the laminates parallel to the grain. Developing composite action between the longitudinal laminated decking and steel girder can bring about considerable saving in steel weights. A much lighter deck makes the wood-steel composite bridge more economical than a concrete-steel composite bridge for cases in which the spans are large. In a continuous span bridge the support moments introduce tension in the deck and the ability of the timber deck to sustain greater tensile stress than concrete can be an added asset.

Csagoly and Taylor [1, 7] experimented with lag bolts and bolted angle shear connectors to achieve the composite action; the connection details are shown in Figure 1.3. A few tests conducted with a specimen, using bolted steel angle set into the deck for shear connection, indicated that the static load capacity of the beams was increased considerably, however, the performance of the beams under cyclic loads was found to be poor [7]. Therefore, further development work along this line was not attempted.

The excellent static load performance of the composite beams and potential dead weight savings prompted a fresh attempt to achieve a better shear connection which can perform satisfactorily under both static and cyclic loads. This report describes recent in-house tests conducted by the Ministry to develop a practical system for steel-wood composite bridges.

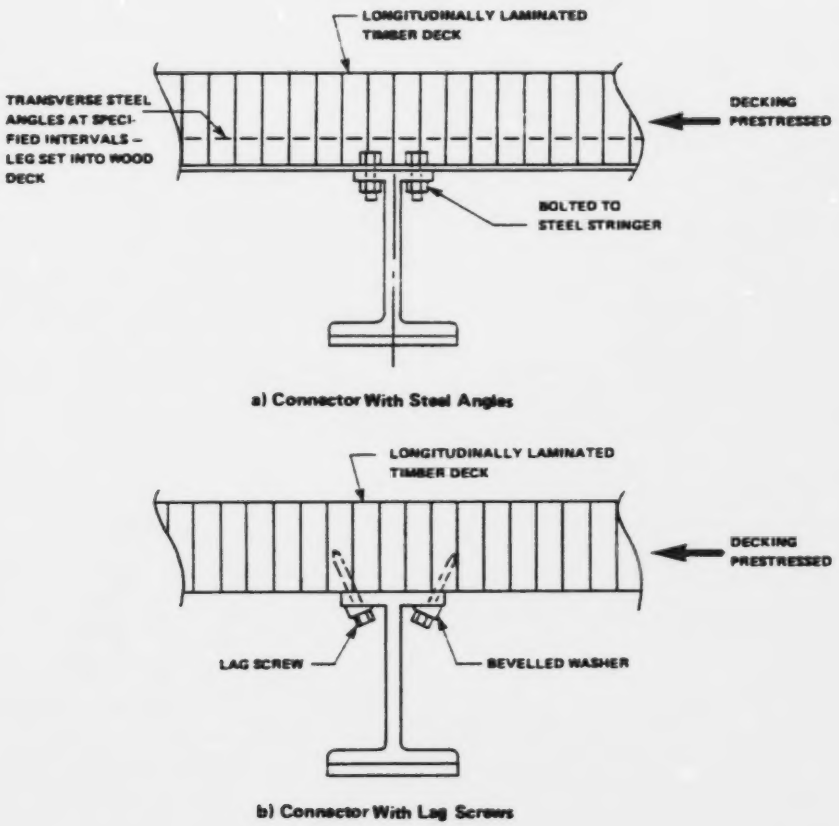

Figure 1.3/ Shear Connectors Proposed by Csagoly and Taylor [7]

2/ ECONOMIC FEASIBILITY OF THE CONCEPT

It is axiomatic that the reorientation of laminates from the transverse to longitudinal direction and making the decking composite with the steel girders will lead to savings in steel girder weights. The actual amount of saving will clearly depend upon such details of the structure as span, width, girder spacing and the like. The steel girder weights at the midspan of a bridge, with seven girders, at a spacing of 1.0 m are compared in Figure 2.1 for various span lengths and for the two kinds of construction, non-composite and composite. It can be shown that for the cross-section under consideration, the steel-wood composite construction results in girder weight savings ranging between 42 and 48%.

One significant question which must be answered before advocating the use of steel-wood composite bridges is: how do these bridges compare in cost with their steel-concrete counterparts? This question is answered for new designs in Figure 2.2 in which cost comparisons between steel-wood and steel-concrete composite bridges are made for one particular cross-section but for various span lengths. The costs of bridges for the two sets of designs were estimated by the Estimating Office of the Ministry. It is expected that, since steel-concrete bridges are regularly built, their cost estimates would be closer to reality. Steel-wood composite bridges, on the other hand, are still untried commodities. Therefore, it is likely that the estimated costs of these structures are on the high side. The effect of the dead weight reduction on the cost of the substructure is also not reflected in the values plotted in Figure 2.2.

Notwithstanding the slight over-estimation of the cost of steel-wood composite bridges, these structures, as can be seen in Figure 2.2, are not economical alternatives to steel-concrete composite bridges for spans of up to 40 m. For larger spans, the cost of the former becomes comparable to that of the latter. However, it is recommended that the concept of steel-wood composite bridges not be applied to such long spans until this form of construction has been applied to shorter spans and their in-service performance is studied over a long period of time.

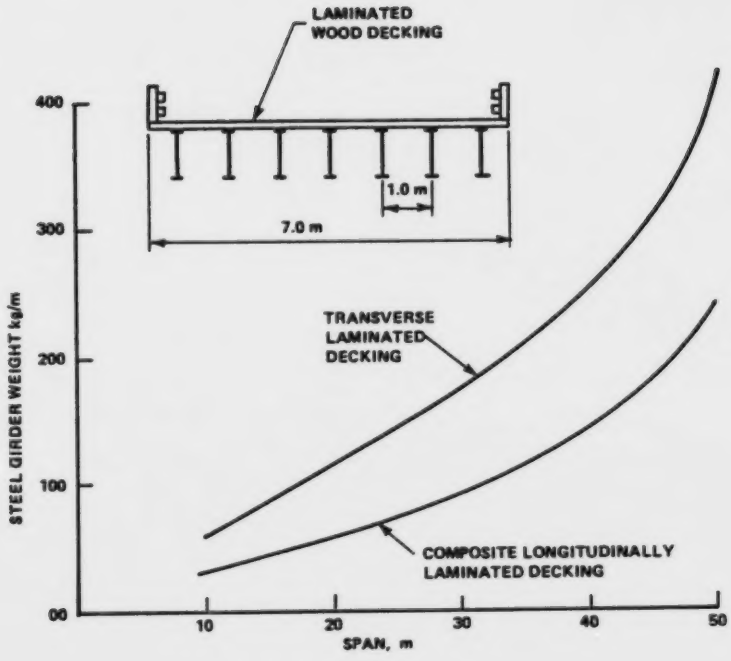

Figure 2.1/ Steel Weight Comparison

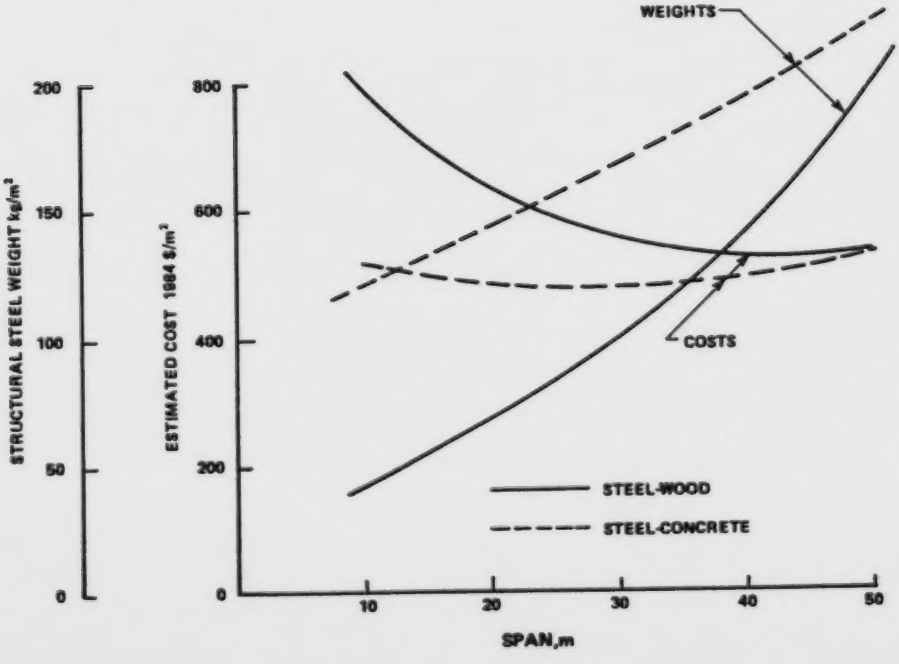

Figure 2.2/ Costs and Steel Weight Comparison

It is interesting to note, in Figure 2.2, that steel-wood composite construction affects a significant reduction in the steel girder weight as compared to the steel-concrete construction. This attribute of the proposed form of construction, together with the considerable reduction in the dead weight of the decking itself, can be used to advantage in the rehabilitation of substandard bridges with sound steel girders but deteriorated non-composite concrete deck slabs.

A five-girder bridge, having a span and width of 30.0 and 14.0 m respectively, is chosen as a vehicle to demonstrate the usefulness of the composite wood decking in the rehabilitation of steel girder bridges. Girders corresponding to different values of the scale-down factor, F, are considered. It is noted that F is obtained according to the OHBDC. F, equal to or greater than 1.0, indicates that the bridge is normal and needs no posting. Smaller values of F indicate the need for posting. When F is smaller than 0.3, the bridge is beyond even posting. It should be replaced.

Posting loads corresponding to level 3 loads (OHBDC, 1983) are plotted in Figure 2.3 for the structure under consideration against different values of F. The Figure also shows the enhancement in the values of F when each of a composite deck slab of 225 mm depth, and a composite wood decking of 200 mm depth, replace the existing non-composite concrete decking. It is noted that the above depths of the decking are commonly used in most cases.

It can be seen in Figure 2.3 that, for the case under consideration, the concrete composite decking can upgrade the structure to normal load carrying level only when F is greater than nearly 0.9. When the steel girders are weaker, i.e., when F is smaller, the composite concrete decking can not upgrade the structure to carry normal loads. The difference in the dead weights of concrete and wood deckings in the structure under consideration is in the order of 105 t, which is about 1.75 times the weight of a single heavy vehicle. It is because of this substantial reduction in dead weight that, as shown in Figure 2.3, the composite wood decking can restore the bridge to standard load carrying capacity even when the scale-down factor is as low as 0.5.

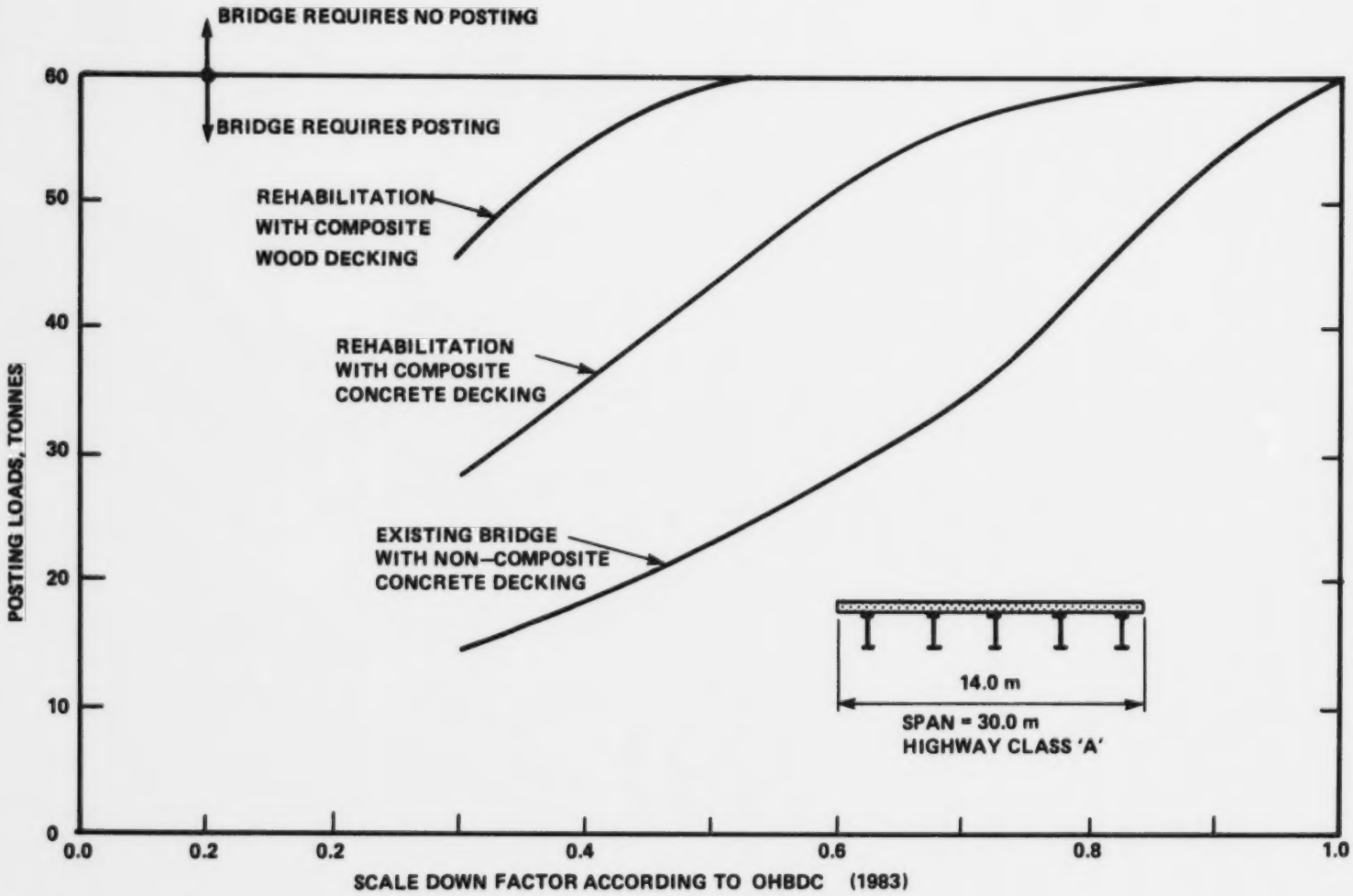

Figure 2.3/ Posting Loads of Bridges Rehabilitated with Timber and Concrete Deckings

It is concluded that, while the concept of steel-wood composite bridges may not yet be economical for new designs, it is a useful and economical one in the rehabilitation of existing bridges with steel girders and deteriorated non-composite concrete deck slabs or transverse laminated wood decks.

3/ SPECIMEN PREPARATION, INSTRUMENTATION AND TESTING

The experimental program undertaken for the investigation was conceived to provide a progression from selecting a suitable shear connecting system with preliminary tests to conducting a more intensive investigation on the selected shear connector, composite beams, composite bridge system under both static and cyclic loads.

3.1/ Preliminary Tests

Preliminary tests were performed on two beams with different types of shear connection system to transfer the interface shear between the steel girder and the decking. In one system, the shear connector consisted of a continuous vertical steel plate welded intermittently to the top flange and embedded between laminates before prestressing. In the other system, the prestressed wood decking was assembled first. Large holes were then drilled in the decking to accommodate clusters of shear studs attached to steel flange and the holes filled with non-shrinking grout or concrete mix. The details of the steel girders, the decking and the shear connections used for each of the two beams are given in Figure 3.1(a) and (b). The decking consists of twelve 50 x 100 x 3050 mm long laminates of select structural No. 1 Jack Pine held together by post-tensioning. Dwiydag post-tensioning bars of 15 mm diameter were threaded through 20 mm holes made in the laminates at 305 mm centres. The tendons bear against 100 x 200 x 10 mm thick bearing plates. The steel beams used are S 150 x 19 kg/m and are 3050 mm long with the yield strength of 300 MPa. The shear connection plate is 90 x 10 thick and 3050 mm long, and the shear studs are 10 mm in diameter x 80 mm long. The shear plate and the shear studs are welded with a manual arc welder.

The test specimen were instrumented with electrical resistance strain gauges, demountable gauges and deflection transducers. Details of the instrumentation and loading are shown in Figure 3.2. The beam and the decking were tested in the following sequence:

a) The naked steel beam;

b) Prestressed wood deck with the steel plates sandwiched between the laminates;

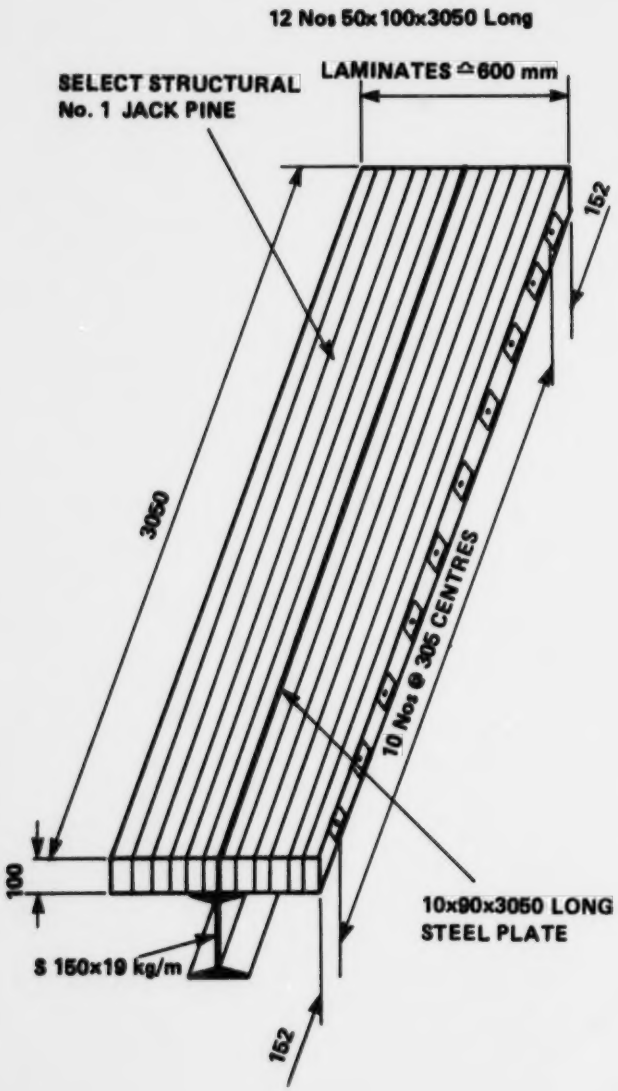

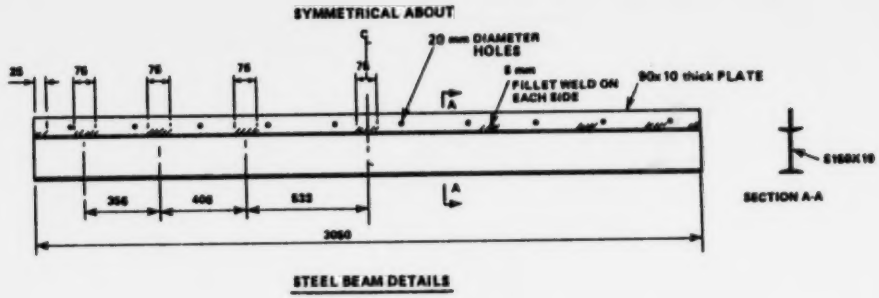

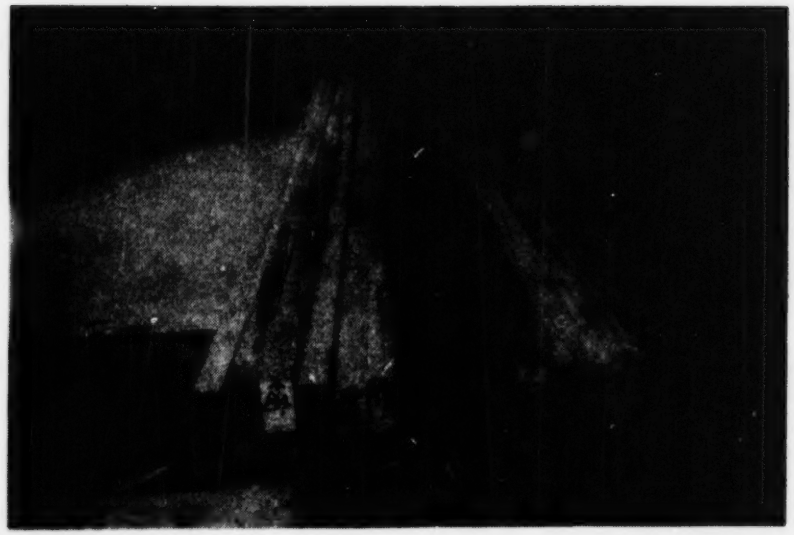

Figure 3.1a/ Composite Beam Using Steel Plate Shear Connector

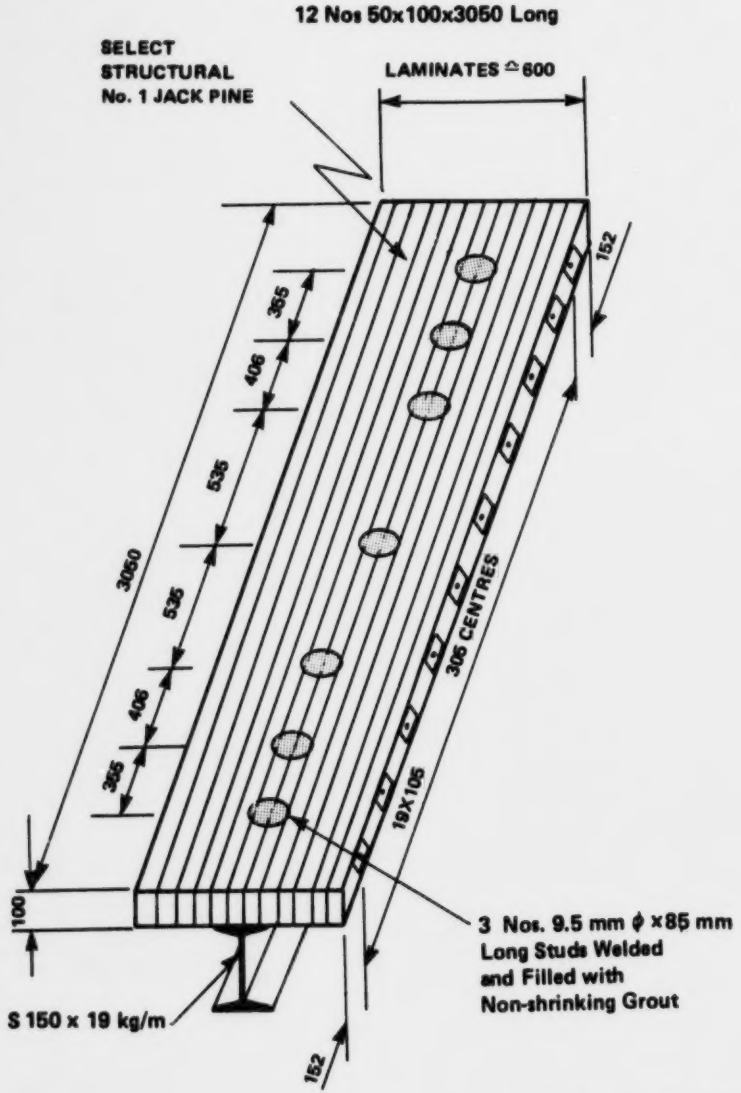

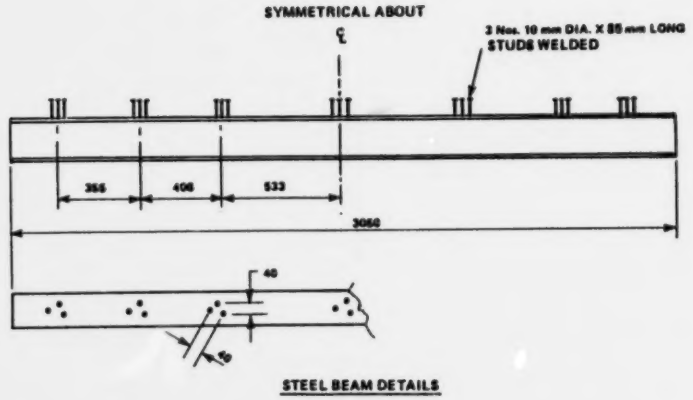

STEEL BEAM DETAILS

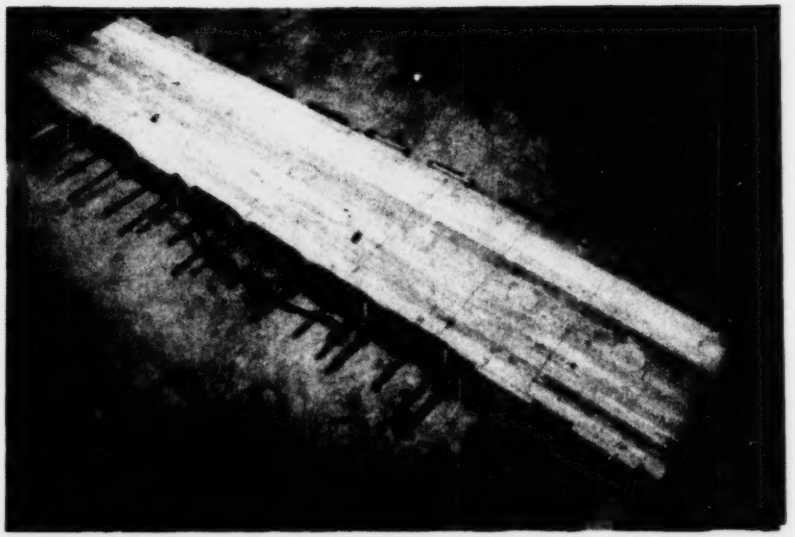

Figure 3.1b/ Composite Beam Using Concrete Bulkhead Shear Connector

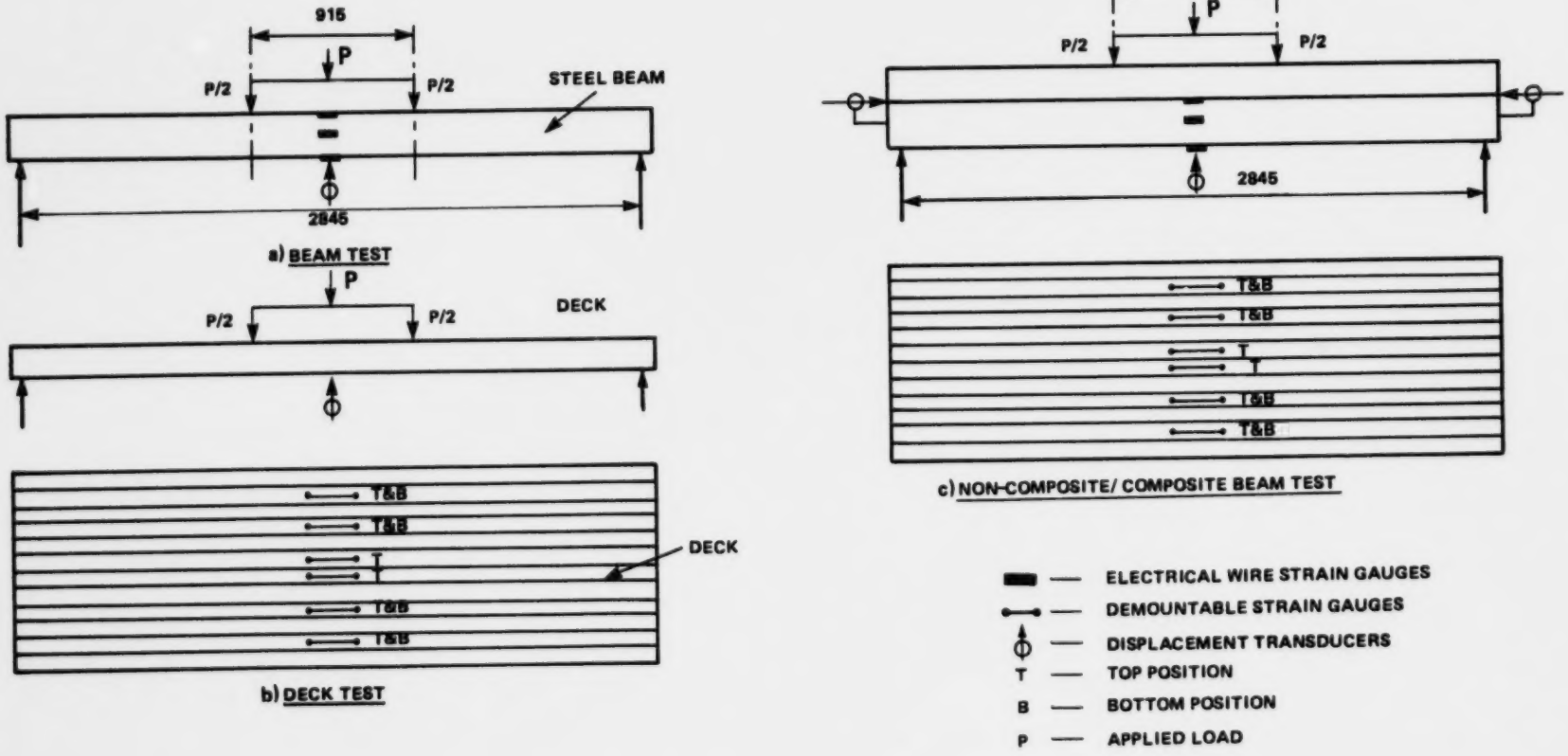

Figure 3.2/ Instrumentation and Loading Arrangement used for Preliminary Beam Tests

c) The above wood deck and steel beam without a mechanical shear connector.

d) The composite beam.

The magnitude of the applied loading, which varied according to the stiffness of each of the specimen, was kept sufficiently large to allow a realistic comparison but kept below levels that can induce inelastic deformations.

The system with concrete bulkhead connector was tested in the following sequence:

a) The naked steel beam
b) Prestressed decking alone
c) The prestressed decking and steel beam without any mechanical shear connection
d) The composite beam

The tool used for drilling large holes in the deck to accommodate shear connectors is shown in Figure 3.3. The composite beam was tested 28 days after the casting of the bulkheads.

The success of a shear connection system in a bridge depends on its ability to sustain cyclic loads. After the completion of static load test, the above two beams were subjected to cyclic loads. The cyclic loading arrangement used is shown in Figure 3.4. The load was applied at the mid span with a 1 Hz cycle and varied from 8 kN minimum to 67 kN maximum. The maximum load of 67 kN applied is considered to be about half the ultimate load capacity of the beam. At frequent intervals, the test was interrupted to test the beam under a static load of 67 kN. The centre span beam deflection and strain on the bottom flange of the steel girder were measured. The specimens were also watched continuously for any signs of fatigue induced distresses.

3.2/ Shear Connectors

Preliminary static load tests indicated the concrete bulkhead connector to be the better one of the two connectors tested. It was also foreseen

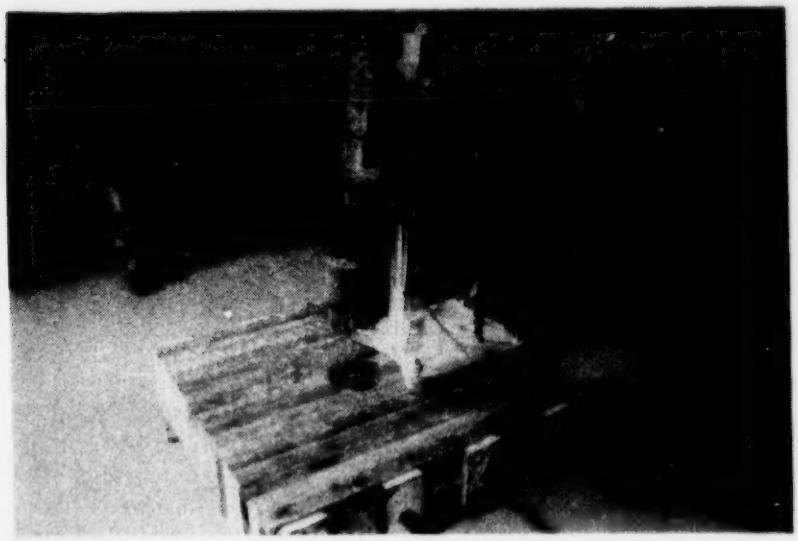

Figure 3.3/ Deck Coring Tool

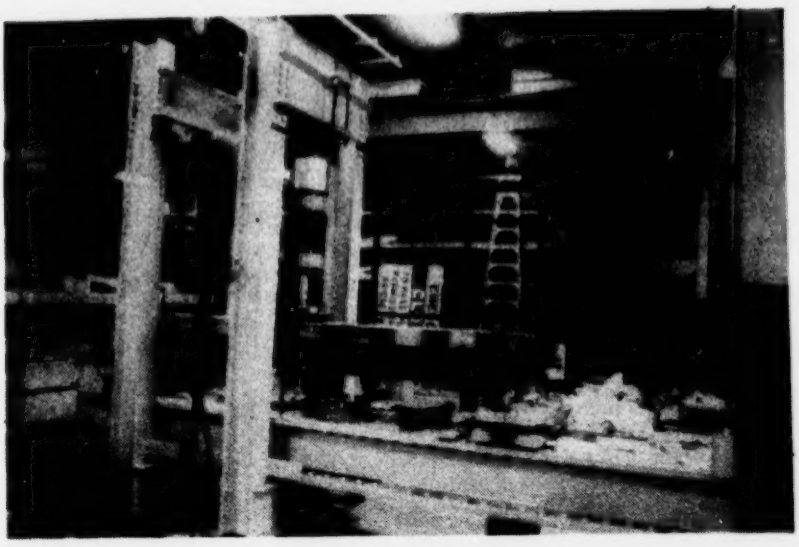

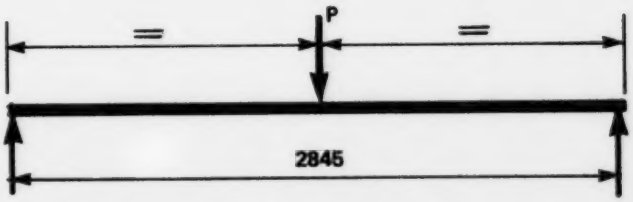

Figure 3.4/ Cyclic Loading of Beams

that the installation of a prestressed deck with steel plate shear connection will lead to significant difficulties in the field. When a longitudinal laminated deck is prestressed laterally, its width is reduced by up to 5% due to transverse compression of wood fibres [8]. If a laminated wood deck with steel plate type shear connector was to be transversely prestressed, the large shortening of the deck width would have to be accommodated by the steel components below the deck. Clearly, the width reduction would necessitate awkward adjustments in the transverse diaphragms and girder bearings. The additional static tests were limited to systems using the concrete bulkhead as a shear connector.

Direct shear tests were made to obtain the ultimate shear load capacity, and the deformation characteristics of the concrete bulkhead shear connector while varying the stud diameter, the diameter of the bulkhead and the type of welding used to attach shear connectors.

Details of specimens used to study the direct shear load characteristics of concrete bulkhead shear connectors are given in Figure 3.5. Two identical post-tensioned decks with twelve 50 x 100 x 1115 mm long laminates of select structural No. 1 Jack Pine were fabricated. In a few cases, select structural No. 1 Spruce Pine Fir was used. The holes for the bulkhead were made using either 100 mm or 150 mm diameter coring tool. The 900 mm long steel beam cross head of was welded with three studs on each flange of the beam. The beam was kept in place and a deck cast with non-shrinking grout. After 2 days of curing, the other decking was kept in place and cast with grout. After a minimum of 20 days of curing, the specimen was placed on the loading rig, instrumented, and tested to failure. Generally, two deflection transducers were used to measure the deformation under applied load; however, for specimen No. 5, demountable gauges were attached to the deck laminates to study the load dispersion through the laminates, see Figure 3.5. The loading was generally applied at approximately 9 to 18 kN intervals; however, the readings were taken at closer intervals as failure load is reached.

Three specimens were subjected to cyclic loads to investigate the fatigue load characteristics of the shear connection used. A full scale specimen with 200 mm deep laminates was also fabricated for the cyclic load tests.

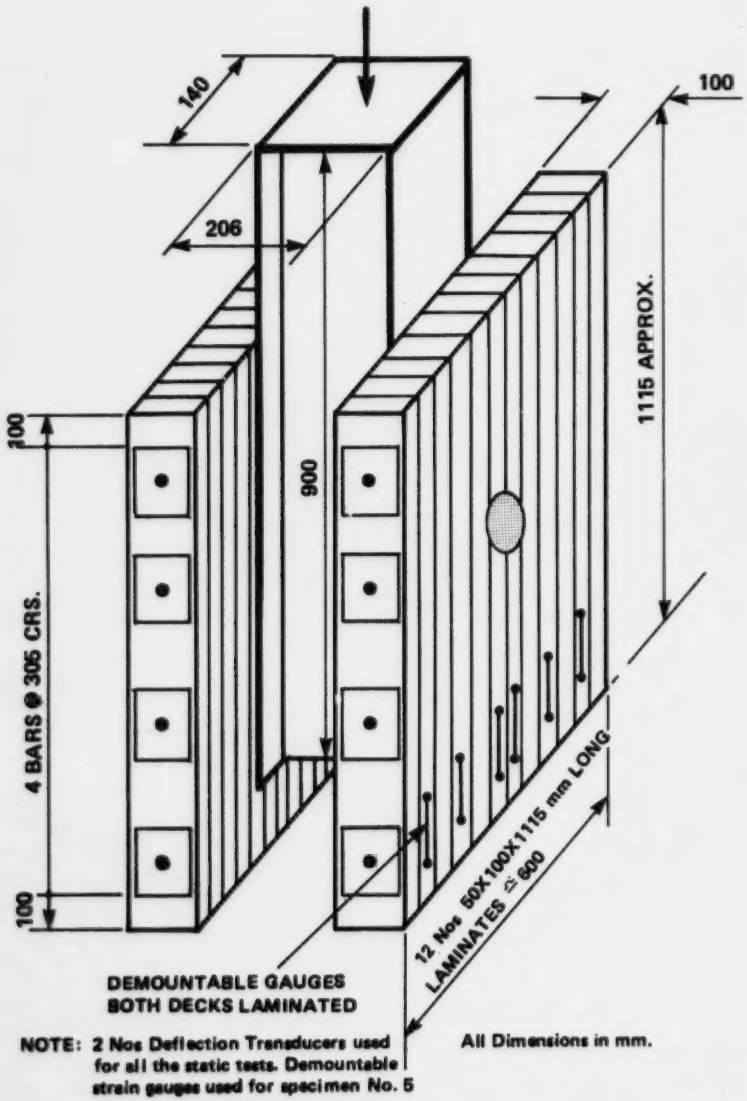

NOTE: 2 Nos Deflection Transducers used for all the static tests. Demountable strain gauges used for specimen No. 5

All Dimensions in mm.

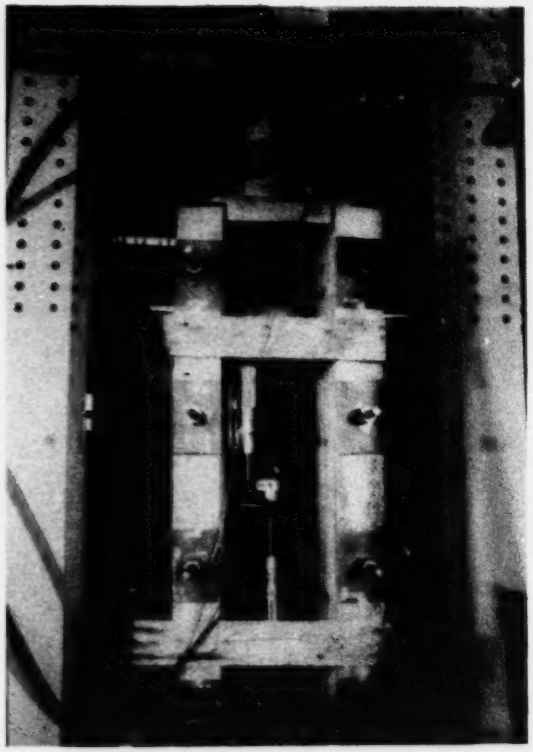

SPECIMEN No.	WOOD TYPE	No. OF STUDS	DIAMETER OF STUDS, mm	TYPE OF WELDING	DIAMETER OF BULK HEAD mm	TEST TYPE
1	Jackpine	6	12.7	Manual Arc Weld	100	STATIC
2	Jackpine	6	15.9	–do–	100	
3	Jackpine	6	12.7	Nelson Stud	100	
4	Jackpine	6	19.1	–do–	100	
5	Spruce	6	19.1	–do–	150	
6	Spruce	6	12.5	–do–	100	CYCLE
7	Spruce	6	19.1	–do–	150	
8	Spruce	6	19.1	Manual Arc Weld	150	

Figure 3.5/ Details of Direct Shear Test Specimens

The details of the full scale specimen together with the test set up used for the cyclic load tests are given in Figure 3.6. Each specimen was placed on the test rig and subjected to a selected maximum and minimum direct shear load at 1 Hz loading rate. The cyclic loading was continued until a shear connection showed a visible sign of distress or the number of cycles exceeded 2 million.

3.3/ Composite Beams

In order to understand the deformation characteristics of the steel-wood composite beams, three composite beams with concrete bulkhead shear connectors were fabricated for testing to failure. The shear connection capacity was varied in each of the beams, to study its effect on the deformation and ultimate strength characteristics of the composite beams. Assuming a compressive stress capacity of the decking to be 20 MPa, the decking used can sustain a 1500 kN axial compressive load. Accordingly, for the three beams, the stud capacity between the midspan of the beam and the beam end was selected to be 312 kN, 780 kN and 1408 kN, respectively.

The details of the three beams fabricated are given in Figure 3.7. It is noted that the beam with 780 kN stud capacity was later used for cyclic load tests instead of static load tests. The decking consisted of fifteen 50 x 100 x 3050 mm long select structural No. 1 Spruce/Pine/Fir laminates. The laminates were drilled with 20 mm diameter holes at 305 mm centres to accommodate post-tensioning rods. The deck was assembled, post-tensioned with 0.70 MPa prestress and drilled with 100 or 150 mm diameter holes. The beam was welded with Nelson studs and the deck beam system assembled and grouted with non-shrinking mortar. The load deformation tests were performed after a minimum of 20 days of curing.

Each specimen was set up on the loading frame and instrumented with electrical wire strain gauges, demountable strain gauges, and deflection transducers. It was intended to obtain sufficient information on the deck strains, beam strains, the slip between the deck and the beam, and the vertical deflections. The instrumentation details are also given in

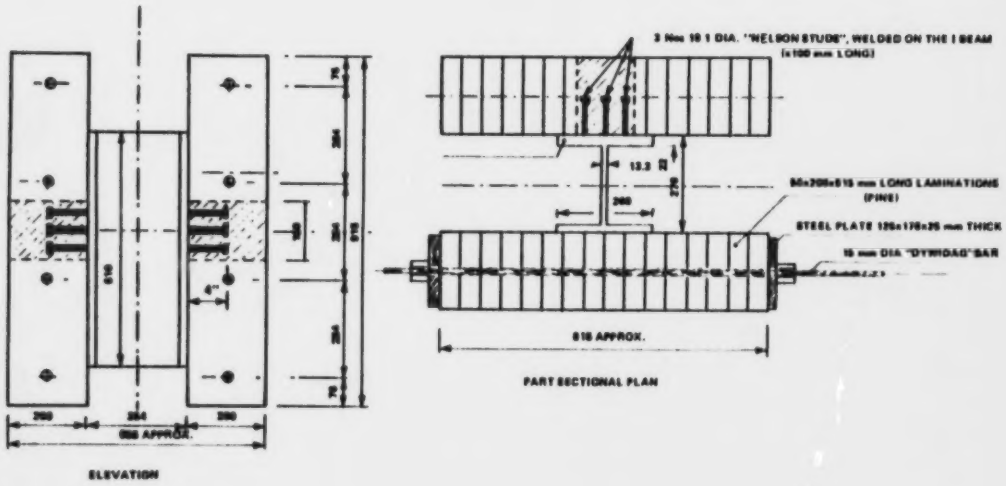

a) Full Scale Specimen for Cyclic Load Test

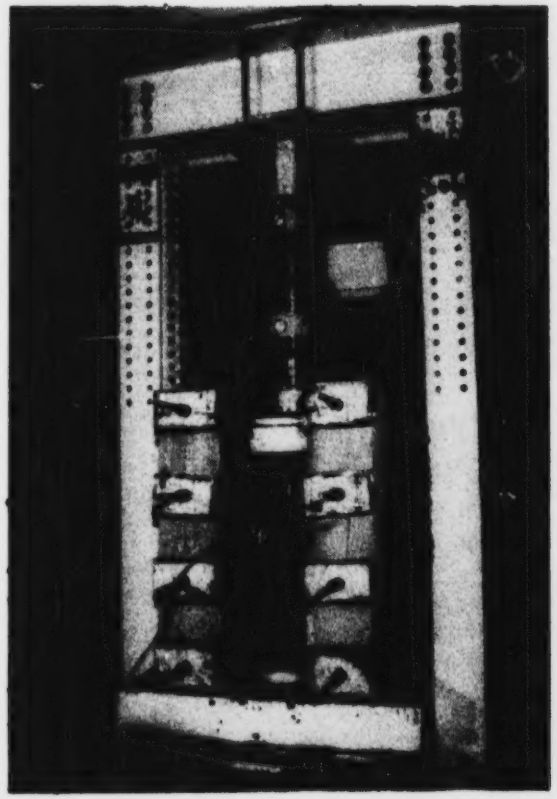

b) A Specimen Under Direct Shear Cyclic Loading

Figure 3.6/ Details of the Full Scale Specimen for Cyclic Loading and a View of the Cyclic Loading Rig

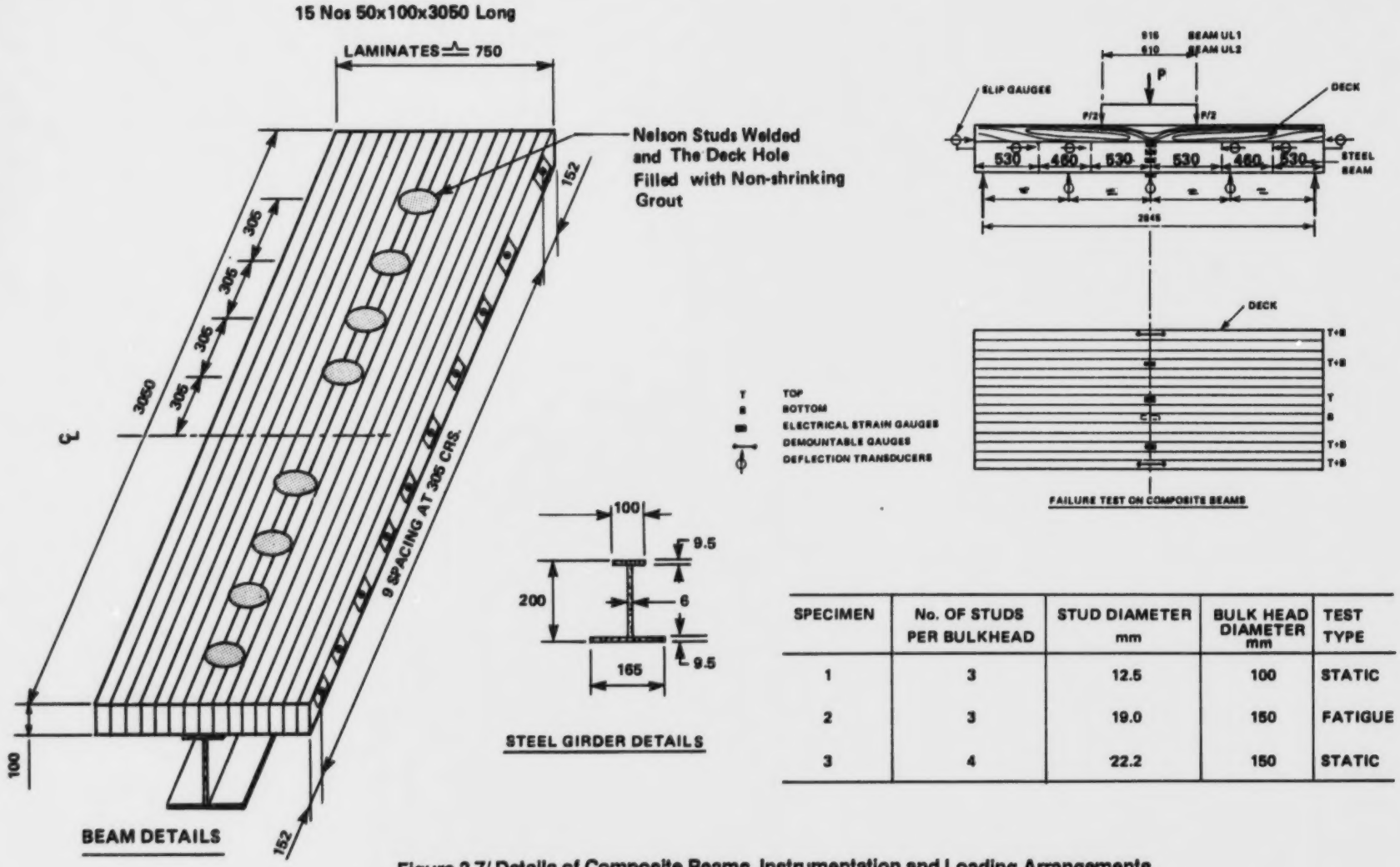

SPECIMEN	No. OF STUDS PER BULKHEAD	STUD DIAMETER mm	BULK HEAD DIAMETER mm	TEST TYPE
1	3	12.5	100	STATIC
2	3	19.0	150	FATIGUE
3	4	22.2	150	STATIC

Figure 3.7/ Details of Composite Beams, Instrumentation and Loading Arrangements

Figure 3.7. A two point loading, symmetrical about the centreline, was applied. The loading was generally applied at 10 to 15 kN intervals, however, the readings were taken at closer intervals as the failure load approached.

In order to develop theoretical models for the prediction of ultimate load capacity of steel-wood composite beams and load deformation characteristics of fully and partially composite beams, the relevant material properties of steel and wood were obtained by tests. After each failure test, about five timber specimens of 50 x 100 x 300 long were removed from the composite beam deck to test for the compressive strength. The specimens were attached with a strain gauge at mid-height of the specimen and loaded to failure in an Instron machine using a loading rate of 16000 N/min. The strains was measured at regular intervals using a portable strain metre. A steel sample was also removed from the girder and tested as per CAN. G40.21-M81 for tensile strength. Timber specimens were also selected from spruce laminates used in direct shear tests and tested for load-deformation characteristics. These tests were performed at the MTC materials laboratory. The results of these tests are given in Figure 3.8.

With the set-up similar to that shown in Figure 3.4, specimen No. 2 was also tested under cyclic loads. The maximum load used was 98.0 kN and the minimum was 13.0 kN with a cycle rate of 1 Hz. The specimen underwent 2 x 10^6 cycles without any loss of stiffness however the bulkheads showed cracking after reaching 100 000 cycles. The observed cracking was generally parallel to the laminates. It is postulated that the concentrated compressive forces exerted by laminate tips to the concrete bulkhead induces the transverse splitting stress which is responsible for cracks. Use of chicken wire mesh to increase the tensile resistance of the bulkhead was thought to be a means to avoid bulkhead cracking. The same beam specimen was disassembled and the remaining bulkhead broken while keeping the shear studs intact. The beam was assembled again and the bulkhead, cast with four layers of wire mesh, had equal distribution along the depth of the timber laminates. One specimen was cured for 20 to 28 days and cyclic loads were applied. Even after 2 x 10^6 million cycles, no cracks could be observed in the bulkhead.

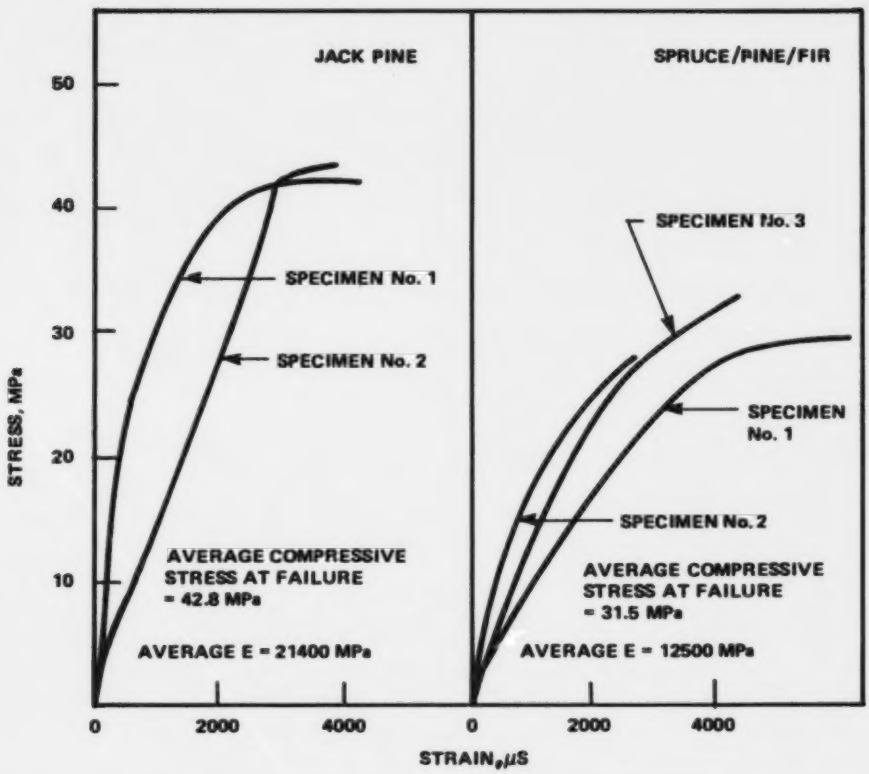

a) TYPICAL STRESS-STRAIN CURVES FOR TIMBER LAMINATES USED

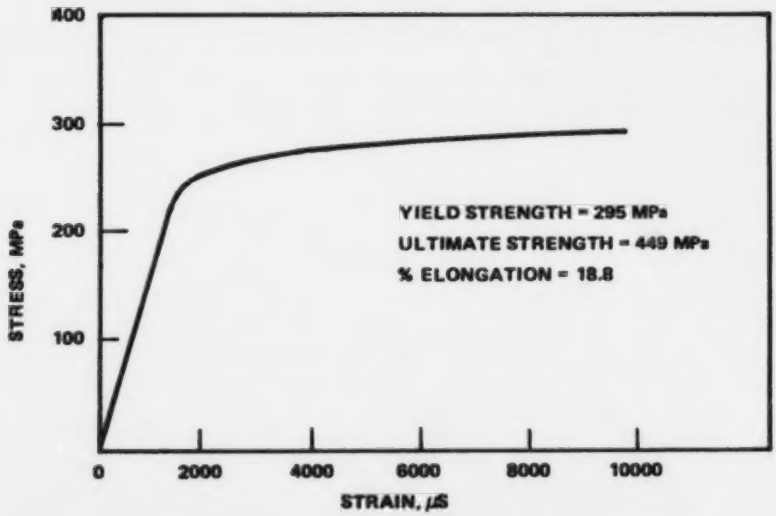

b) TYPICAL STRESS-STRAIN CURVE FOR SPECIMEN TAKEN FROM STEEL GIRDER

Figure 3.8/ Properties of Timber and Steel Used

3.4/ Model Composite Bridge

A half scale model bridge was designed so that the behaviour of a composite bridge incorporating the concrete bulkhead shear connection system could be studied. The bridge was designed according to the OHBDC with reduced live loads to account for the scale effects. The design calculations are given in Appendix 'A' and the details of the bridge structure in Figure 3.9. The bridge consisted of 6.96 m long and 2.782 m wide longitudinally laminated decking, held together by nailing and prestressing rods at 305 mm centres. A continuous channel of C75 x 7 kg/m section was used as the bearing plate for prestressing rods. The decking was supported longitudinally by four W 200 x 30 kg/m steel girders at 0.865 m centres and transversely by three diaphragms, two at the end supports and the other at the midspan. Each diaphragm consisted of a C130 x 10 kg/m channel. The shear connection was made by using 15.8 mm diameter, 90 mm long Nelson studs installed in 100 mm diameter bulkheads.

The 50 x 100 mm laminates were drilled with 20 mm diameter holes at 305 mm centres to accommodate prestressing rods. These laminates were nailed together. The laps necessary to achieve the required length of 6.096 m were staggered according to the OHBDC. Once the full width of the deck was nailed together, the channel were attached and the whole deck prestressed to an average stress of 0.70 MPa. The steel beams were fabricated with brackets to receive the channel diaphragms. After completion of the tests on the deck and the non-composite bridge, 100 mm diameter holes were cored in the deck, the shear studs welded, the bridge assembled and the holes filled with non-shrinking grout. The bulkheads were cured for a minimum of 20 days before the tests.

The decking was initially instrumented and simply supported along two lines, as shown in Figure 3.10. It was then subjected to patch loads and a knife edge load to study the effects of these loads on the stressed and unstressed deck. Also, results of this test were used to obtain the average elastic modulus of the decking. The decking was then supported over three line supports, as shown in Figure 3.10 and loaded with full size and half size wheel pads. It was intended here to study the effects

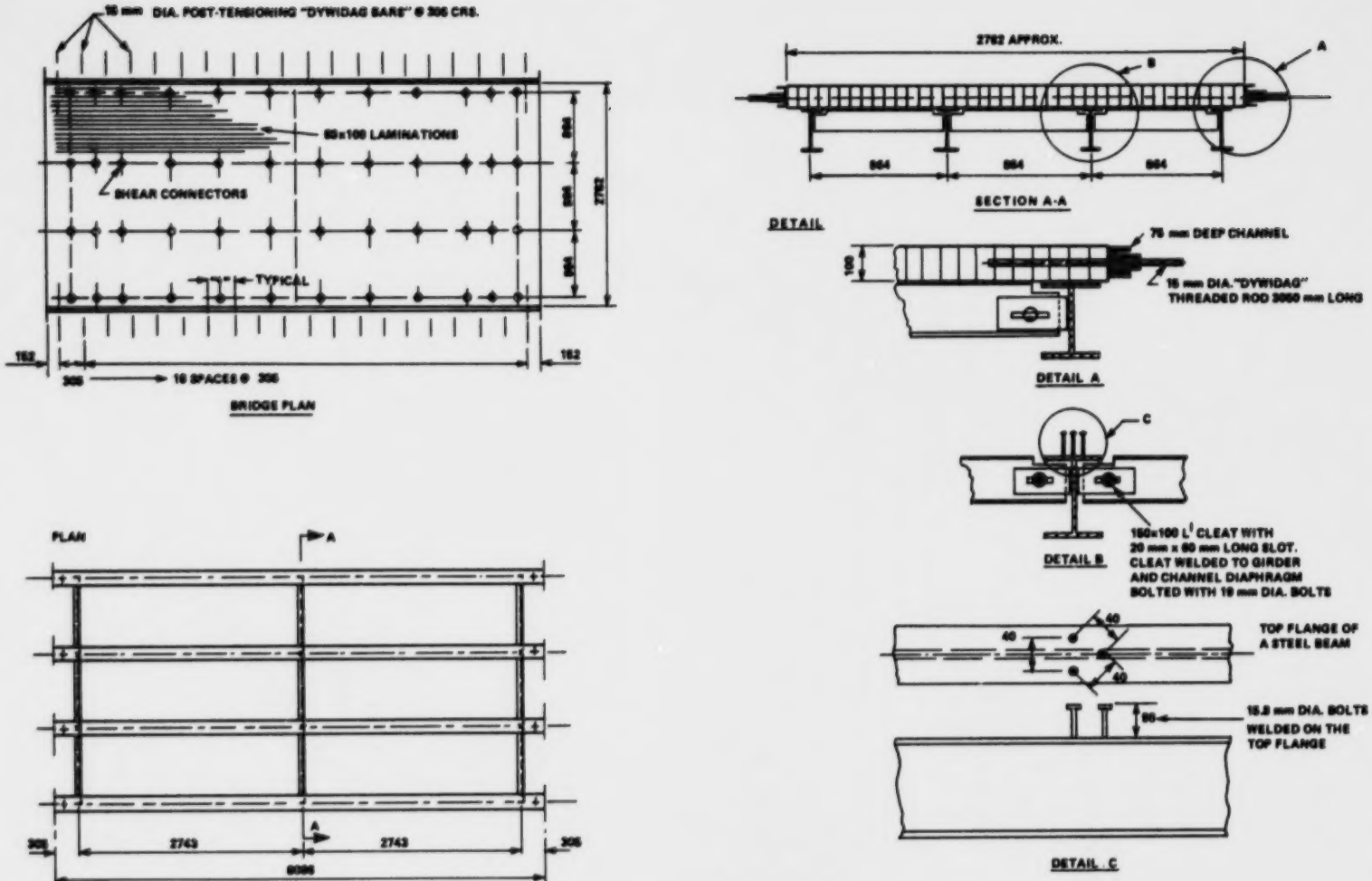

All dimensions are in mm.

Figure 3.9/ Model Bridge Details

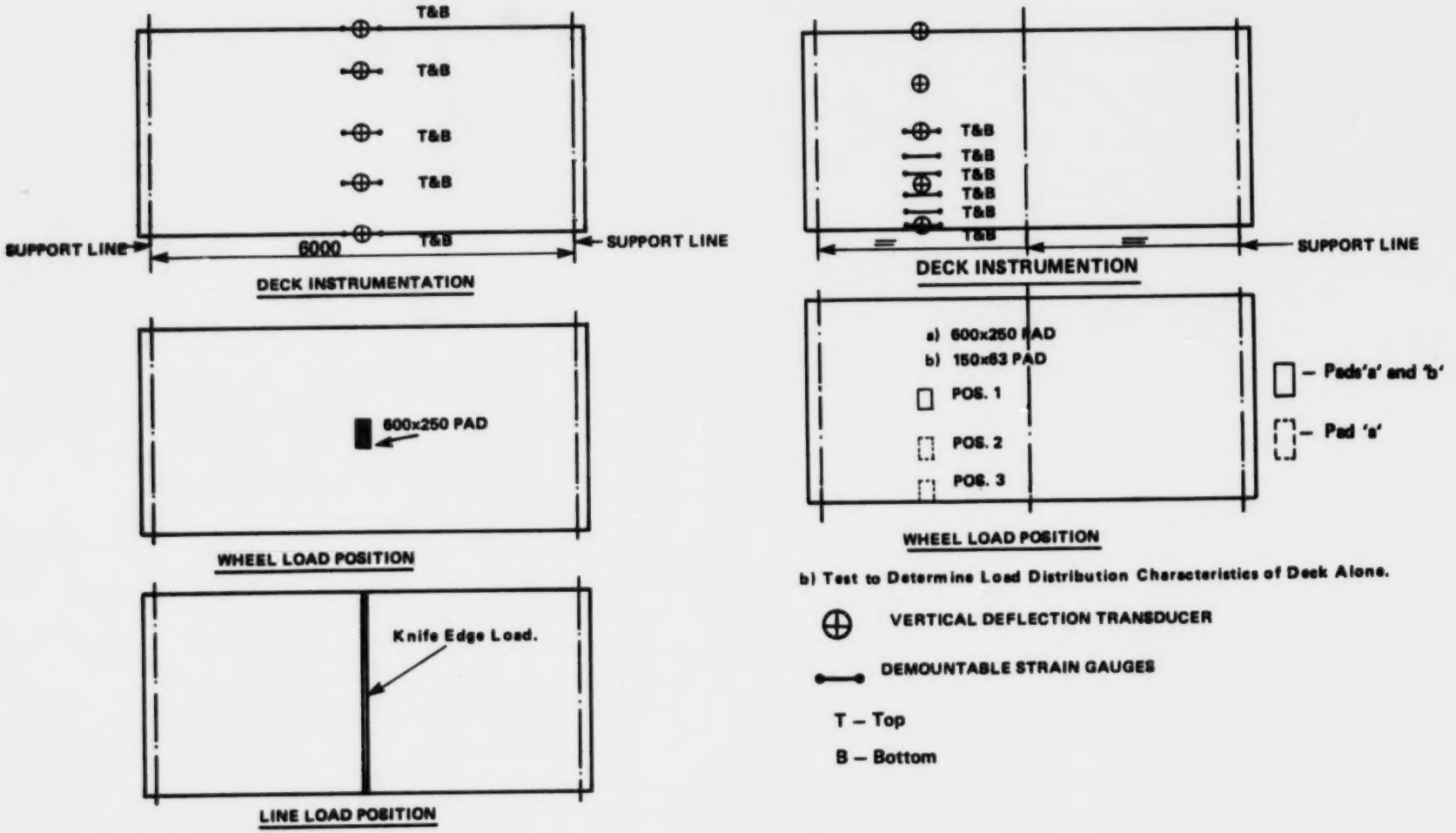

Figure 3.10/ Instrumentation and Testing of the Deck

of the wheel pad size on the deformation and strains induced on the decking. The half scale pad was used to make the test compatible with the half scale model of the bridge.

The decking was later placed on the steel grid and the bridge was instrumented as shown in Figure 3.11. A view of the bridge under test loading is shown in Figure 3.12. The decking was initially loaded with wheel loads placed at positions shown in Figure 3.11. The loads were applied at 5 to 8 kN intervals to a load level that was kept lower than the level that can cause permanent deformations. At each load level, the results were recorded through a data aquisition system. These tests were repeated for single axle and dual axle load cases. The positions of the single axle loads and the dual axle loads are given in Figure 3.11.

After the deck was made composite it was tested in a similar way as the non-composite bridge. The loads applied were indeed greater than those applied for the noncomposite bridge because of the greater rigidity of the composite system.

After the static load tests were completed, the bridge was tested under cyclic loading. A dual axle load was selected for the cyclic test, the details of which and the instrumentation are given in Figure 3.13. A maximum dual axle load of 67 kN and a minimum load of 12.0 kN was used for the test. The loading rate used was 1.0 Hz. The cyclic loading was interrupted at regular intervals to measure the girder deflections, midspan strains, and deck deflections directly under the loading pads.

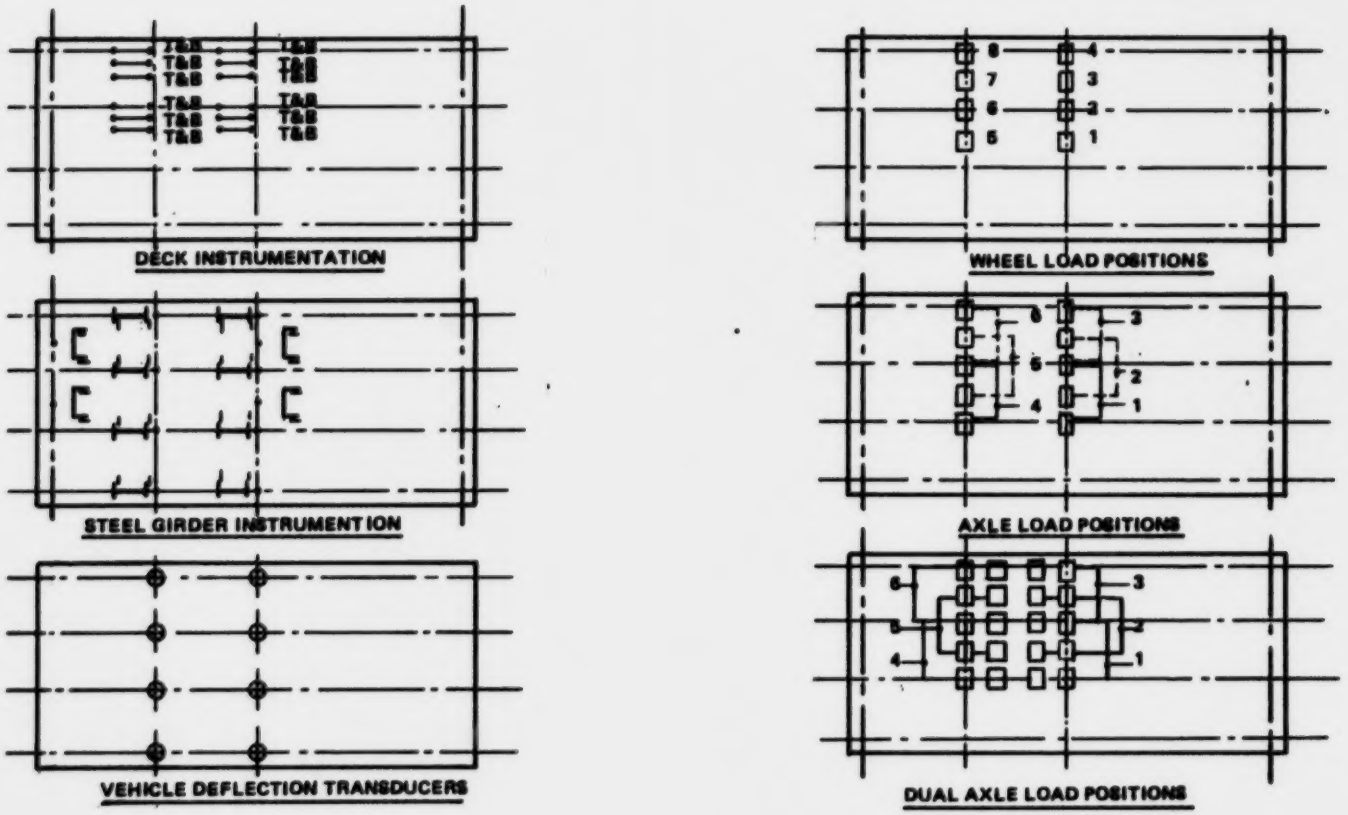

Figure 3.11/ Instrumentation and Testing of the Model Bridge

Figure 3.12/ A View of the Model under Test Loading

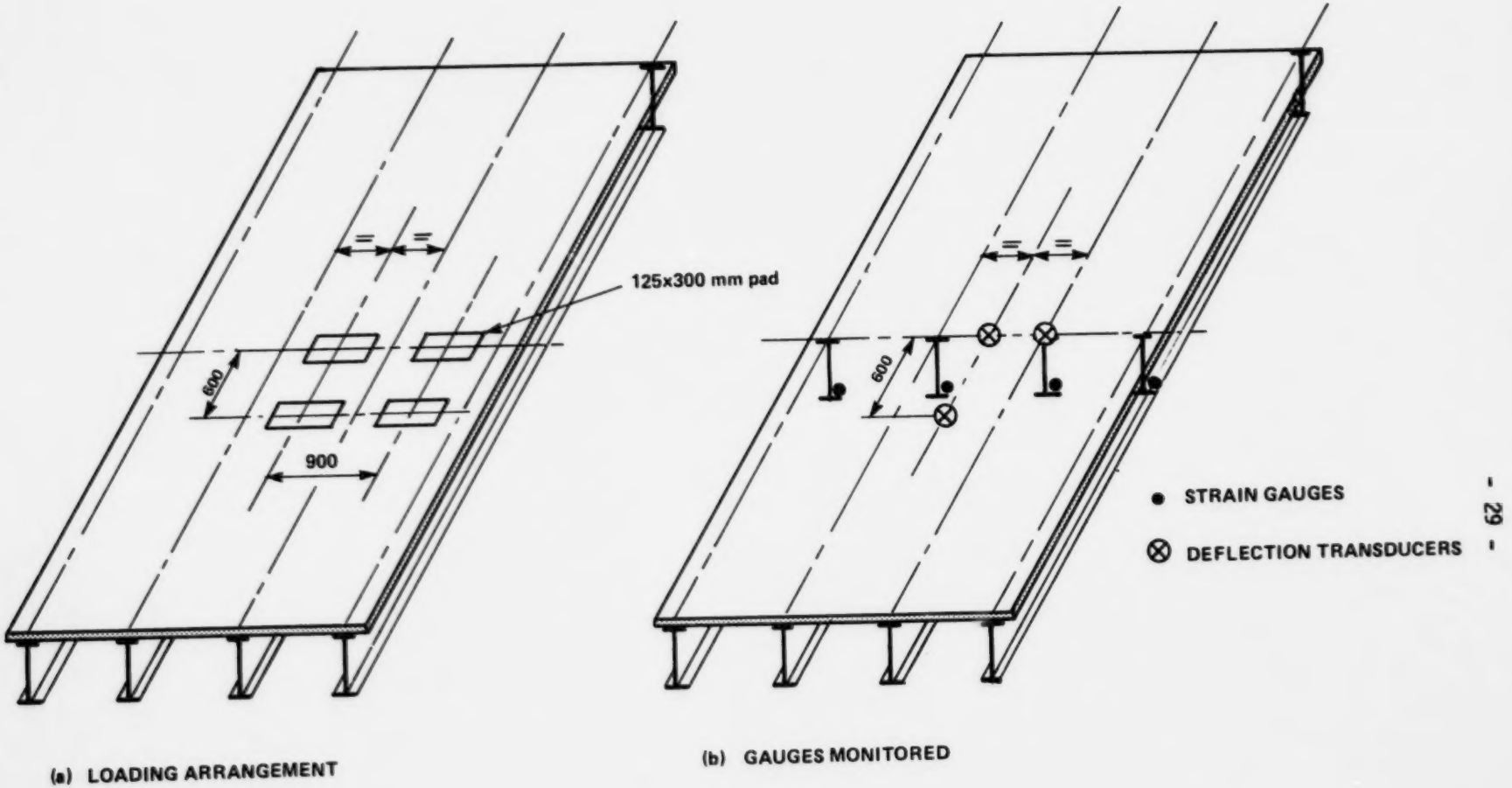

Figure 3.13/ Cyclic Loading of the Model Bridge

4/ PRELIMINARY TESTS

4.1/ Static Load Tests

The test results obtained for the system using steel plates as a shear connector are summarized in Figure 4.1 and Table 4.1. Clearly, the composite beam performance is much better than that of the non-composite beam or the steel girder alone. The stiffness of the composite beam compared to the steel girder increased by approximately 125% for a midspan deflection of 5 mm. The end slip between the deck and the steel girder are also shown in the figure. The slip for the non-composite beam was found to be reversible and was about 1.8 mm under the applied load of 76 kN. The composite beam had a slip of less than 0.05 mm for the applied load of up to about 65 kN. When the load exceeded 65 kN, there was a loud gun shot-like noise accompanied by an instantaneous slip of approximately 0.15 mm. Under higher loading, the rate of slip increase was reduced and the gradient of load-slip curve became almost equal to that observed in the initial loading stage. When the load was released, there was a permanent slip of 0.15 mm, approximately equal to the sudden slip movement described earlier.

It can be seen in Table 4.1 that the steel strains are much lower for the composite girder than those of the non-composite girder or the steel girder alone. Similarly the deck strains are also reduced indicating the additional rigidity offered by the composite action. Going from a naked girder system (which effectively corresponds to the bridge with transverse laminated decking) to the composite bridge affects a reduction of live load stresses in the top flange of up to 99%, as shown in Table 4.3. The table also lists the stress reductions when one goes from the non-composite system with longitudinal laminates to the composite system. It can be seen that these reductions are also substantial which confirms the advantage of reorienting the laminates of the decking.

The test results obtained for the system using concrete bulkhead as shear connection are summarized in Figure 4.2 and Table 4.2. Again, the

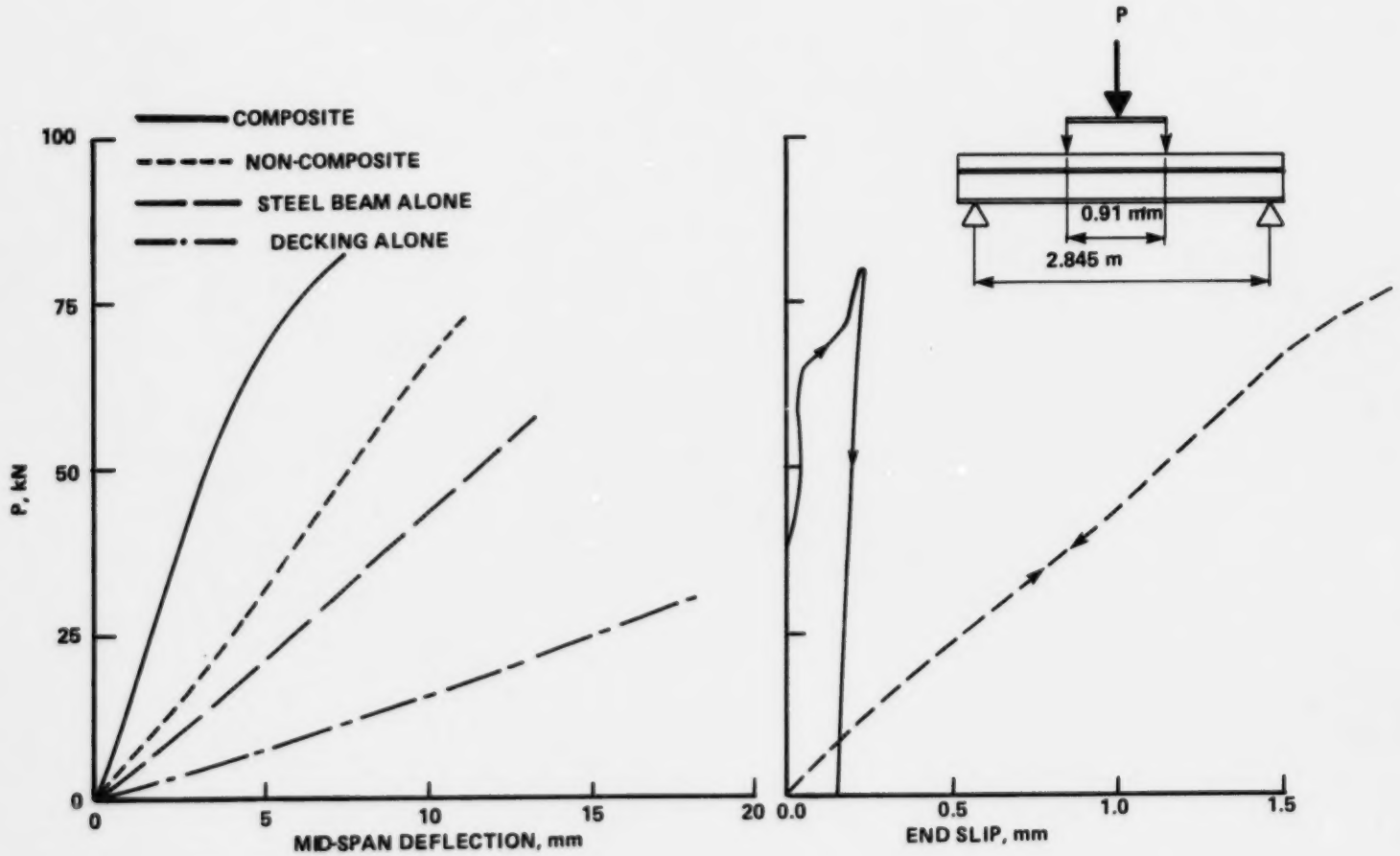

Figure 4.1/ Load Deformation Characteristics of Beam with Steel Plate Shear Connection

Table 4.1/ Strains Measured in the System Tested for Steel Plate Shear Connection

BEAM TESTED	MEASURED STRAINS,μS		
	APPLIED LOAD,kN 25	50	70
Steel Beam	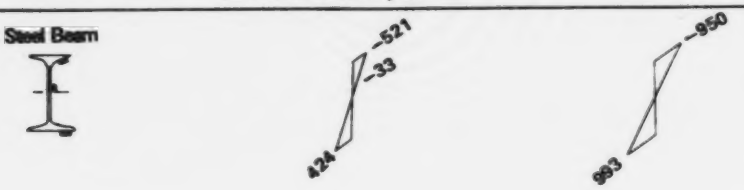		N/A
Timber Deck	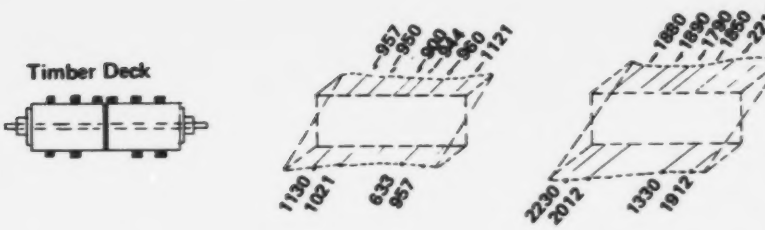		N/A
Steel-Wood Non-Composite	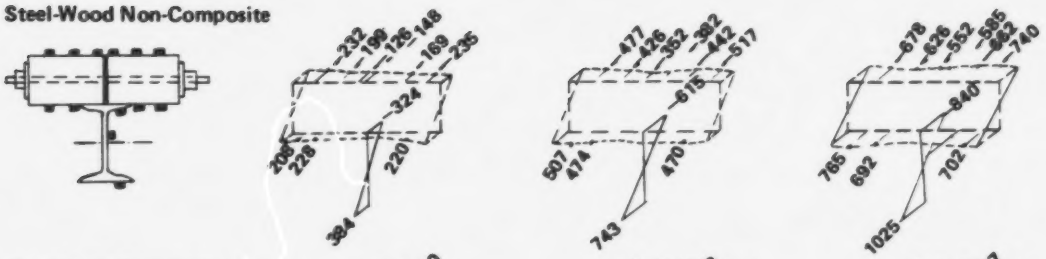		
Steel-Wood Composite	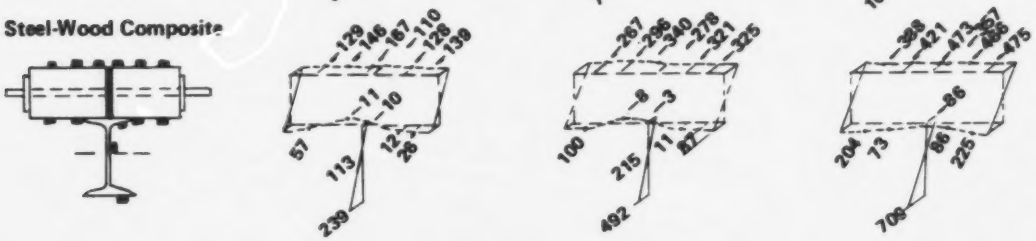		

▬ – Strain Gauge Locations (Typ.)

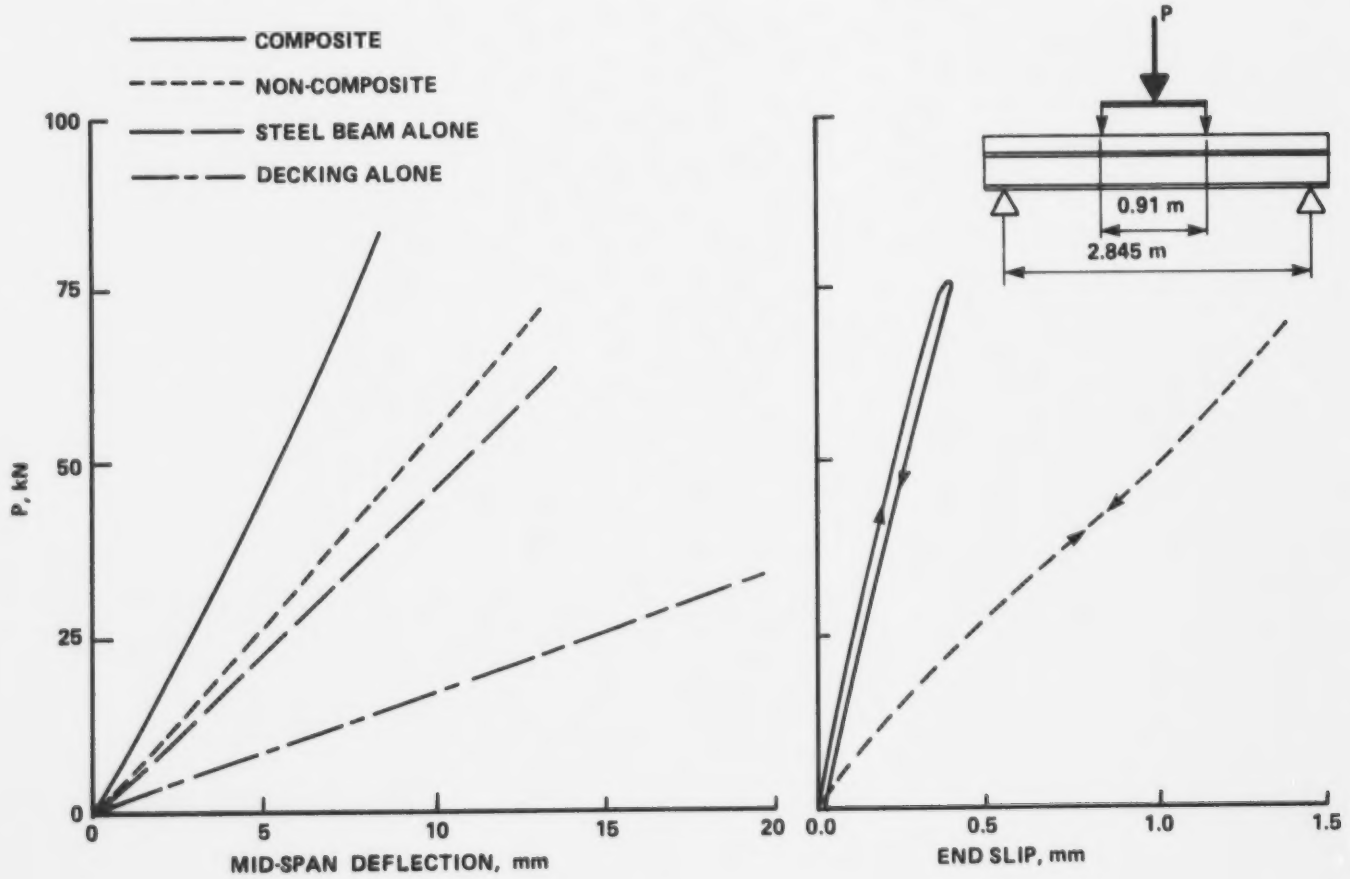

Figure 4.2/ Load Deformation Characteristics of Beam with Concrete Bulkhead Shear Connectors

Table 4.2/ Strains Measured in the System with Concrete Bulkhead Connection

BEAM TESTED	MEASURED STRAIN, μS		
APPLIED LOAD,kN	25	50	70
Steel Beam	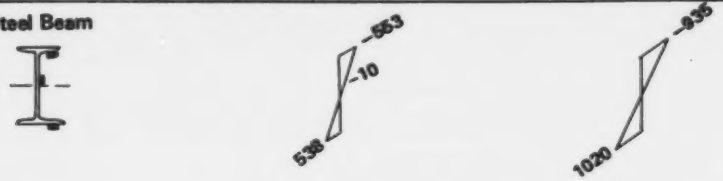		N/A
Timber Deck	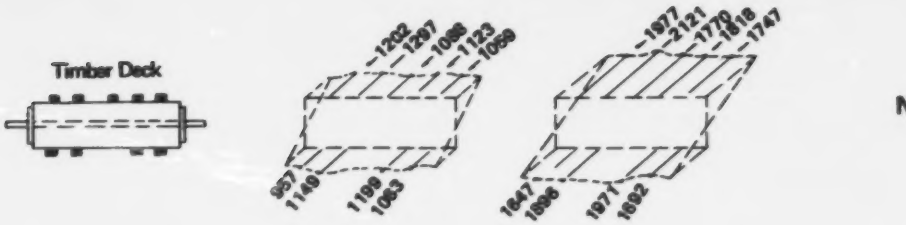		N/A
Steel–Wood Non Composite	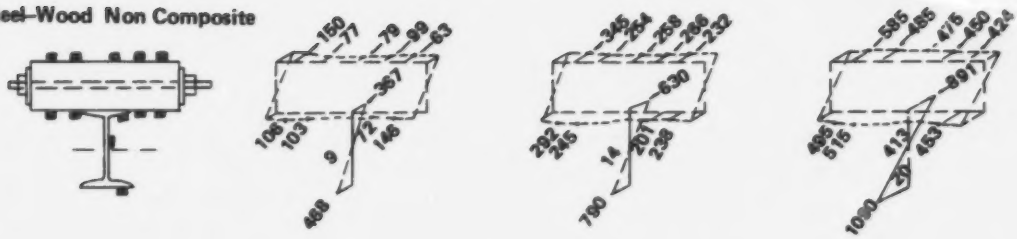		
Steel–Wood Composite	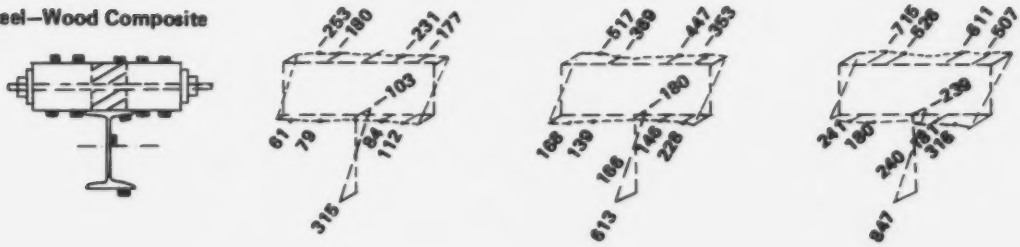		

■ – STRAIN GAUGE LOCATION (TYP.)

composite beam behaved much better than the non-composite beam or the steel girder alone. The stiffness of the composite beam compared to the steel girder increased by approximately 102% for a midspan deflection of 5 mm. This increase is about 23% smaller than that for the first system, however, the higher rigidity of the first beam is also due to the additional steel plate.

The slip curve for this composite girder is linear and there were no signs of sudden movements similar to that observed for the steel plate shear connection system. The maximum recorded slip under a load of 75 kN was approximately 0.4 mm and about twice that for the former system. The slip was, however, totally recoverable. It can be seen in Table 4.2 that the steel strains are much lower for the composite girder than those of the non-composite system or the steel girder alone. Comparing the deck strains between the non-composite girder and the composite girder, there is an increase in top fibre strains and a reduction in bottom fibre strains. The percentage reductions or increase in stress observed for the deck and steel girder under various loads are also given in Table 4.3. The development of composite action between the deck and steel girder can increase the deck top fibre compressive stress and reduce the deck bottom fibre stress, similar to that observed for this beam. However, the reductions observed in the deck stresses for the first beam are thought to be due partly to the additional rigidity offered by the welded steel plate.

A comparison of the load deflection curves for the two composite systems given in Figures 4.1 and 4.2 will readily show that the system with plate shear connector is stiffer than that with the bulk head connectors. However, these figures also show that an irreversible slip can take place in the former, thus casting a doubt on the integrity of the system for long term, heavy, repeated loads.

4.2/ Fatigue Tests

The two beams described in Section 4.1 were also tested under cyclic loading in which the maximum bottom flange stress was varied from 40 to 200 MPa at 1 Hz. After a certain number of cycles, each beam was tested under static loads to observe any loss of stiffness caused by the cyclic loading. The results from these static tests are given in Figure 4.3 for

Table 4.3/ Observed Stress Reductions

BEAM TYPE	APPLIED LOAD KN	STEEL TO COMPOSITE		NON COMPOSITE TO COMPOSITE			
		Steel, Top	Bot.	Deck, Top%	Bot.	Steel, Top	Bot.
Steel Plate Shear Connection	25	99	44	26	90	96	33
	50	99	50	41	95	99	34
	70	-	-	33	80	89	30
Concrete Bulk Head Shear Connection	25	81	41	-123	23	72	33
	50	81	40	-54	33	71	22
	70	-	-	-18	51	73	22

- ve ≡ an increase in stress

beams with the two shear connectors. It can be seen that in the beam with steel plate connection, there is no loss of stiffness even after 2 x 10^6 cycles of loading. However, after 2 million cycles hairline cracks extending over lengths of up to 35 mm were observed at the welds which connected the steel plate to girder flange. Views of this beam are shown in Figure 4.4.

In the second test, the shear connectors which were installed by manual welding failed in the manner shown in Figure 4.5. Since the beam with these connectors could not be tested under static loads before the failure occurred, the effect of cyclic loading on degradation of the composite beam stiffness could not be fully established.

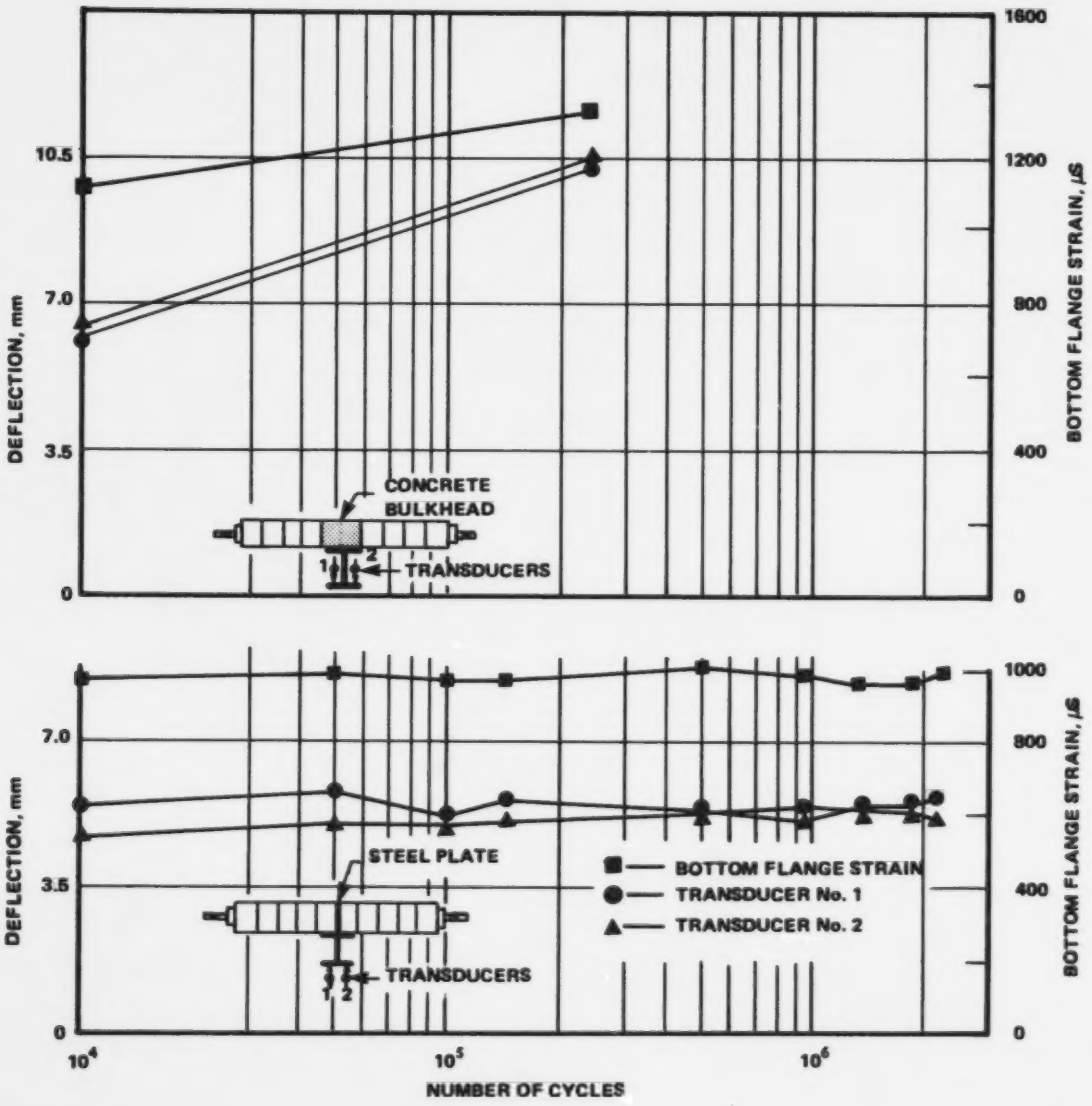

Figure 4.3/ Performance of Preliminary Test Beams under Cyclic Loads

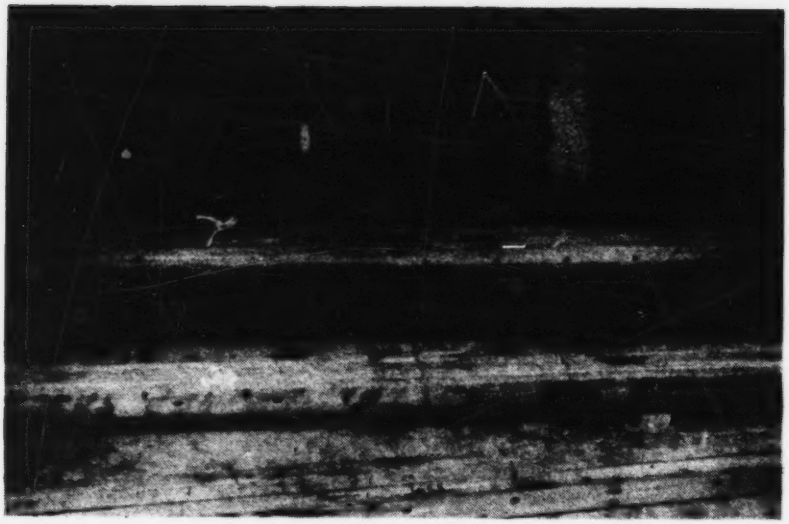

a) DISMANTLED BEAM

b) CRACKING OF THE SHEAR PLATE ADJACENT TO WELD LINE

Figure 4.4/ Cracking Observed on Shear Connector Plate after $2X10^6$ Cycles

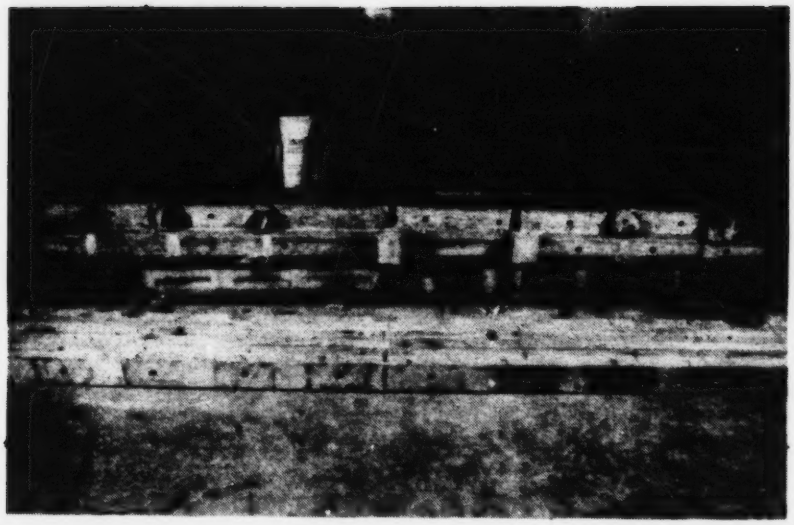

b) DISMANTLED BEAM

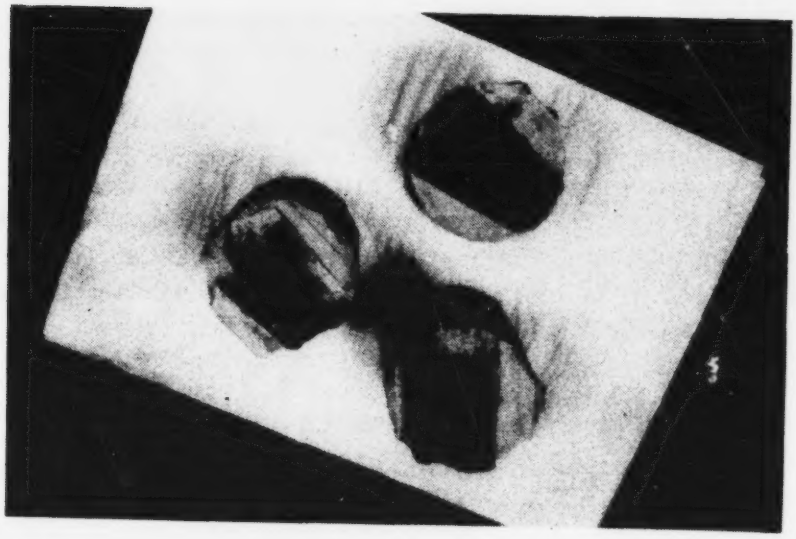

c) A VIEW ON FAILED BULKHEADS

Figure 4.5/ Fatigue Failure Observed on Concrete Bulkhead Shear Connector with Manually Arc Welded Shear Studs

5/ BULKHEAD SHEAR CONNECTOR

5.1/ Shear Strength

To establish the ultimate strength and the load-slip characteristics of the bulkhead shear connectors under direct shear loading, five specimens were tested under static loads. Details of the stud diameters, the type of welding and concrete bulkhead diameter used are given in Figure 3.5. The load deformation curves are plotted in Figure 5.1. All five load-slip curves are mostly similar. The deformation at the first yield point varied between 1 and 4 mm. After the initial yield, the failure load remained constant while the shear connector underwent considerable deformation. The load-slip curve generally took a down turn when the slip value reached approximately 15 mm. Typical shear connector failure mode observed during the static load test of the connectors is shown in Figure 5.2. The failure is generally caused by the failure of the weld or stud material just above the weld. The studs undergo considerable bending before the weld or studs break off.

To study the problem of shear lag in the deck, specimen No. 5 was extensively instrumented. The laminate stress distribution for this specimen is illustrated in Figure 5.3 for different loads. The deck consists of spruce laminates and an 'E' value of 12 500 MPa for this material, given in Figure 3.8, is used to convert strains to stress value. The stresses on the laminate directly under the bulkhead are always the maximum and the stress drops fairly rapidly as one moves away from the bulkhead. The peak stress, average stress and the ratio between these two stresses for various load levels are given in Table 5.1. The ratio varies between 0.30 and 0.62, however, it generally remains around the 0.50 mark. The average to peak ratio obtained can be useful in studying the behaviour of wood-steel composite beams and to establish a methodology to design wood-steel composite beams.

Similar to the case of studs cast in concrete deck, the strength of the bulkheads set in timber laminates can depend on the stud diameter, deck elastic modulus and laminate ultimate compressive strength. In addition, the shear strength of the bulkhead can depend on the bulkhead diameter. The number of tests performed is not large enough to correlate

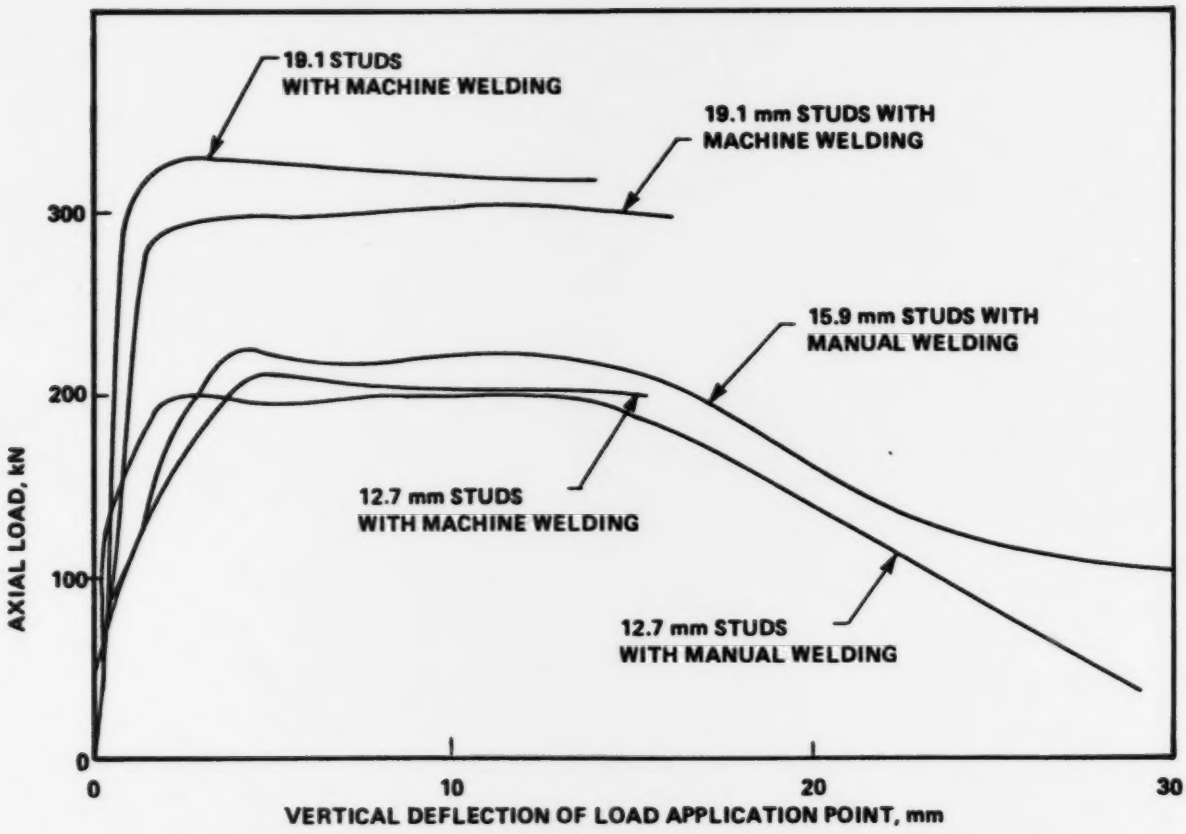

Figure 5.1/ Load Deformation Characteristics of Bulkhead Shear Connectors

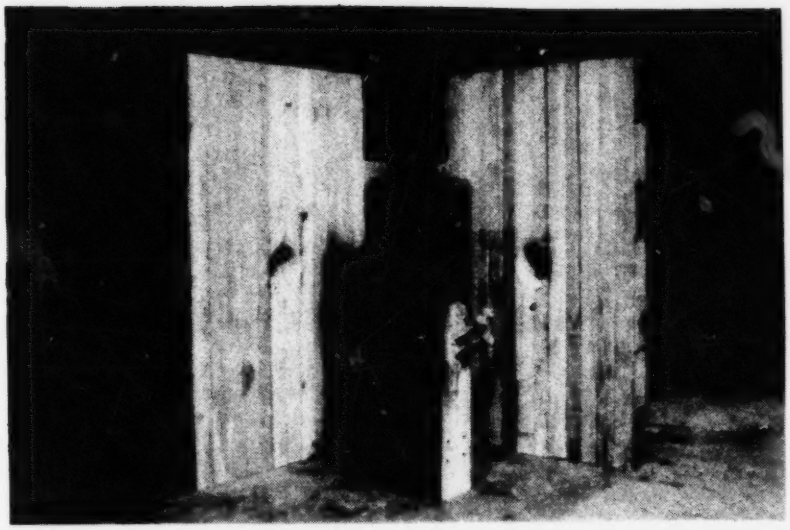

a)Dismantled Direct Shear Specimen

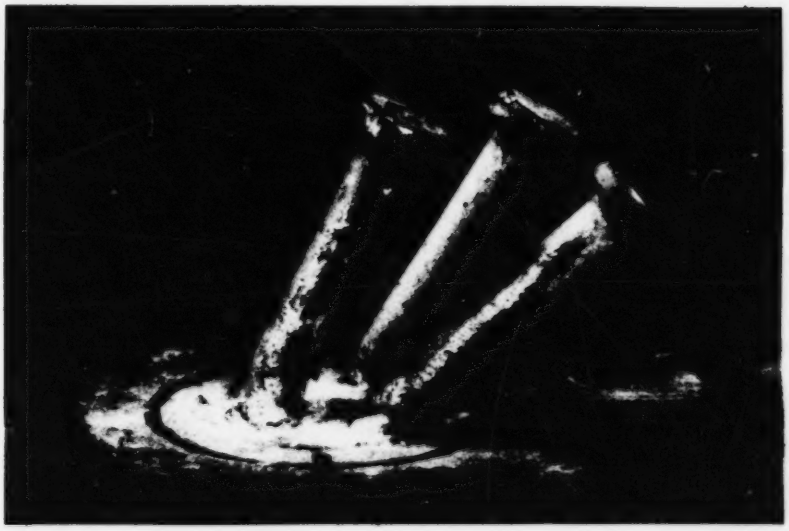

b) Studs After Failure

Figure 5.2/ Typical Shear Connector Failure Mode

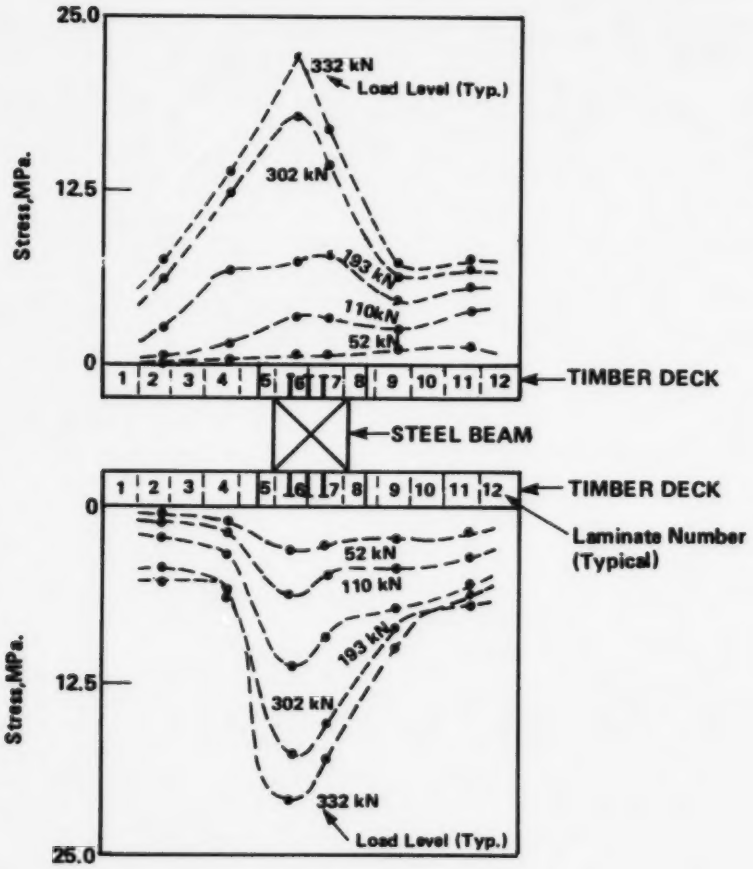

Figure 5.3/ Laminate Stress Distribution under Direct Shear Loads

Table 5.1/ Average and Peak Stresses in the Laminated Deck Under Direct Shear Load

LOAD, kN	DECK NUMBER	PEAK STRESS, MPa	AVERAGE STRESS, MPa	RATIO $\frac{\text{AVERAGE STRESS}}{\text{PEAK STRESS}}$	
52	1	1.25	0.38	0.30	
	2	3.75	1.76	0.47	
110	1	3.75	2.06	0.55	
	2	6.50	2.94	0.52	
193	1	7.75	4.86	0.62	
	2	11.50	6.04	0.53	
					0.50
302	1	17.75	9.40	0.53	
	2	17.75	8.76	0.49	
332	1	22.12	10.95	0.49	
	2	21.25	10.04	0.47	

the dependence of shear strength on each of the above parameters. All the direct shear test specimens were made of Jack Pine laminated deck except for the specimen No. 5, which was made of spruce laminates. The ultimate compressive strength and elastic modulus of the laminates were tested and found to be 42.8 MPa and 21400 MPa respectively for Jack Pine and 31.5 MPa and 12 500 MPa respectively for Spruce. If the bulkhead shear strength relationship is similar to that of the shear connectors in concrete decks, i.e., $Q_r = 0.4*d^2* f'_c*E_c$, then specimen No. 4 must have much greater shear strength than specimen No. 5. In fact, the reverse happened; ie., specimen No. 5 has 8% greater capacity than that of specimen No. 4. This increase is thought to be due to greater bulkhead diameter reducing the bearing stress and deformations in the laminates. These observations suggest that the bulkhead shear strength relationship is somewhat different to that established for the shear connectors in concrete deck.

The shear connector strength values related to the diameter of the studs are given in Figure 5.4(a). The limited number of test results shows a straight line relationship. The manual arc welded studs and the Nelson studs give approximately equal direct shear strength value for stud diameters closer to 12 mm. However, the strength of manually arc welded studs is lower than that of the Nelson studs as the diameter of the studs increased above 12 mm. For this reason, the results of manually arc welded studs and Nelson studs are treated separately. In the case of manually arc welded studs, the weld material is placed on the perimeter of the studs. For small diameter studs, the penetration of the weld provides a uniform weld to the shank, but for studs with larger diameters, the penetration can be insufficient to provide a uniform weld. The lack of penetration reduces the stud capacity. For Nelson studs, the weld is uniformly applied between the stud shank and beam flange as shown schematically in Figure 5.4(b). Additional tests are required to test the effects of various parameters affecting bulkhead shear strength.

The results of static load test after two specimens were subjected to different cycles of loading are summarized in Figure 5.5. The specimen which had studs attached using manual arc welding failed within 5.0×10^4 cycles and no deformation results are available. The next specimen, containing 12.5 mm diameter Nelson studs with 100 mm bulkhead, failed at

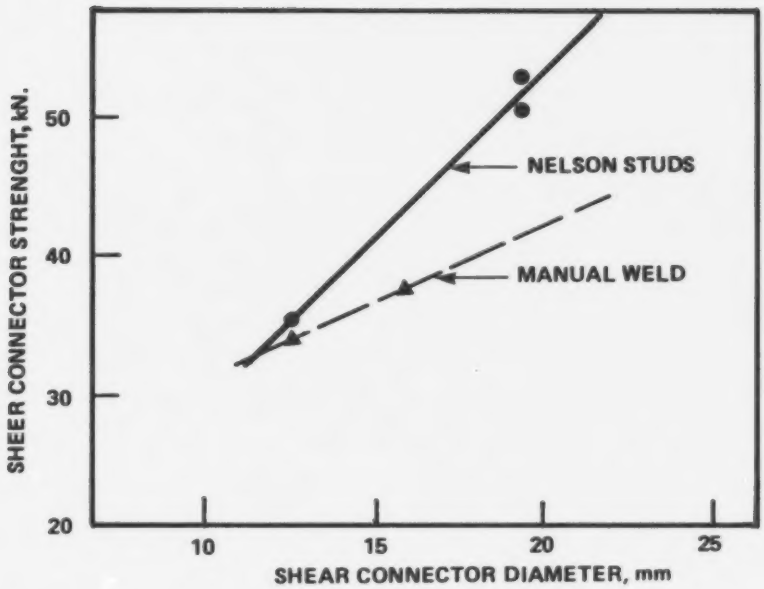

a) STUD SHEAR STRENGTH RELATED TO STUD DIAMETER AND TYPE OF WELD USED

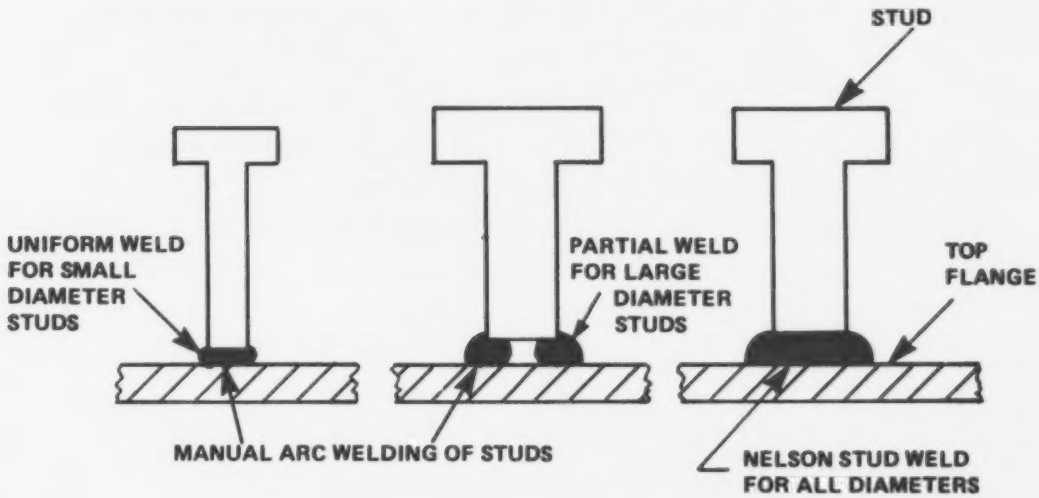
STUD
UNIFORM WELD FOR SMALL DIAMETER STUDS
PARTIAL WELD FOR LARGE DIAMETER STUDS
TOP FLANGE
MANUAL ARC WELDING OF STUDS
NELSON STUD WELD FOR ALL DIAMETERS

b) WELD UNIFORMITY AFFECTED BY THE TYPE OF WELD USED

Figure 5.4/ Stud Shear Strength Related to Stud Diameter and Type of Weld

approximately 1 x 10^6 cycles. The bulkheads remained intact and did not show any signs of cracking. The studs failed at the weld location (as shown in Figure 5.6) and did not show signs of local bending as was observed in the case of static load tests. The cyclic direct shear load applied was 89.2 kN which is about 43% of the ultimate strength obtained by direct shear tests. Cyclic loads allowed for the studs (i.e., using the stress range) for various class of bridges, as specified by OHBDC, are given in Table 5.2. As can be seen by the table, for the applied cyclic load, the above direct shear specimen is expected to sustain approximately 1 x 10^5 cycles (Clause C-2). The specimen was able to sustain 1 x 10^6 cycles, however, which is 10 times that required by the OHBDC. Clearly, a reduction in applied cyclic shear load would substantially increase the number of cycles sustained.

The specimen containing 19.05 mm studs and using 150 mm diameter bulkhead withstood 2 x 10^6 cycles without showing any signs of distress. The applied cyclic load was 102.6 kN which is, approximately 31% of the ultimate direct shear load. The applied shear load is about 25.0% over that required for Class 'A' bridges in Ontario and the specimen withstood 2 x 10^6 cycles without loss of stiffness and showing signs of distress.

The cyclic load tests was performed on the full scale direct shear specimen shown in Figure 3.6. The load was cycled between 111.0 kN and 9.0 kN. The results of the static tests performed on the specimens at regular intervals is given in Figure 5.6. The specimen underwent 2.04 x 10^6 cycles without any visible increase in the static deflection. The bulkhead did not exhibit visible cracking until the end of the test.

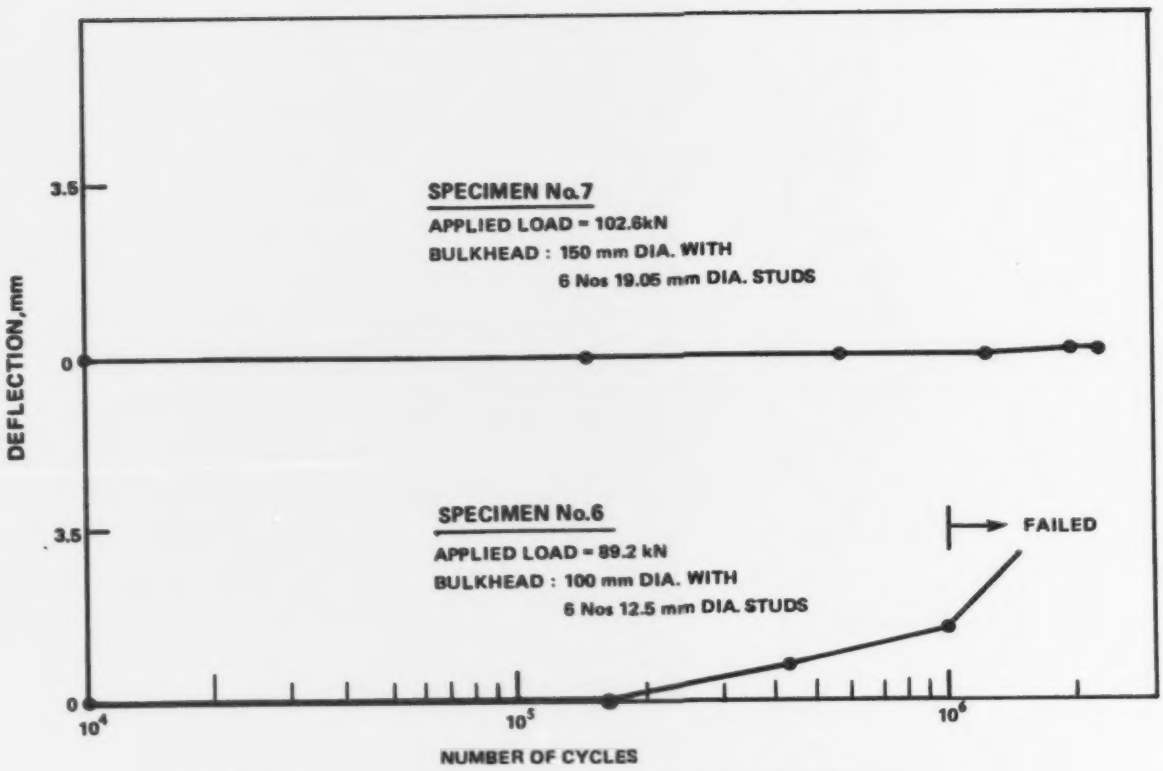

Figure 5.5/ Performance of Bulkheads Under Direct Shear Cyclic Loads

Table 5.2/ Fatigue Load Resistance of Bulkhead Shear Connectors as per OHBDC

Bolt Diameter, mm	Fatigue Load Capacity of Direct Shear Specimens (as per OHBDC), kN			
	Class C-2 for 100 000	Class C-1 for 500 000	Class B for 2 000 000	Class A over 2 000 000
12.5	84.6	62.5	47.8	35.3
19.1	196.6	145.3	111.1	82.0

Figure 5.6/ Stud Failure Mode due to Cyclic Loading

6/ COMPOSITE BEAMS

6.1/ Load-Deformation Characteristics

Two beams were tested to study the ultimate load and the load-deformation characteristics of wood-steel composite beam. In the first beam (identified as Beam UL1) shear buckling of web at the end supports was observed at a high load level which caused a marginally premature failure. A view of the failed beam is shown in Figure 6.1(a). In order to avoid such failure mode, shear stiffeners were welded to the second beam which is identified as Beam UL2. As can be seen in Figure 6.1(b), the web stiffening eliminated the shear buckling failure mode observed in the first beam.

The load-deflection curves of the two beams at midspan tested are shown in Figure 6.2(a). These curves appear generally bi-linear with the initial gradient remaining constant until the deflection reaches approximately 15 mm. The gradient, then, reduces considerably but remains more or less constant until the deflection reaches approximately 75 mm and the beam fails. Although Beam UL2 carried higher moments than Beam UL1, the load-deformation graphs are not appreciably different. This is so because the loading arm used in each of the test was different. In order to illustrate the difference in the moment capacities of the two beams, the applied midspan moment is shown related to midspan deflections in Figure 6.2(b). Initially, both beams show nearly equal stiffness yet the failure moment capacity of Beam UL2 is about 28% more than that of Beam UL1.

Decks under direct shear tests gave a peak-to-average stress ratio of 0.50 up to failure loads, indicating that only 50% of the deck width is effective in compression. The beam deflections obtained with 50 and 90% effective deck width are also shown in Figure 6.2(a). Although Beam UL1 is designed as a partially composite beam, for deflection calculations it is assumed to be fully composite (similar to Beam UL2). Clearly, within the elastic limits of the composite beam, the use of 50% deck area gives a reasonably accurate estimation of beam stiffness. For serviceability limit states, it seems reasonable to use 50% of the effective deck area in the calculation of beam stiffness.

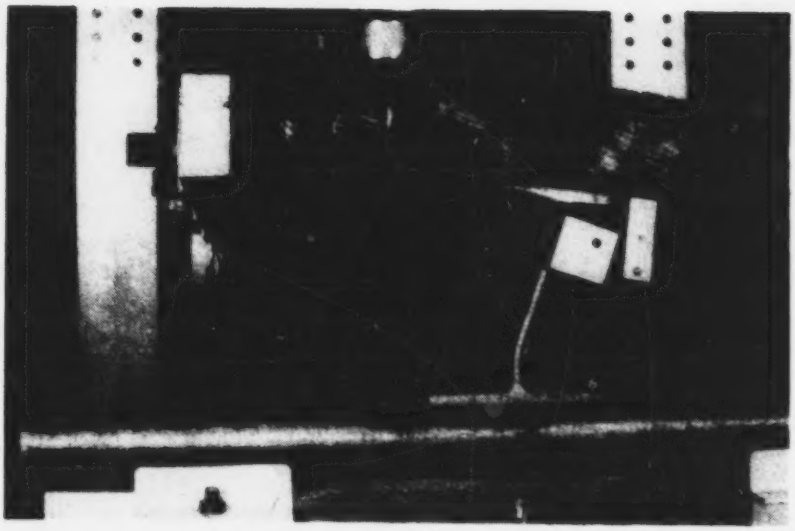

a) Failure of Beam UL1

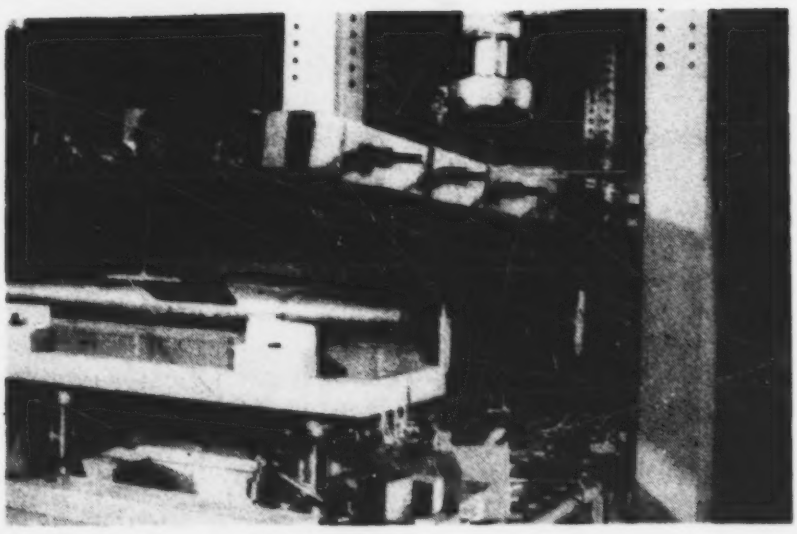

b) Failure of Beam UL2

Figure 6.1/ View of the Beam Failure Modes

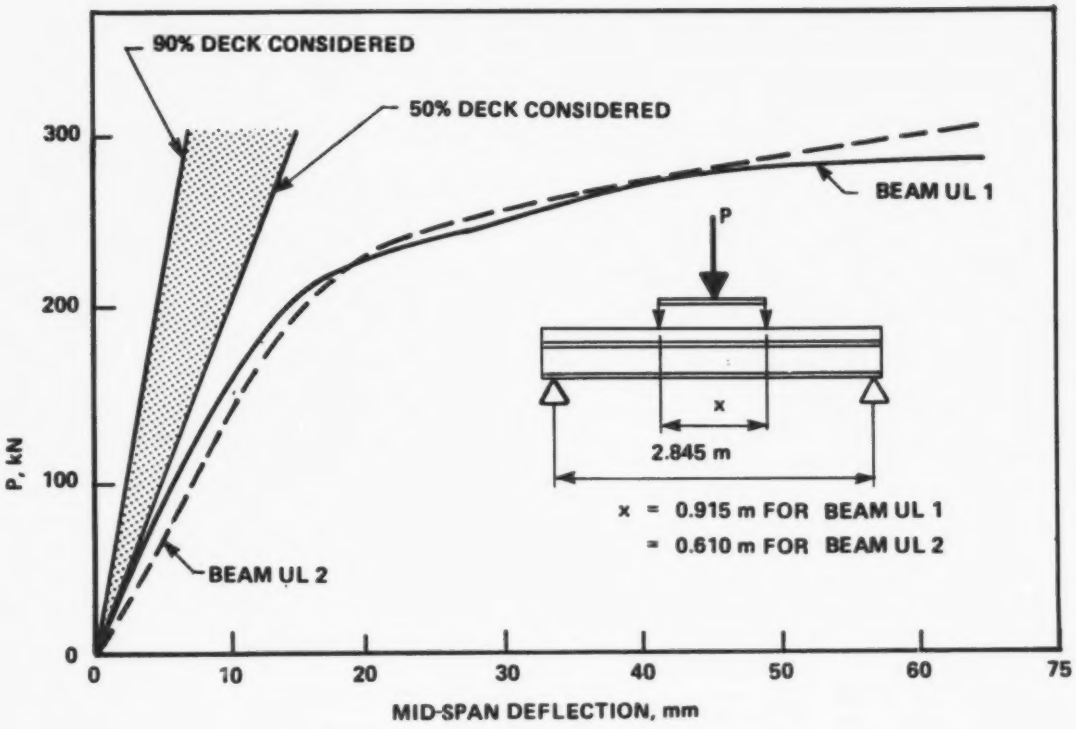

a) Applied Load Related to Mid-span Deflection

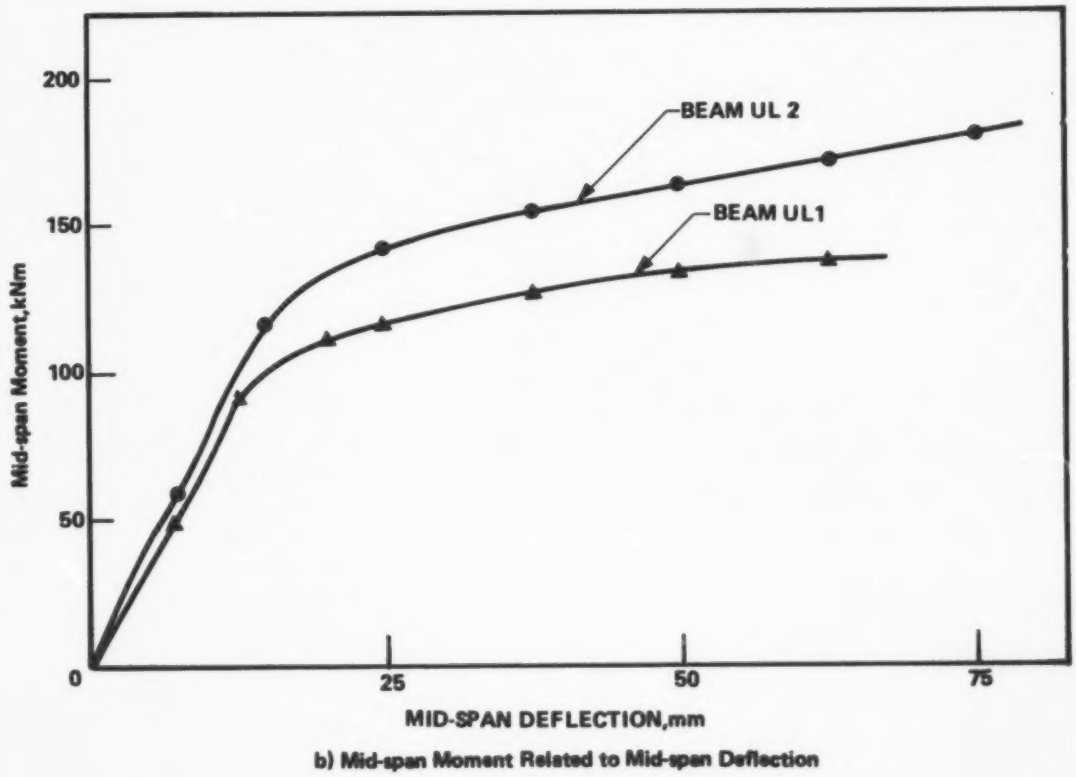

b) Mid-span Moment Related to Mid-span Deflection

Figure 6.2/ Load Deformation Characteristics of Beam UL1 and UL2

oth the beams are identical except for the strength of shear connection provided in each of them. Beam UL1 had four 100 m diameter bulkhead with three 12.5 mm diameter Nelson studs per bulkhead between the centre span and the beam end, while Beam UL2 had four bulkheads with four 22.2 mm diameter Nelson studs per bulkhead. The total direct shear strength capacity of the bulkheads between the centre span and the end for Beam UL1 is approximately 312 kN and that of Beam UL2 is approximately 1408 kN. The deck is initially considered to have direct compressive strength of approximately 1500 kN. Therefore, Beam UL1 was designed to fail by failure of shear studs and Beam UL2 by the deck failure. It should be noted that spruce-pine laminates used for the deck were later found to have a compressive strength of 31.5 MPa, as shown in Figure 3.8, and hence, the deck is capable of sustaining 2362 kN axial compressive load. If allowance is made for the shear lag within laminated decks, the deck capacity can be approximated to 1180 kN (50% of 2360 kN). This indicates that the failure mode assumed in the initial design of Beam UL1 and Beam UL2 remains unaffected.

The bulkheads remained in very good condition after Beam UL1 had failed. Careful breaking of the mortar cover showed that the studs had not undergone any noticeable deformation as shown in Figure 6.3. The Beam UL2, which in any case was not expected to fail by shear connector failure, also showed that the bulkhead and the studs remained unaffected by the beam failure. These observations confirm that the actual force induced by the deck is generally lower than that calculated theoretically.

The above phenomenon was also observed by several researchers who studied the behaviour of steel-concrete composite beams. Although it is difficult to measure the load carried by the shear connector in a composite beam, Slutter [9] measured indirectly the forces induced on the shear connectors in composite beams and concluded that the strength of shear connectors in beams are generally higher than the strength of shear connectors in pushout specimens. Also, the shear connector experiences lower loads in a beam than was theoretically evaluated. King [10] also observed that the stud stresses obtained theoretically are about 25% greater than the actual stress induced and remarked that the difference can be much greater in most practical cases. Therefore, it can be concluded that the shear connectors of the test beams remained unaffected by the beam failure, especially for Beam UL1, due to the fact that the

a) View of Shear Connector in Beam UL1 After Beam Failure

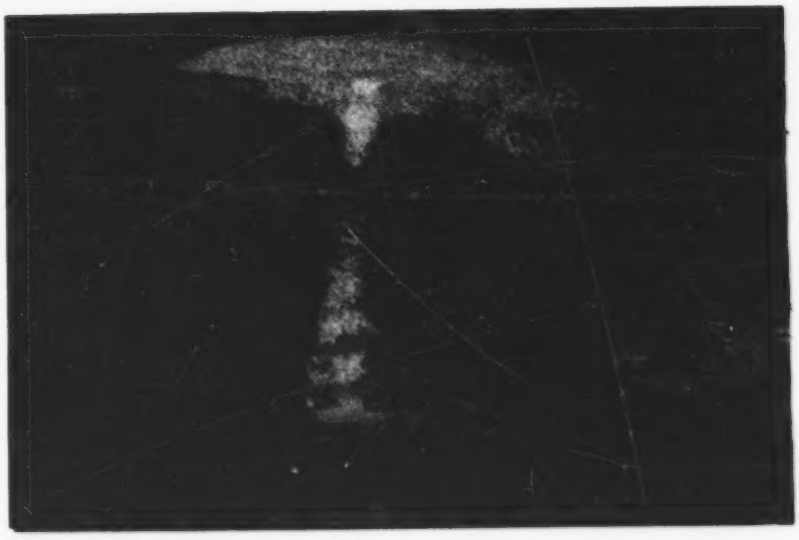

b) View of Shear Connector in Beam UL2 After Beam Failure

NOTE; In both Cases the Bulkhead Was Intact after Failure, but Was Broken by a Hammer to Exhibit the Condition of the Shear Connectors.

Figure 6.3/ Condition of Shear Connectors After Beam Failure

theoretically estimated force on the shear connector is much lower than calculated.

McGarraugh [11] studied the load-midspan deflection characteristics of light weight concrete deck/steel girder composite beams for various levels of shear connection strength. The results of these tests showed that the initial gradients are only marginally affected by the level of shear connection resistance provided. The difference between the ultimate strength of the beam having 34 and 100% shear connection was approximately 20%. Chapman [12] tested a series of beams with normal concrete and varying total shear connector capacity between 36% and 131% of the deck strength. The observed difference between the ultimate strengths was approximately 22% and the initial gradient remained unaffected by the level of shear connector strength. The present test results and the above observations lead to the following conclusions:

1) the stud shear connectors in the composite beam does not experience the theoretically estimated shear loads;
2) the initial gradient of the load-midspan deflection curve is marginally affected by the level of shear connection resistance provided between the steel girder and the timber deck;
3) the ultimate strength of steel-wood composite beam is increased by approximately 28% for an increase in shear connection capacity from 26 to 119%; i.e., the beam capacity increase at a much lower rate compared to that of the shear connection capacity.
4) Published data obtained from tests using normal or light-weight concrete-steel girder composite beams indicated almost similar characteristics.

6.2/ Load-Slip Characteristics

The slip between the deck and the steel girder measured at various locations on the beams are given related to applied loads in Figure 6.5 for various load levels. The slip at the ends of the girders is

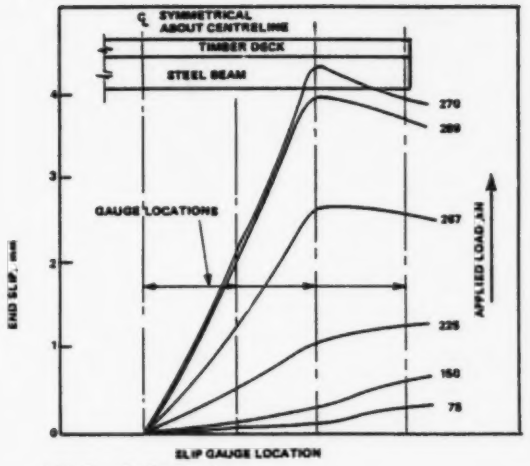

1) Slip Curve for Beam UL1

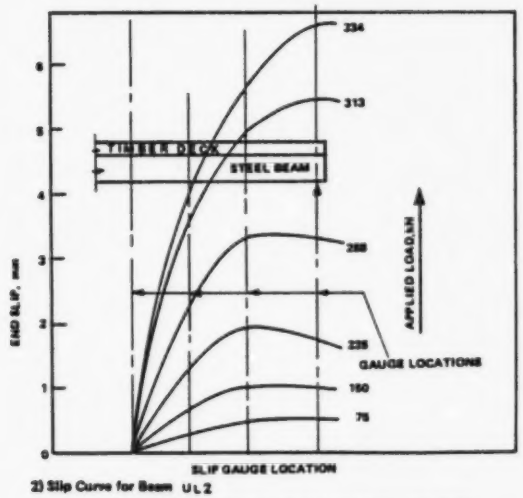

2) Slip Curve for Beam UL2

a) Slip Curves Obtained for Steel–Wood Composite Beams

Figure 6.5/ Load-Slip Characteristics

generally greater than the slip at the interior locations for lower applied loads. After about 70% of the ultimate load was applied, the shape of the slip curve changed rapidly and the slips were generally maximum near the centre of the shear span. Chapman [12] reported the load-slip characteristics of concrete-steel composite girders. In general, the load-slip behaviour of timber-steel composite beam is similar to concrete-steel composite beam; however, the slip measured for the timber-steel composite beam is substantially higher (approximately 6.5 mm for a half beam length of 1.5 m) than the slips measured for the concrete steel-composite beams (approximately 1.5 mm for a half beam length of 3.05 m).

6.3/ Stress Distribution

Strains measured on the deck and the steel girder at the centre span under various loads are given in Table 6.1(a). The corresponding stress values are given in Table 6.1(b). The appropriate stress-strain curves obtained for the deck laminates and steel girders in Chapter 3 were used to convert the strains to stress values. As evident from the tables, for Beam UL1, the bottom fibres of the deck in the middle portion are under compression until the load exceeds 225 kN. The bottom fibres of Beam UL2 is, however, in tension throughout. As expected, the top of deck for both the beams are in compression throughout. Another feature to note is that the deck stress and strains are generally convexed at the centreline, indicating that the laminates bearing directly against the bulkhead undergo greater deformations than the laminates away from the bulkheads. Direct shear tests showed similar but more pronounced convexity. However, for the beam, the convexity is more evident at the bottom of the deck than the top.

The stress diagrams given in Table 6.1(b) were used to obtain the moment resisted by the section and this is compared against the actual moment applied on the beam in Table 6.2. A computer program was developed to calculate these moments from the stress diagrams and is explained in Appendix B. As evident from the table, the moment values obtained from measured strains compare well with the actual applied moments.

Table 6.1a/ Strains Measured at Various Applied Load Levels

APPLIED LOAD, kN	MEASURED STRAIN, μS	
	BEAM UL 1	BEAM UL2
75 (16.8)	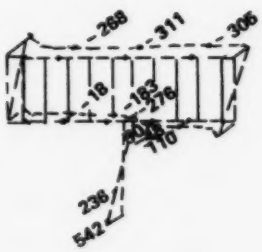	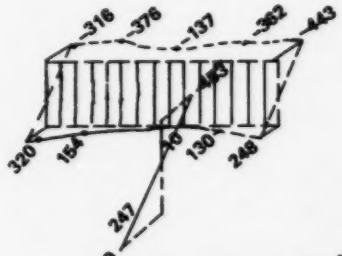
150 (33.6)	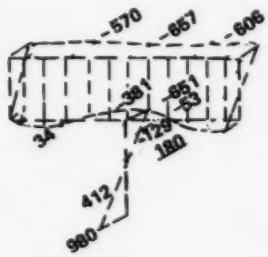	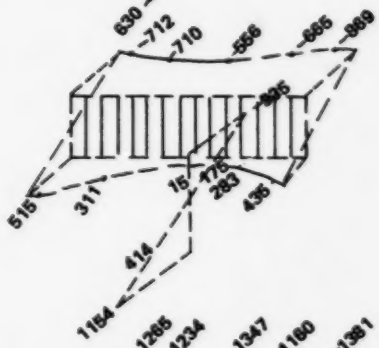
225 (50.4)	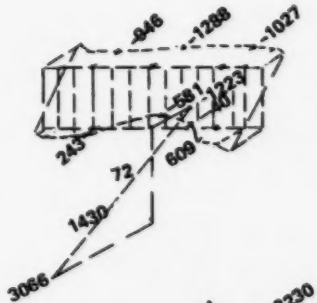	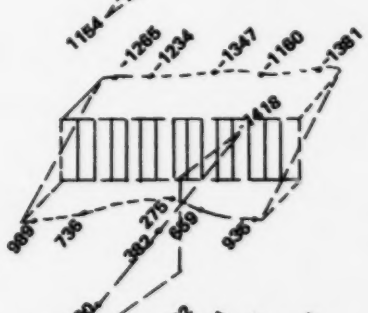
ULTIMATE LOAD	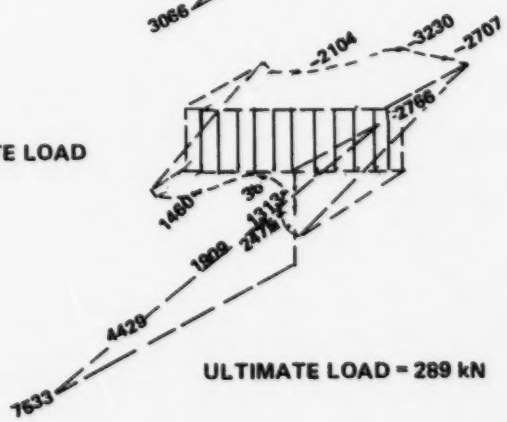 ULTIMATE LOAD = 289 kN	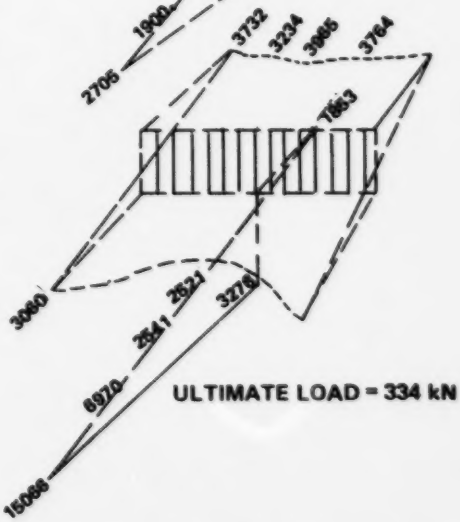 ULTIMATE LOAD = 334 kN

( ) Load in kips.

Table 6.1b/ Stress Measured at Various Applied Load Levels

APPLIED LOAD,kN	MEASURED STRESS, MPa	
	BEAM UL1	BEAM UL2
75 (16.8)	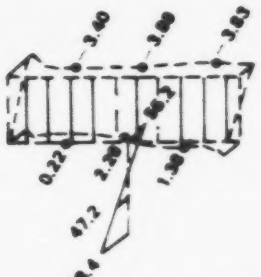	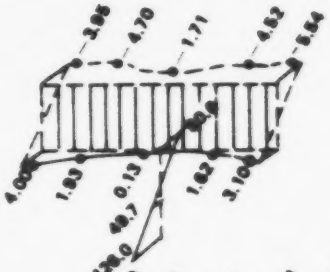
150 (33.6)	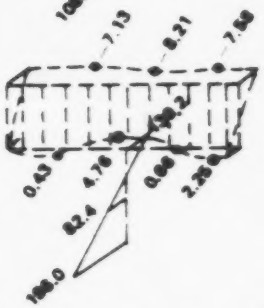	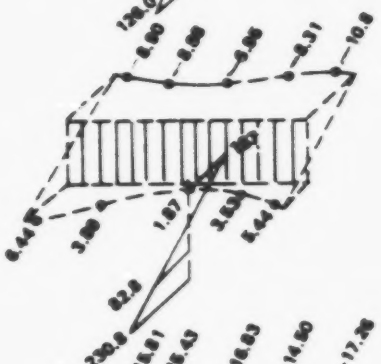
225 (50.4)	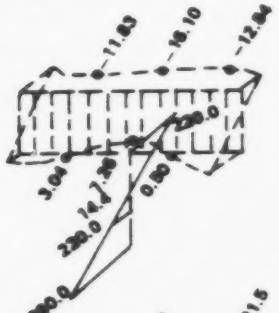	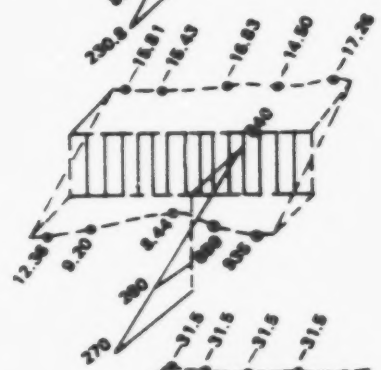
ULTIMATE LOAD	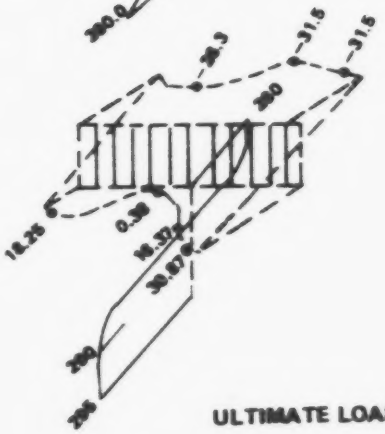 ULTIMATE LOAD 298 kN	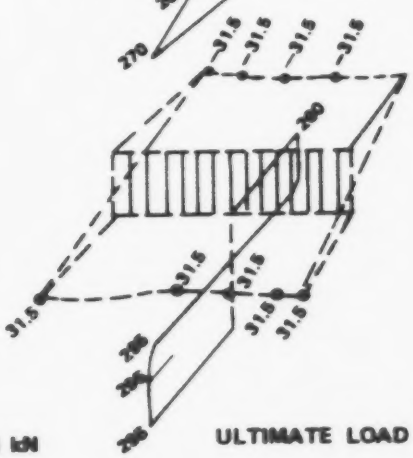 ULTIMATE LOAD 334 kN

( ) Load in kips.

Table 6.2/ Comparison of Actual Moment to that Calculated Using the Strain Measurements

APPLIED LOAD, kN	Moment, kNm,	BEAM UL1		BEAM UL2	
		Actual	Calculated	Actual	Calculated
75.0		36.0	31.1	43.0	32.8
150.0		72.3	60.1	86.0	64.2
225.0		108.5	117.2	129.0	118.1
Ultimate load Beam UL1 = 289.0 Beam UL2 = 334.0		139.4	143.2	191.0	168.0

6.4/ Ultimate Strength

The ultimate load tests were performed on timber-steel composite beams to understand a load-deformation characteristics of these beams and to establish a procedure to design such beams. Undoubtedly, a design method for these composite beams cannot be established with just two beam tests. Since the composite beam behaviour is shown to be mostly similar to concrete steel composite, it is thought that the design procedure in use for concrete-steel composite beams could be used to calculate the ultimate moment capacity of timber-steel composite beams.

The theory originally proposed in Reference 9 and generally used in the OHBDC is considered accurate for predicting closely the actual moment of resistance of concrete-steel composite beams. In this approach, the ultimate compressive strength of concrete deck and the ultimate shear connection capacity of the shear connectors provided are calculated and the least of the two values is taken to calculate the section plastic neutral axis and the corresponding ultimate moment of resistance. Similar methods are adopted except for timber-steel composite beams. Two additional assumptions are made and these are as follows:

1/ Only 50% of the laminated timber deck capacity is considered to be effective in compression; and
2/ the shear connector capacity in laminated timber deck is equal to 50% of that obtained by direct shear tests.

The first assumption is made to account for the stress distribution observed on the laminated decks under direct shear tests. The tests showed that only 50% of the laminated deck width used can be considered effective in compression. Also, the use of 50% deck width gave theoretical beam stiffness much closer to the actual. The second assumption is made to account for the condition of the shear connectors observed after the failure test of the two beams (see Section 6.1). The shear connectors did not show visible signs of experiencing the full deck compressive load (i.e., 50% of the deck compressive strength) when the beams (Beam UL1 and Beam U12) failed. It is most surprising that Beam UL1, which had a shear connection capacity of 312 kN and a deck capacity

of 1180 kN (0.5 x 2362) did not fail by shear connector failure. In fact, the shear connectors did not show any visible deformation after beam failure (see Figure 6.3). Consequently, it was confirmed earlier that shear connector experiences much less shear load than theoretically evaluated. A 50% reduction in the shear connection capacity is considered adequate to allow for the above observed effect. Although 50% shear connection capacity is used for ultimate beam strength calculations, it is not recommended to physically reduce the number of connectors used in a composite beam.

The ultimate moment capacity of the two beams, Beam UL1 and Beam UL2, calculated using the proposed method is given in Table 6.3. Estimated moment capacity is less than actual moment value and about 79 and 94% of the actual value for Beam UL1 and Beam UL2 respectively. This is a conservative estimate and until further test data are gathered, the above method can be used to calculate the moment of resistance capacity of timber-steel composite beams.

6.5/ Fatigue Tests

The results of the cyclic load test performed in the composite beam fabricated with those used for ultimate load tests (shown in Figure 3.7) are given in Figure 6.6. This beam had shear connections of ultimate direct shear capacity of 780 kN (approximately). The specimen underwent 2×10^6 cycles without loss of stiffness or increase in the bottom flange strains. However, the bulkhead began to crack when the number of cycles reached approximately 100 000 cycles. The crack propagation observed on each of the bulkheads is also illustrated in Figure 6.6. The innermost bulkhead was the first one to crack while the outermost bulkhead remained uncracked until the end of 2×10^6 cycles.

The bulkheads are compressed on either side parallel to laminate direction as shown in Figure 6.6. At the centre span, the compressive force is a maximum while this force reduces parabolically to zero towards the ends. Therefore, for the innermost bulkheads, the compressive force induced is a maximum and the shear load is a minimum, while for the outermost bulkhead, the compressive force induced is a minimum and the

Table 6.3/ Comparison Between the Actual and Theoretical Moment of Resistance Values

Beam Type	% Shear Connection	Moment of Resistance, kNm		Ratio
		Test	Theory	
Beam UL1	26	140.0	110.0	0.79
Beam UL2	119	180.0	169.3	0.94

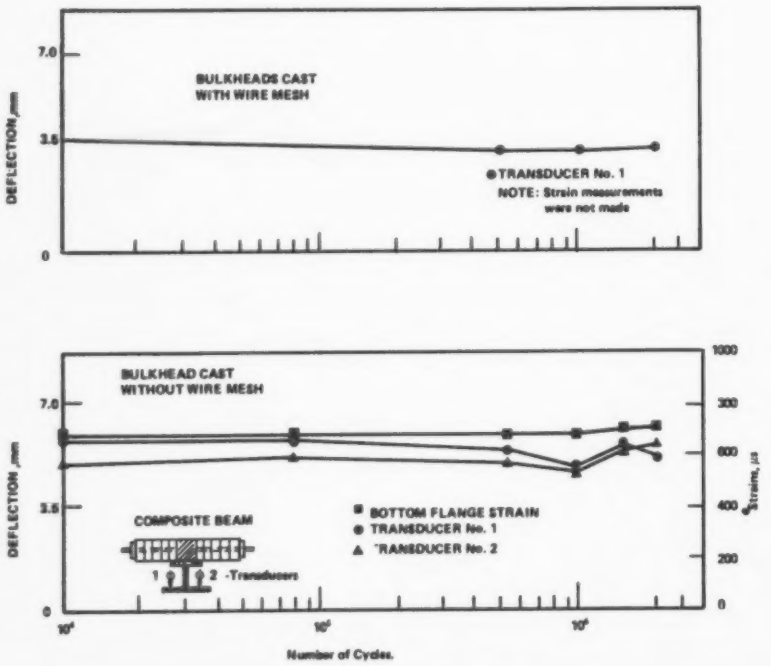

BULKHEAD CRACKING OBSERVED AT VARIOUS CYCLES

No. OF CYCLES		COMMENTS
100 000	———	Hair line cracks
500 000	———	Crack widened and additional cracks formed
1 000 000	– – – –	– DO –
2 000 000	·····.····	Considerable movement within the bulkhead along the cracked lines was observed. This movement was highly pronounced for the bulkheads closer to mid-span.

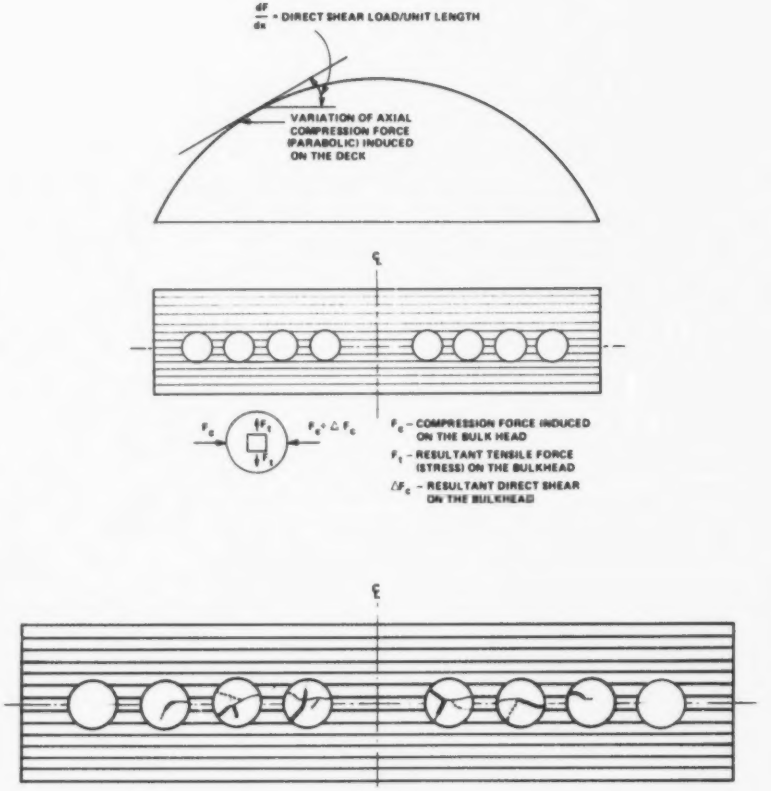
dF/dx = DIRECT SHEAR LOAD/UNIT LENGTH
VARIATION OF AXIAL COMPRESSION FORCE (PARABOLIC) INDUCED ON THE DECK
F_c – COMPRESSION FORCE INDUCED ON THE BULK HEAD
F_t – RESULTANT TENSILE FORCE (STRESS) ON THE BULKHEAD
ΔF_c – RESULTANT DIRECT SHEAR ON THE BULKHEAD

BULKHEAD CRACKING AT VARIOUS CYCLES

Figure 6.6/ Results of Cyclic Load Tests Performed on Composite Beam

shear load is a maximum. Equal and opposite compressive force on the bulkhead induces the tensile stresses along the axis perpendicular to the laminate axis; when it exceeds the allowable stress, cracks develop in the bulkheads. The innermost bulkhead cracks first because the tensile stresses induced on the bulkheads depends on the magnitude of compressive force and not on the magnitude of the direct shear load. Cracking of bulkheads was not encountered when both Beam UL1 and Beam UL2 were tested under static load where the tensile stresses induced on the bulkheads can be substantially higher. Although the tensile stresses in the bulkhead under cyclic loading can be substantially less than the tensile stresses experienced by the bulkheads under static failure tests, the cyclic loading appears to reduce the tensile strength of the mortar, culminating in bulkhead cracking. The dismantled beam with the cracked bulkheads is shown in Figure 6.7. One of the bulkheads has cracked up in such a way that, unless it is confined within the timber laminates, the bulkhead will not be able to sustain shear loads. However, there was no visible reduction in stiffness observed from the deflection and strain measurements. It is possible that the shear load was redistributed among the other undamaged bulkheads.

Although the beam did not show reduction in strength characteristics until 2×10^6 cycles, the cracking of the bulkhead is considered unacceptable. Ways of improving the bulkhead fatigue tensile strength was considered. The use of wire mesh in layers distributed across the depth of the bulkhead was considered as a workable option. The dismantled beam was assembled again and cast with new bulkheads. The results of the cyclic load test performed on this beam specimen is also given in Figure 6.6 as evidence that the the beam deflection remained constant until another 2×10^6 cycles. No cracking was observed in any of the bulkheads, suggesting that the use of wire mesh improved the fatigue tensile strength of the bulkhead to the required level. It is worth noting that the shear connection and the beam elements underwent 4×10^6 cycles in total without any sign of distress. The present test, however, confirms that the bulkhead, suitably reinforced, is able to sustain cyclic loads experienced by bridge beams.

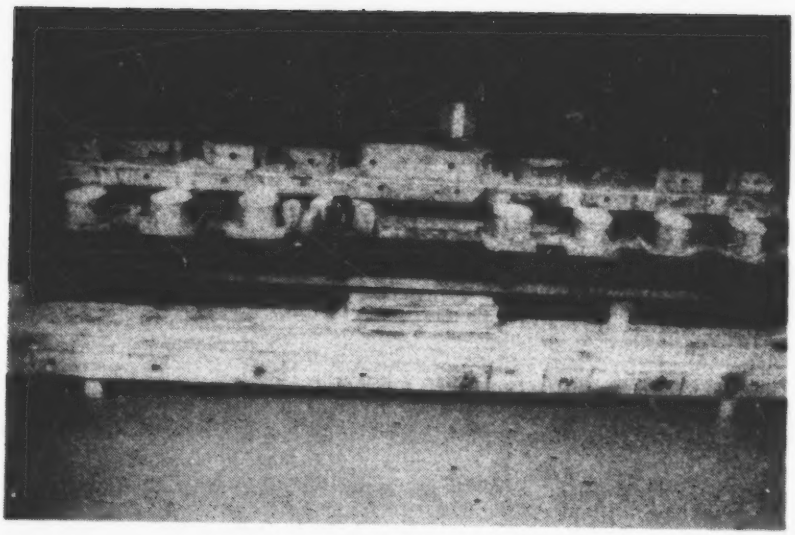

Figure 6.7/ Bulkhead Cracking due to Cyclic Loading

7/ COMPOSITE BRIDGE

The test results obtained by a series of static tests performed on the half scale bridge before and after introducing the composite action is discussed in this section. However, initially the timber deck fabricated for this bridge was tested using patch or line loads for unstressed and stressed condition of the deck and the results of the tests are also discussed.

7.1/ Timber Deck

The deck deflection and strains observed under patch (two sizes) and the line loads are given in Figure 7.1. By prestressing, the deck deflection and strains are reduced, by 25 to 9% respectively, under patch loads. Earlier tests performed by Taylor [3] on Hebert Creek Bridge gave about 40 and 12% reductions in deflection and strains respectively under dual axle load weighing 371 kN. The lower percentage reduction obtained presently may be due to the fact that, unlike Hebert Creek Bridge, the this deck was not exposed to deleterious conditions of weather and traffic loads. Hebert Creek Bridge was indeed considerably deteriorated before MTC upgraded the bridge by the post-tensioning technique. The line load deflections and strains are little affected by the deck stressing. Unlike patch loads, the line load forces all the laminates to participate in resisting the applied loads; therefore the deck deflections are not affected by the application of prestressing. As expected, the deck deflections and strains under line loads are generally lower than that under patch loads. Figure 7.1(b) shows the deck deflections and strains due to patch load positioned at various transverse locations of the deck. Edge loading gives rise to greater deck deflections and strains. The use of a larger sized loading pad reduces the deck deflections and strains, the greatest reduction being at the centre of the pad.

7.2/ Steel-Wood Model Bridge

The steel-wood model bridge was tested before and after introducing composite action to evaluate the effects of composite action under various types of loading. The bridge was tested using wheel, axle and

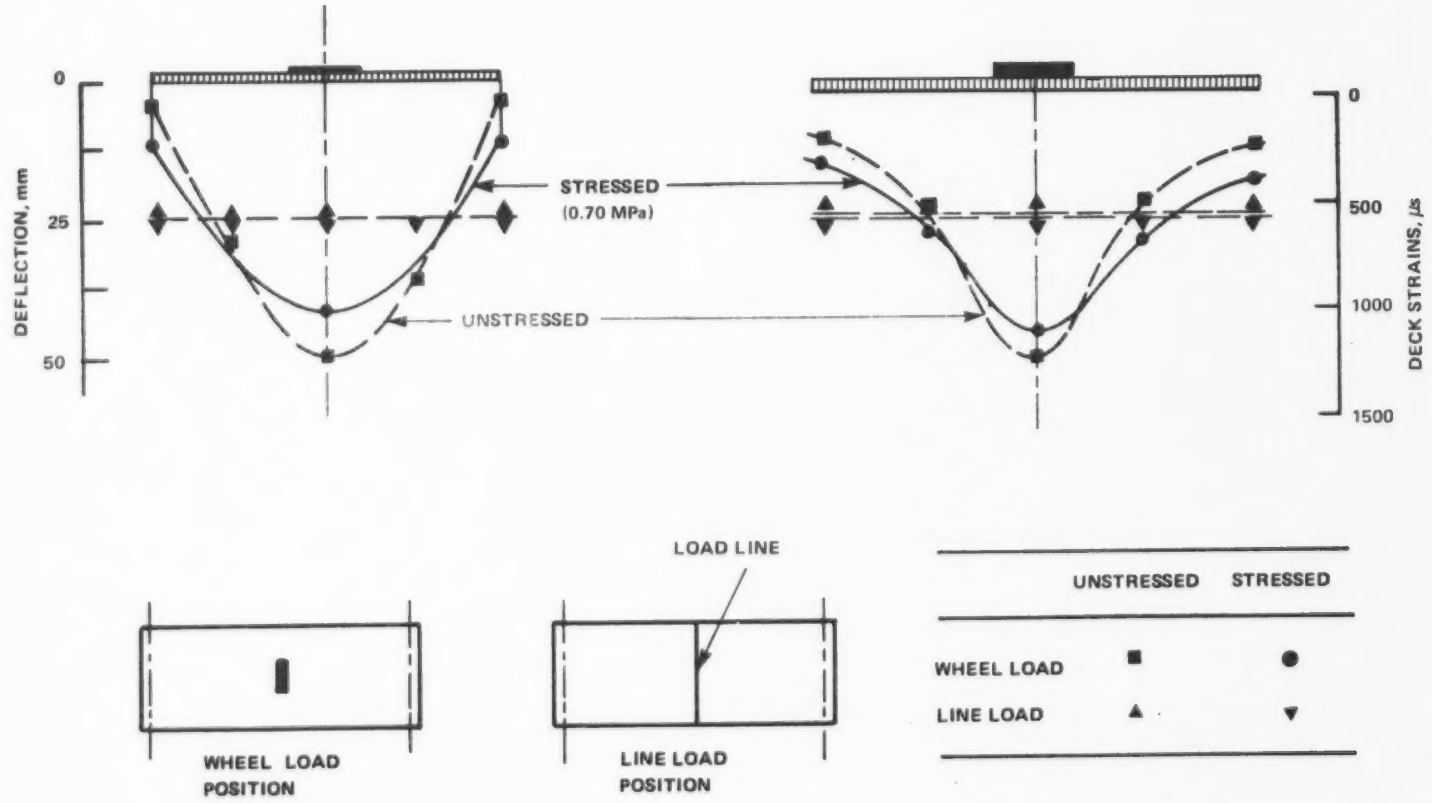

Figure 7.1a/ Effects of Wheel and Line Loads on Unstressed and Stressed Laminated Wood Deck

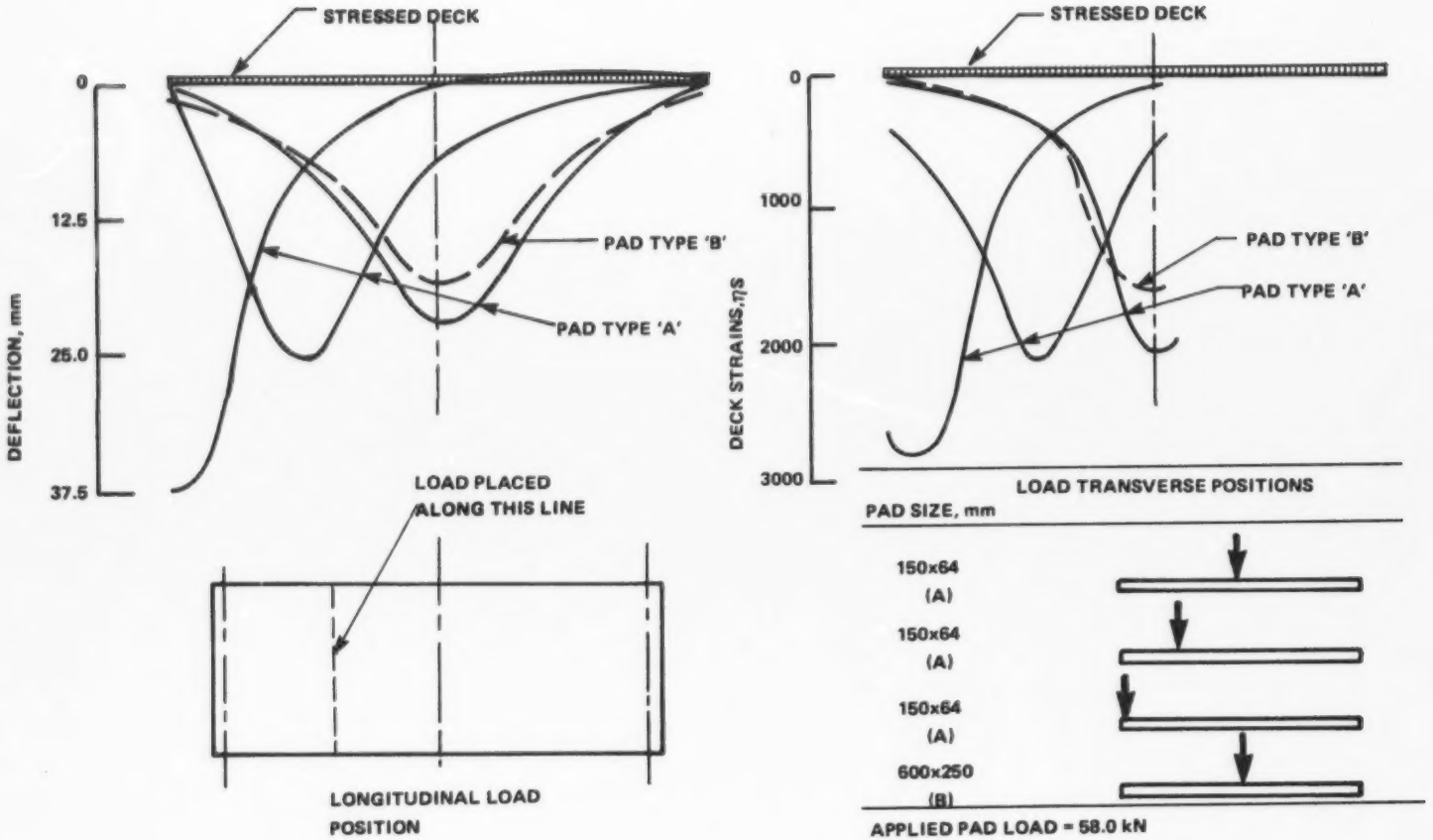

Figure 7.1b/ Effect of Pad Size on Deck Deflections and Strains

dual axle loads at various locations and the deck and girder responses were recorded. Typical bridge deflections observed for selected loading conditions are shown in Figures 7.2(a),(b) and (c). The development of composite action generally increases the rigidity of the bridge which, in turn, reduces the deck deflection. The reduction in bridge deflection is observed to be greater for axle and dual axle type loads than for the wheel loads. The deck and steel girder strains were measured for all the loading cases and Figure 7.3 shows a typical strain diagram obtained under dual axle-type loads. The strains at the top and the bottom of the deck and the steel girder are reduced by the composite action between the timber deck and steel girder.

The bridge tested is a half scale model. The performance of the full scale bridge under serviceability and ultimate limit state loads defined by OHBDC is equivalent to the performance of the model under one quarter of OHBDC loads. The bridge deflections, and the deck and girder strains under serviceability and ultimate loads of wheel, axle and dual axle type are given in Figures 7.4(a) through (f). As observed earlier, the bridge deflections, deck and girder strains are generally reduced by the composite action. The average reductions corresponding to midspan loads are given in Table 7.1. The observed reductions are 29 to 37% for deck deflections, 40 to 67% for girder top flange stresses, 12 to 20% for girder bottom flange stresses, 15 to 34% for the strains of deck top fibre, and 12 to 53% for the strains at the bottom of the deck. Under the equivalent ultimate loads, the deck and the steel girder strains are well within the elastic limits of approximately 1500 μs for the steel used and approximately 2000 μs for the Jack Pine laminates used for the deck. The tests conducted by applying equivalent serviceability and ultimate loads prove conclusively the advantage of using composite action between the timber deck and steel girders.

7.3/ Grillage Analysis

Evaluation of member forces and deformations of a bridge structure using grillage analogy is fairly accurate, simple to use and requires very little computer processing time. It was decided to compare the observed

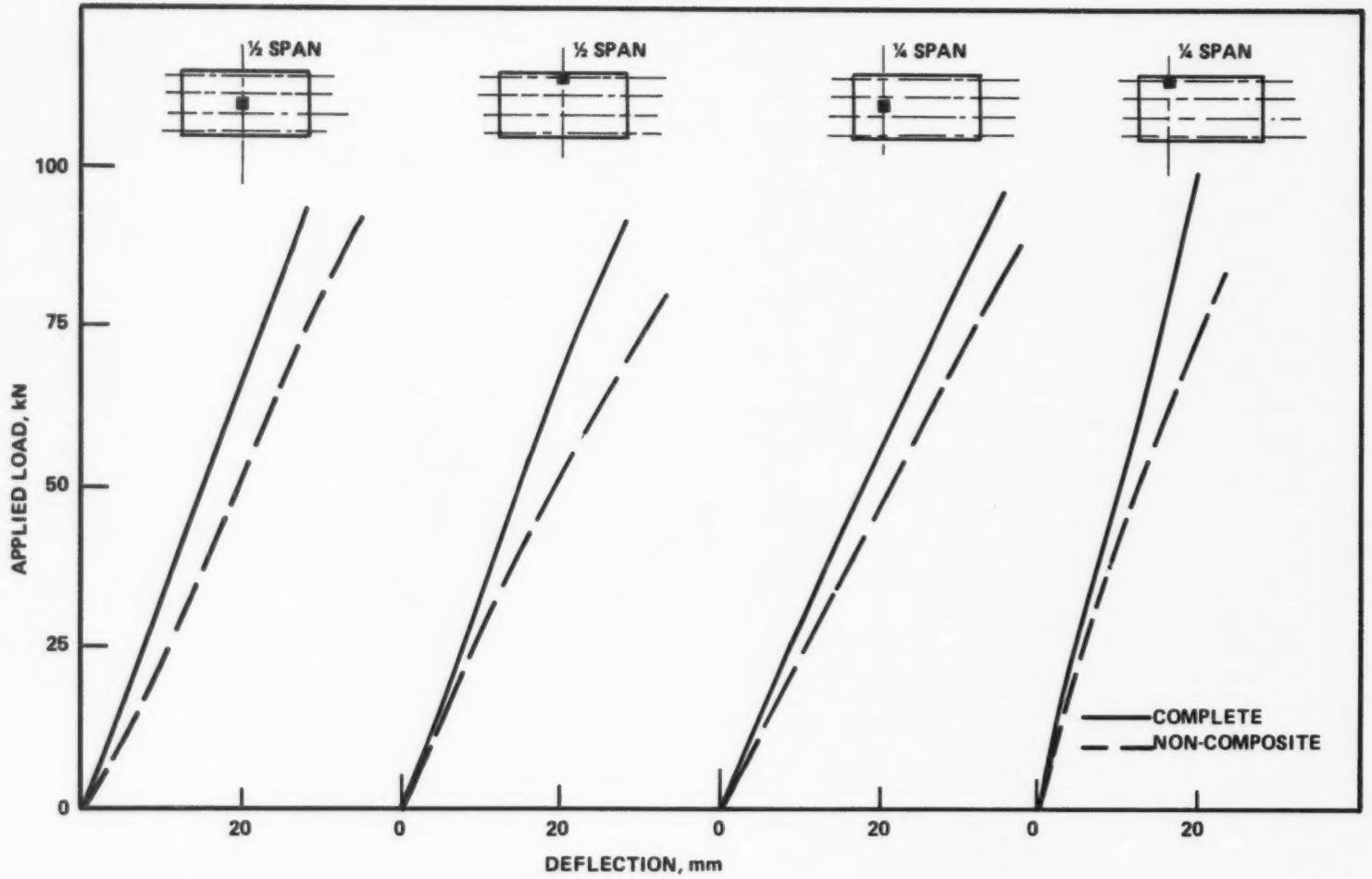

Figure 7.2a/ Comparison of Deck Deflections Under Wheel Loads

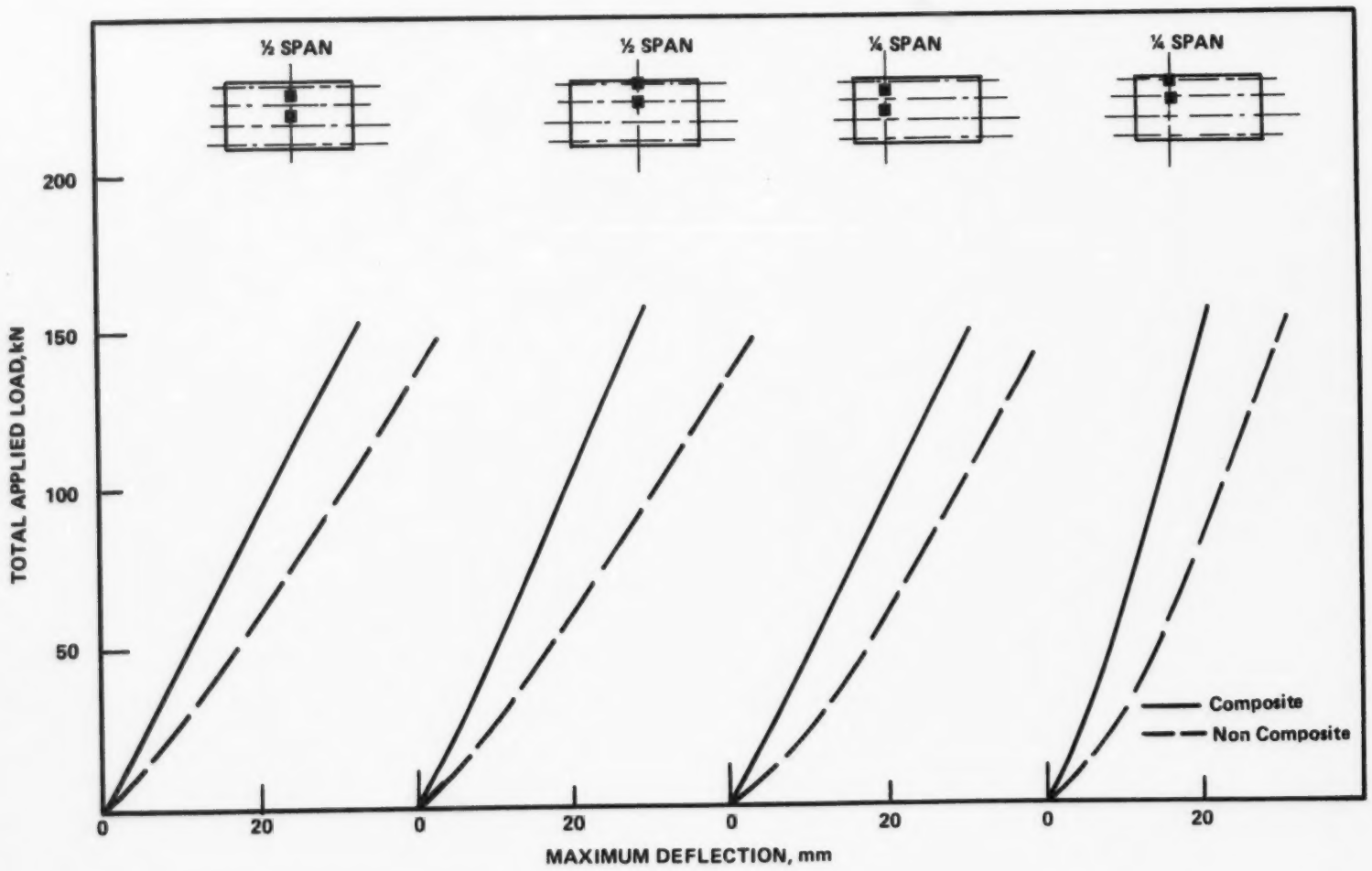

Figure 7.2b/ Comparison of Maximum Deck Deflections under Axle Loads

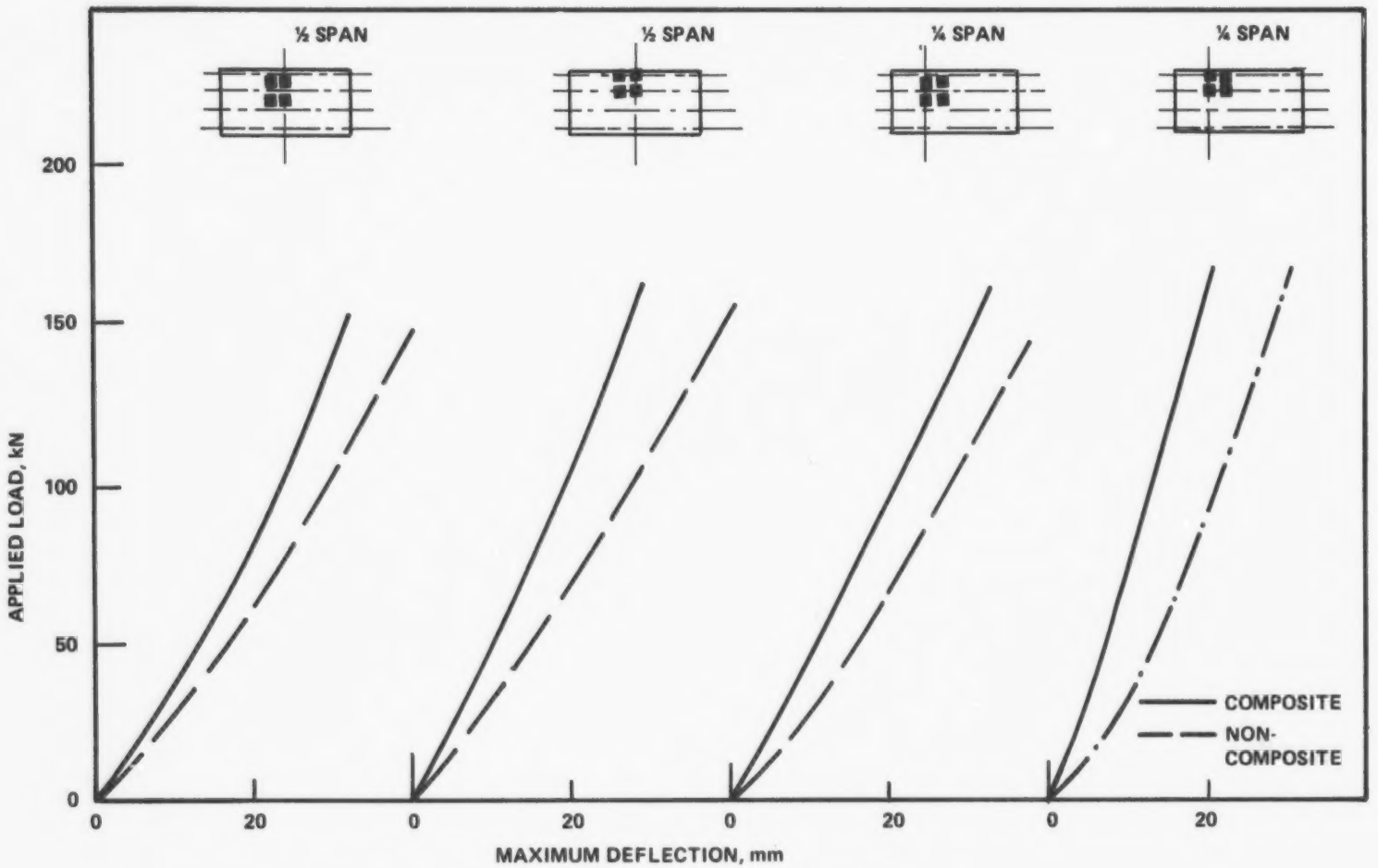

Figure 7.2c/ Comparison of Maximum Deck Deflections Under Dual Axle Loads

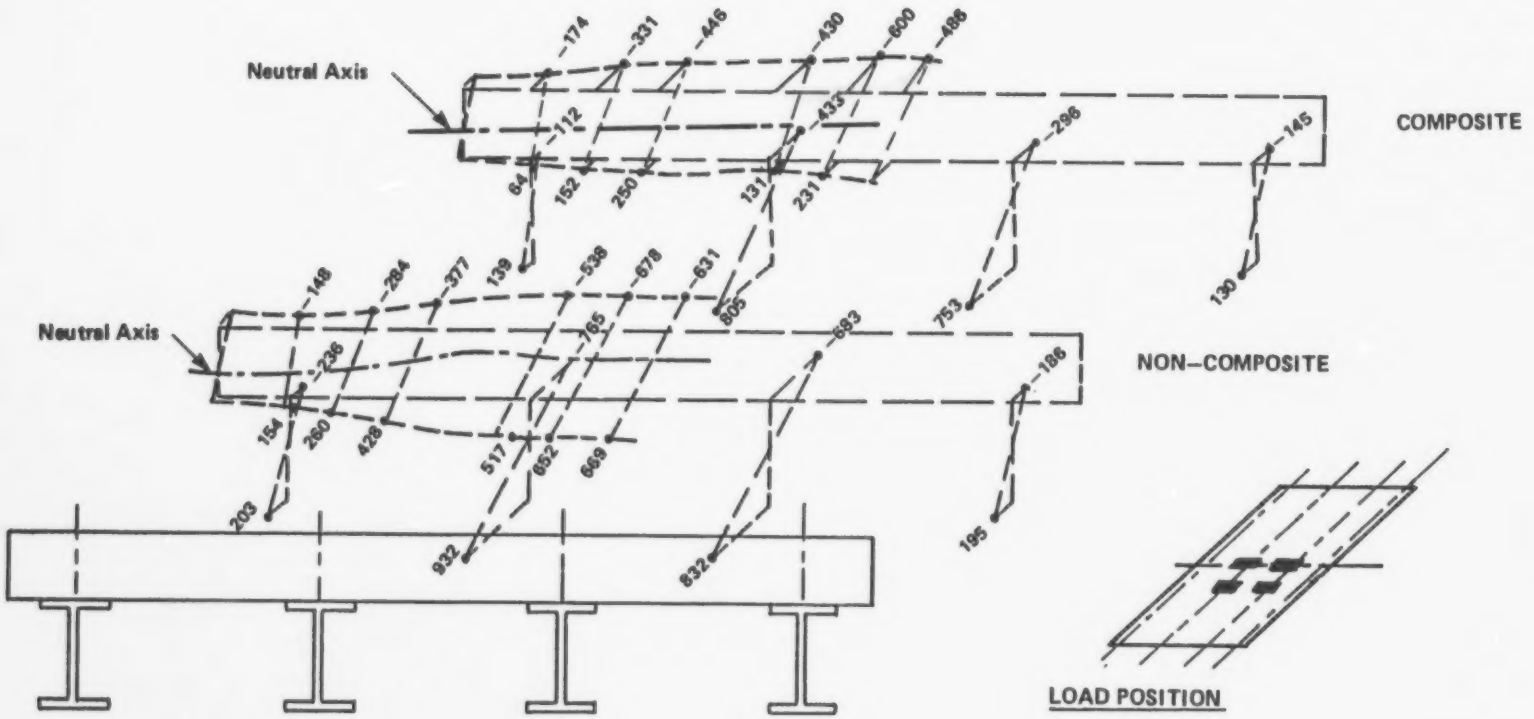

Figure 7.3/ Comparison of Strains Induced Under a Dual Axle Load

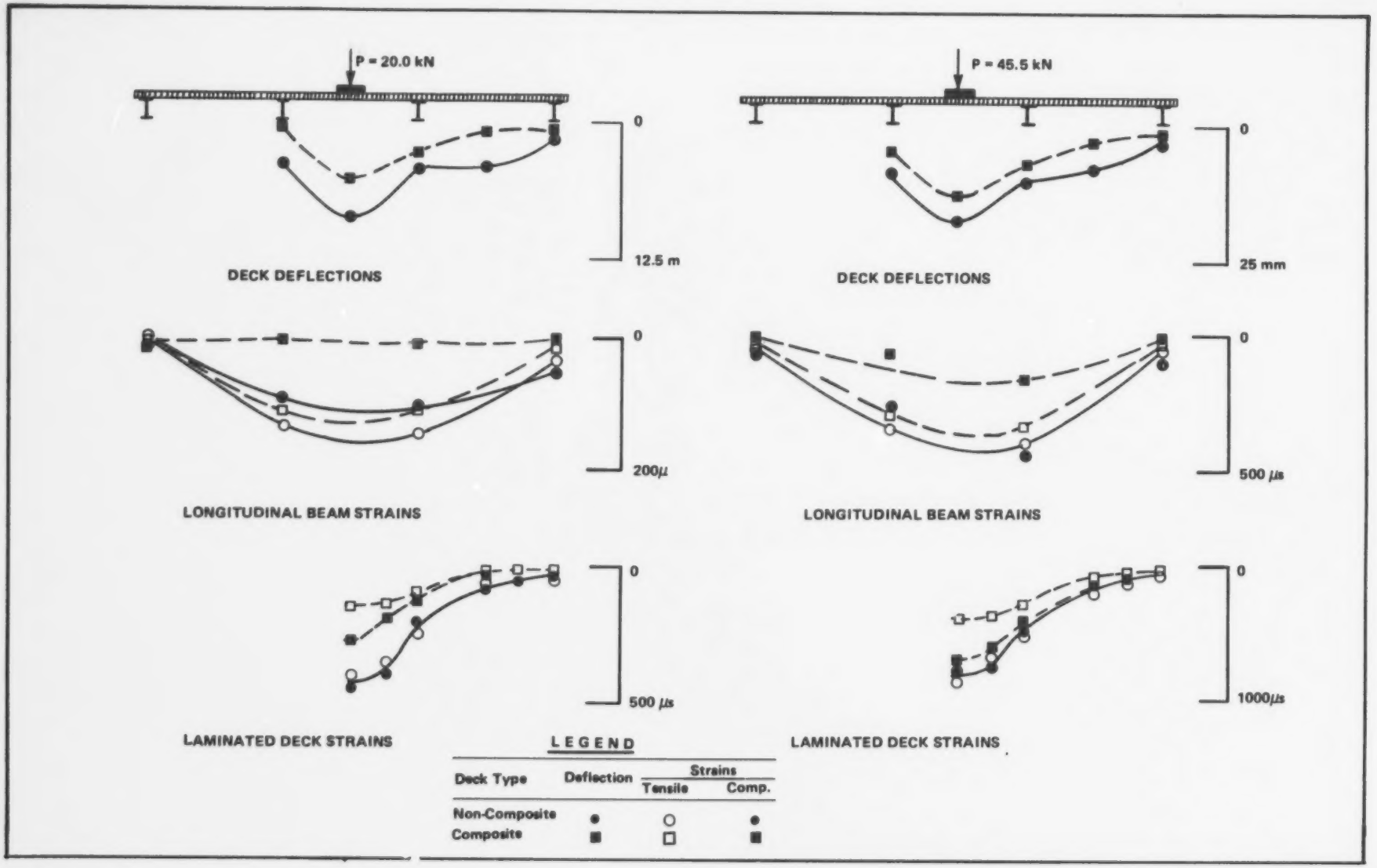

Figure 7.4a/ Behaviour of Composite Bridge Under Wheel Load, WHL1

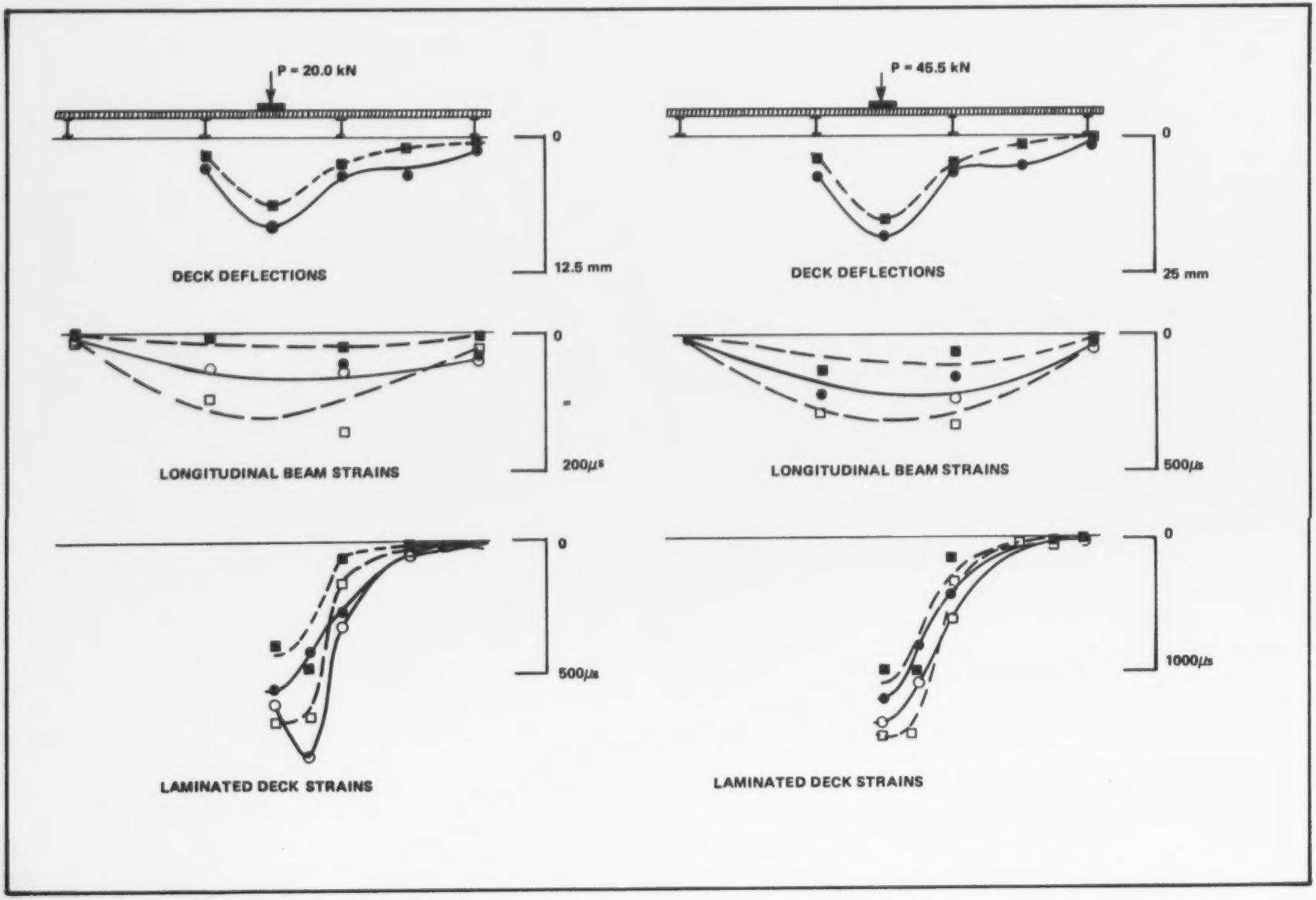

Figure 7.4b/ Behaviour of Composite Bridge Under Wheel Load, WHL5

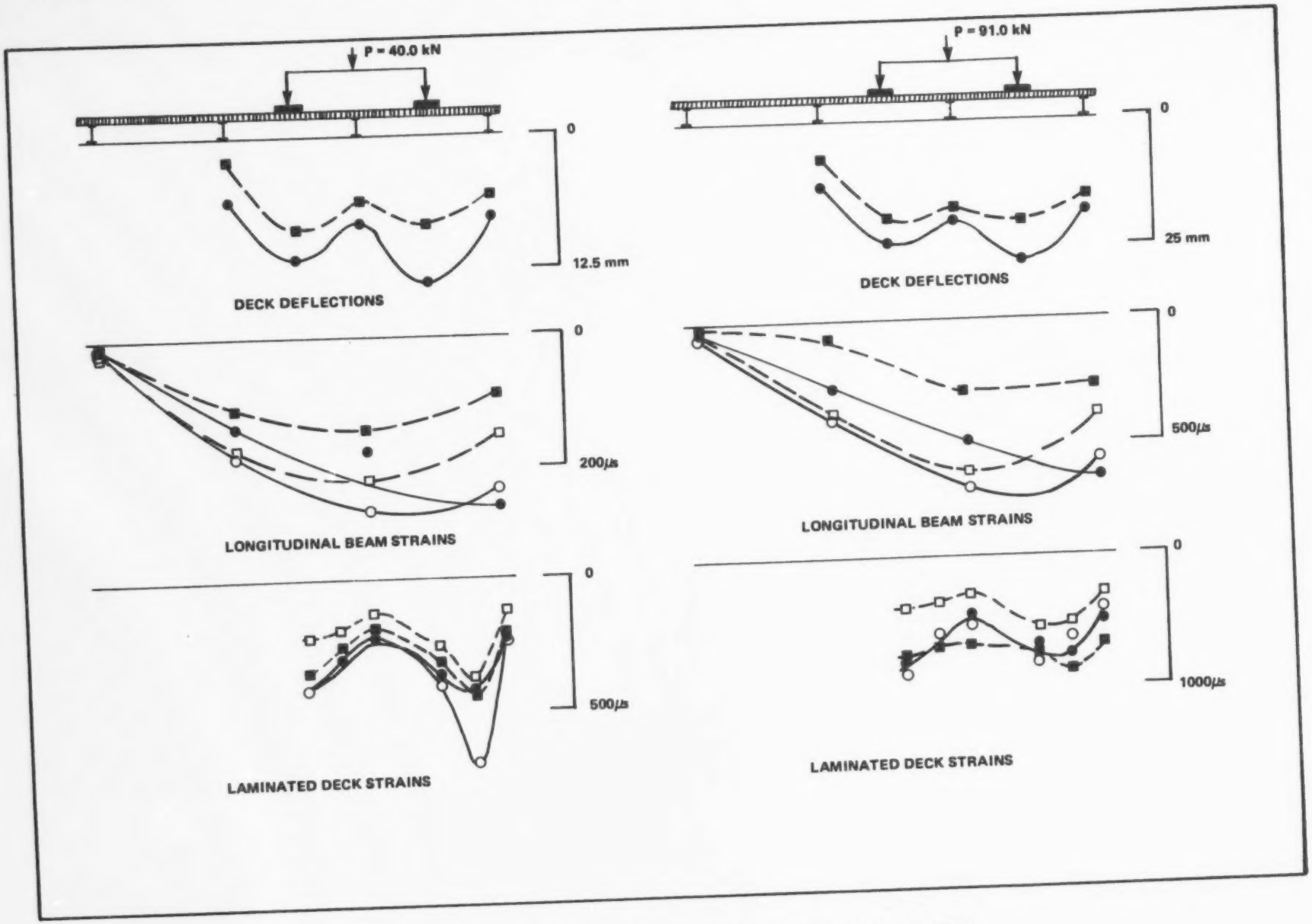

Figure 7.4c/ Behaviour of Composite Bridge Under Axle Load, AXL2

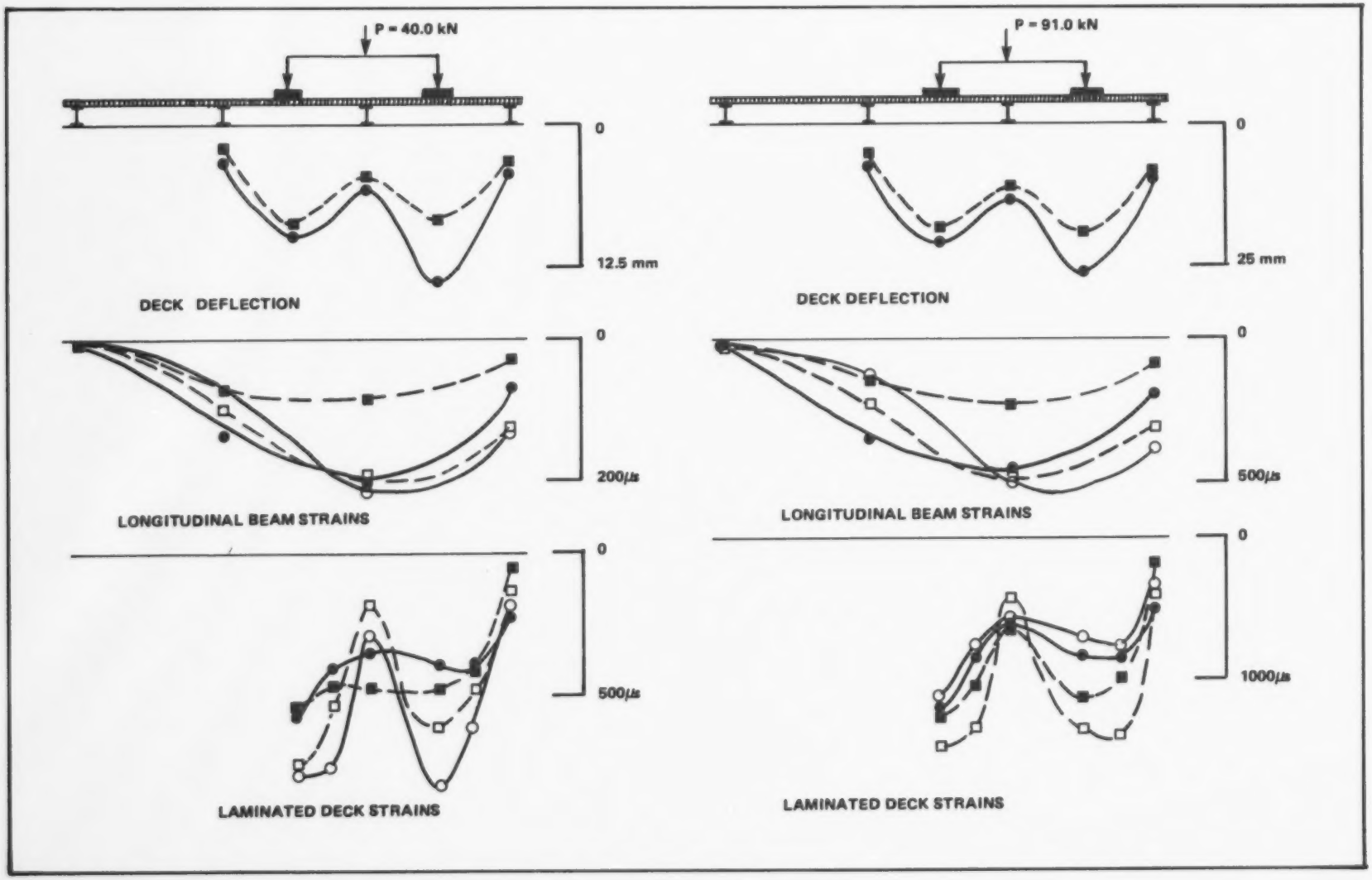

Figure 7.4d/ Behaviour of Composite Bridge Under Axle Load, AXL5

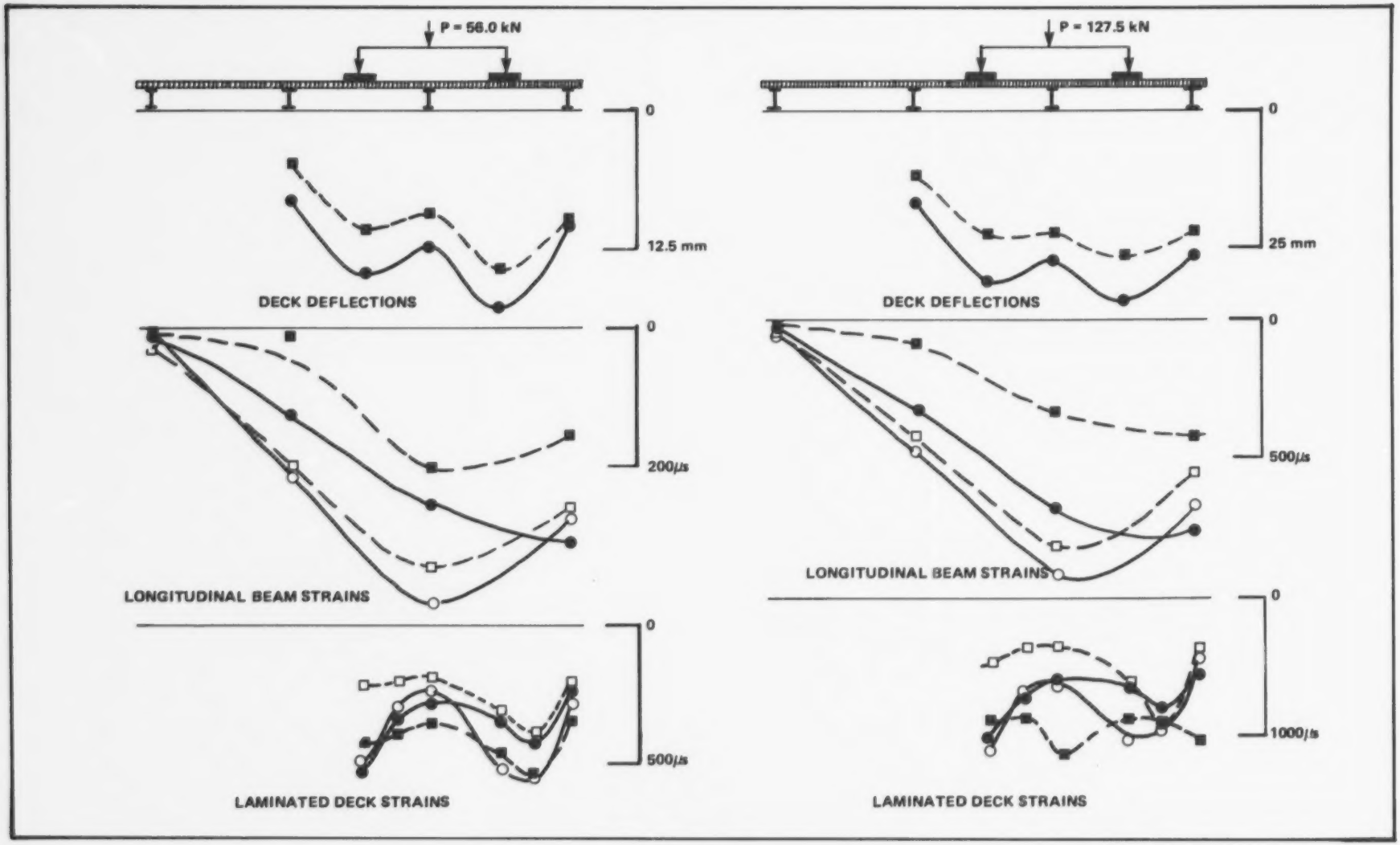

Figure 7.4e/ Behaviour of Composite Bridge Under Dual Axle Load, DAXL2

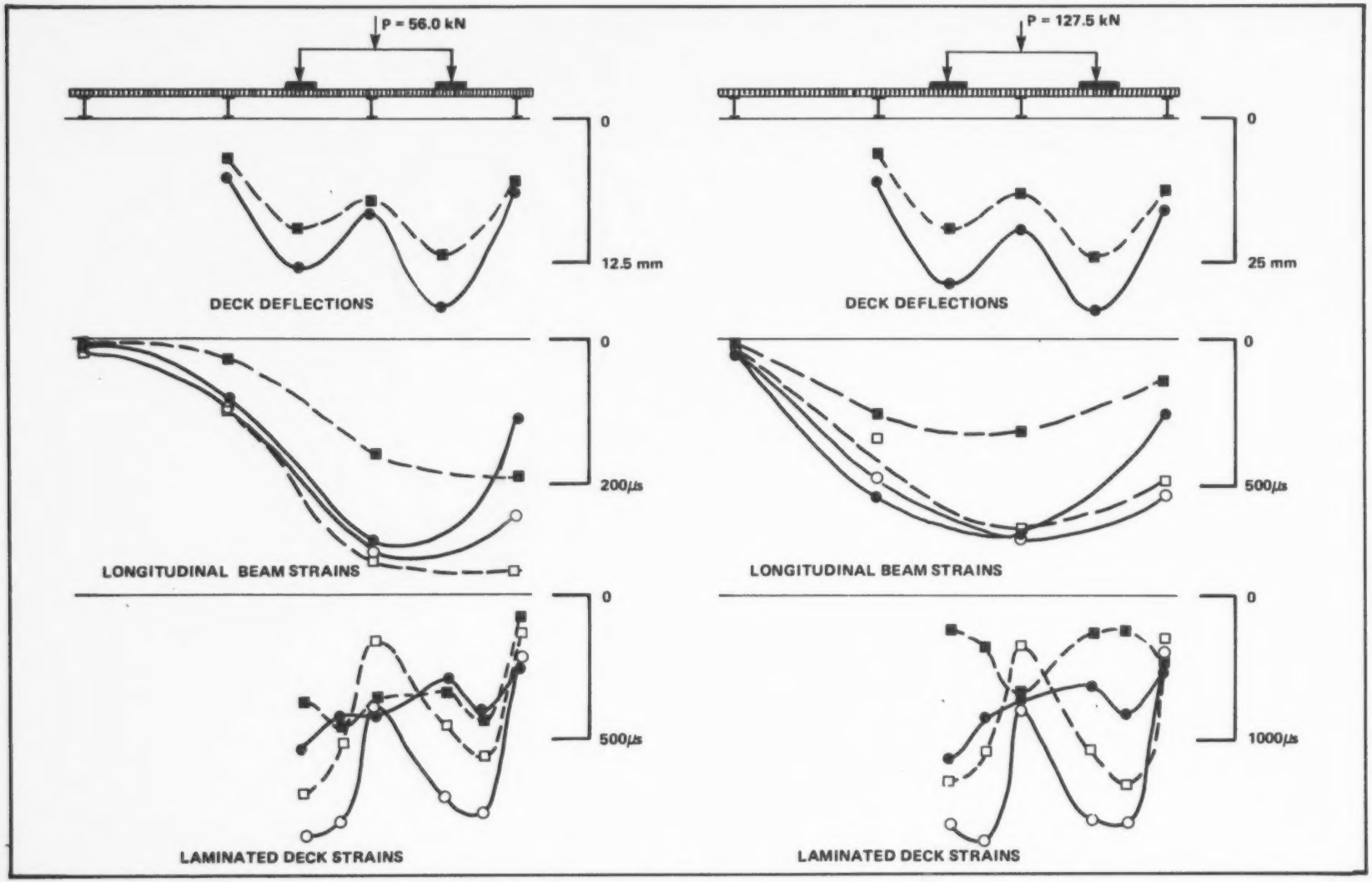

Figure 7.4f/ Behaviour of Composite Bridge Under Dual Axle Load, DAXL5

Table 7.1/ Average Reduction of Stress and Delections Observed on the Deck for Midspan Load

		Averaged Reductions of Stress and Deflections.%					
		Wheel Load		Axle Load		Dual Axle Load	
		Ser.	Ult.	Ser.	Ult.	Ser.	Ult.
Deck Deflections		33.0	30.0	37.0	34.0	29.0	31.0
Steel Beam Stress	Top	49.0	67.0	40.0	50.0	35.0	49.0
	Bot.	18.0	12.0	16.0	20.0	13.0	15.0
Wood Deck Stress	Top	34.0	28.0	16.0	23.0	3.0	-15.0
	Bot.	34.0	12.0	45.0	36.0	53.0	33.0

- ve indicates an increase

bridge behaviour, i.e., deflections and stresses with that given by grillage analysis. The grillage analysis of the bridge is idealized by seven longitudinal beams and twenty-one transverse beams. The longitudinal beam properties required for the grillage analysis were calculated by considering 50% of the deck area to be composite with the girder. The transverse beam properties were calculated corresponding to transverse elastic modulus (E_T) of timber laminates.

The theoretical and actual values of bridge deflections, the steel girder bottom fibre stress and the timber deck top fibre stresses, for selected loading types are given in Tables 7.2, 7.3 and 7.4, respectively. The load types WH1, AXL2 and DAXL2 were applied at the midspan of the bridge with a channel diaphragm running directly under the loads. The load types, WH5, AXL5 and DAXL5, were applied at the quarter span of the bridge where the laminated deck was the only transverse medium. The deck deflections and the stresses given in the tables are along the transverse section of the bridge at which the loads were applied, i.e., at midspan or quarter span. As can be seen, the theoretical deflections compare reasonably well with the measured deflections. In general, however, theoretical maximum deflections for each load case are lower than the actual deflections. The differences between the maximum theoretical and the corresponding deflections are greater at the diaphragm location (i.e., midspan) than at the middle of the deck panel (i.e., quarter span).

The observed greater differences between the deflection values at the midspan are thought to be due to overestimating the stiffening effect of the diaphragm by the grillage analysis. The smaller size load used for the model testing may have also increased the deflections local to the pad location. It has been observed during the tests on the timber deck that the deck deflections increased substantially when the pad size was halved. The difference between these deflections, however, is reduced considerably for the composite bridge deck. Notwithstanding the above discrepancy between the peak deflection values, it is concluded here that, for design needs, the grillage analysis can estimate the actual deflections sufficiently accurately.

Table 7.2/ Comparison Between Theoretical and Actual Bridge Deflection

LOAD TYPE		NON-COMPOSITE Loc. 1	2	3	4	5	COMPOSITE 1	2	3	4	5
WH1	Theoretical	4.8	5.3	4.9	2.8	0.7	3.2	3.6	3.2	1.8	0.3
	Actual	3.8	8.9	4.4	4.2	1.2	0.6	5.1	2.8	1.3	0.8
WH5	Theoretical	3.1	6.4	3.1	1.0	0.1	2.0	5.2	2.0	0.4	0.1
	Actual	2.8	8.4	3.8	2.2	0.7	1.5	6.4	2.5	0.8	0
AXL2	Theoretical	5.7	7.8	9.1	8.5	7.2	3.6	5.1	6.0	5.8	4.9
	Actual	6.1	11.4	7.6	13.3	7.6	2.0.	8.9	5.7	8.3	5.7
AXL5	Theoretical	4.1	5.6	6.9	5.7	4.2	2.0	5.3	3.9	5.5	2.2
	Actual	2.8	9.5	5.7	13.9	3.2	1.9	8.3	4.4	8.3	3.2
DAXL2	Theoretical	7.6	10.5	12.7	11.6	9.8	6.7	9.9	12.1	11.2	9.4
	Actual	7.6	14.6	12.0	17.8	10.0	5.1	10.7	9.5	14.6	10.2
DAXL5	Theoretical	4.9	9.5	8.8	10.0	5.6	4.3	9.9	8.4	10.6	5.4
	Actual	4.6	12.7	8.3	16.8	6.4	3.2	9.5	7.0	12.1	5.1

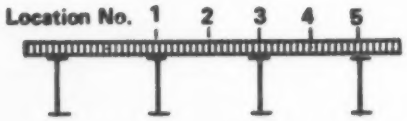

BRIDGE SECTION

Table 7.3/ Comparison Between Theoretical and Actual Girder Stress at Bottom Flange

LOAD TYPE		NON-COMPOSITE			COMPOSITE		
		Loc. 1	3	5	1	3	5
WH1	Theoretical	37.9	37.9	4.9	31.1	31.1	2.8
	Actual	30.0	30.0	6.0	24.0	24.0	2.0
WH5	Theoretical	31.9	31.9	0.64	25.9	25.9	1.4
	Actual	24.0	22.0	4.0	20.0	26.0	0.0
AXL2	Theoretical	43.3	70.4	53.6	34.2	58.1	21.3
	Actual	38.0	52.0	48.0	37.0	44.0	30.0
AXL5	Theoretical	31.7	61.6	32.6	24.7	35.3	16.9
	Actual	18.0	42.0	24.0	18.0	40.0	22.0
DAXL2	Theoretical	59.9	99.9	72.9	45.3	82.3	54.6
	Actual	44.0	80.0	56.0	40.0	68.0	52.0
DAXL5	Theoretical	43.2	83.7	48.3	33.5	68.8	37.9
	Actual	20.0	60.0	48.0	20.0	60.0	60.0

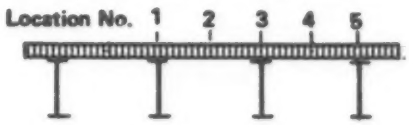

BRIDGE SECTION

Table 7.4/ Comparison Between Theoretical and Actual Deck Top Fibre Stresses

LOAD TYPE		NON-COMPOSITE					COMPOSITE				
	Loc.	1	2	3	4	5	1	2	3	4	5
WH1	Theoretical	0.89	0.85	0.39	0.39	0.10	1.94	0.62	1.94	0.23	0.19
	Actual	2.50	4.50	2.50	0.50	0.25	1.50	3.00	1.50	0.25	0
WH5	Theoretical	0.75	8.44	0.75	0.10	0.01	1.62	4.00	1.62	0.26	0.08
	Actual	3.00	8.00	3.00	0.50	0	0.50	4.00	1.00	0.25	0
AXL2	Theoretical	1.02	1.30	1.64	1.21	1.28	2.13	0.89	3.60	0.70	3.09
	Actual	-	4.00	2.25	3.50	1.80	-	3.30	1.80	3.00	1.90
AXL5	Theoretical	0.75	7.89	1.45	6.85	0.78	1.54	7.43	3.16	6.38	1.86
	Actual	-	6.00	3.60	4.00	2.20	-	5.20	4.80	4.90	0.50
DAXL2	Theoretical	0.49	11.86	12.36	1.84	1.74	2.83	1.30	5.17	1.23	4.19
	Actual	-	15.20	12.60	3.20	2.20	-	4.00	3.60	4.50	3.00
DAXL5	Theoretical	1.02	5.87	2.81	5.28	1.15	2.09	5.23	4.31	4.70	2.75
	Actual	-	5.30	3.80	3.20	2.50	-	3.80	3.80	3.30	0.75

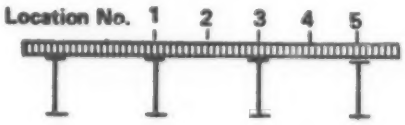

BRIDGE SECTION

The beam stresses calculated using the theoretical moment obtained from the grillage analysis are compared against the actual stresses measured in the test in Table 7.3. As can be seen, the actual stresses are generally lower than those obtained theoretically. The difference is greater for non-composite bridges. However, since the stresses are not seriously overestimated, the grillage analysis can be used to analyse and design practical wood-steel composite bridges.

The theoretical deck top fibre stresses are generally greater than the actual deck stresses where the transverse medium is only the laminated deck. On the other hand, where the transverse medium is the deck and diaphragm, the actual stresses are very much greater than the theoretical values. The comparison between the stresses at the midspan of the bridge become tolerably close for composite bridges. Since the deck stresses are critical at the quarter span where the bridge has no transverse diaphragm (1/4 span) and across this section, the theoretical deck stresses are marginally greater than the actual values. The grillage analysis can be effectively used to analyse and design timber-steel bridges.

7.4/ Cyclic Load Test on the Model Bridge

The cyclic load test on the model was performed using a dual axle load. The total dual axle cyclic load varied between 67 and 12 kN. The maximum cyclic load applied is kept closer to serviceability load value of 56.0 kN for dual axle load (as per OHBDC). The results of the tests are given summarized in Figure 7.5. The model underwent almost 3×10^6 number of cycles without appreciable loss of stiffness. The deflections remained almost constant. Similarly, the strain measurements remained reasonably constant till the end of the cyclic test. The maximum recorded strains on the bottom flange were in the girder No. 2 and averaged around 450 μs, corresponding to a stress of about 90 MPa. For Class A, the allowable stress range as per OHBDC is 165 MPa. Although the applied stress range is lower than that for Class A category structures, the fact that the structure withstood loads equivalent to

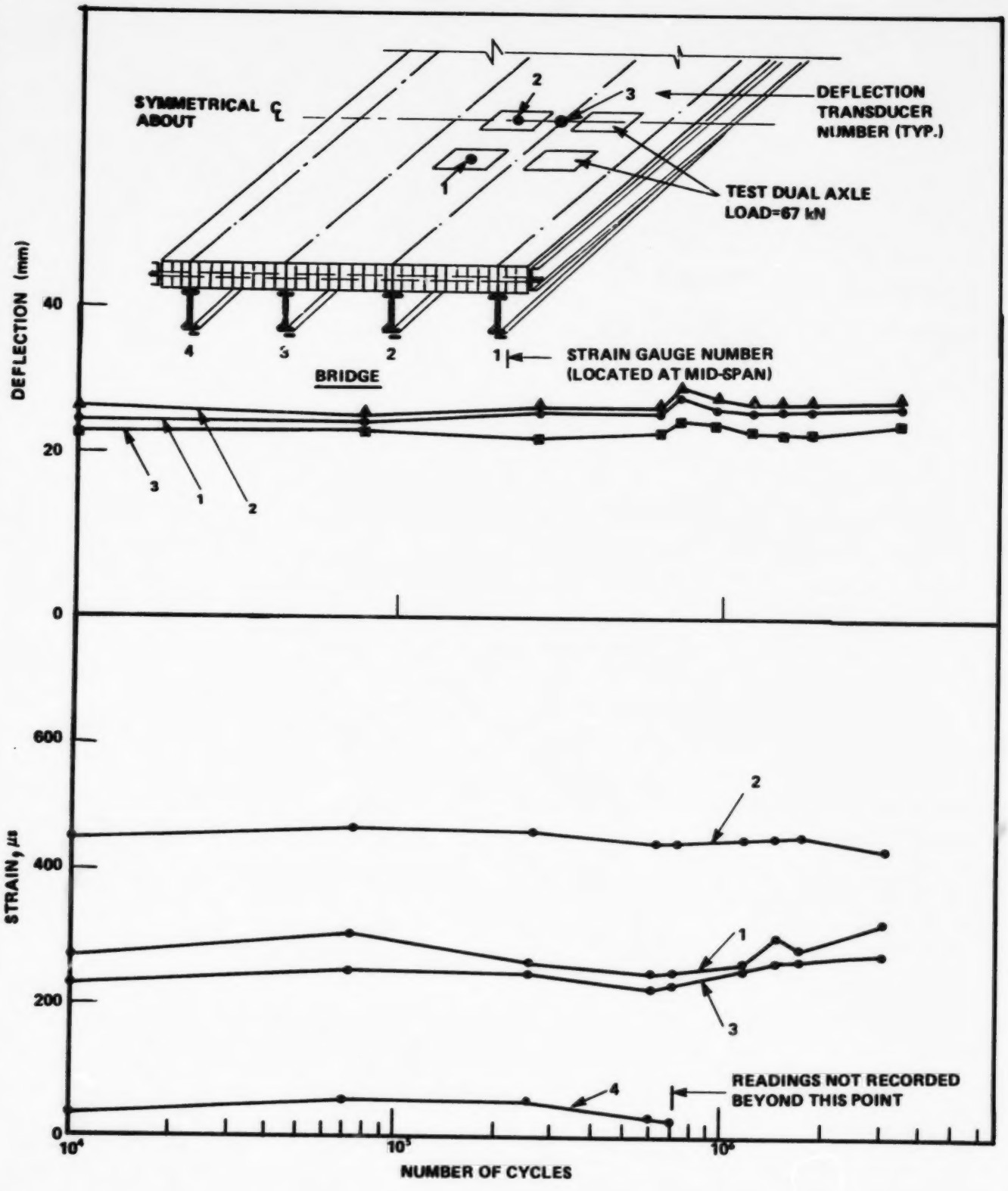

Figure 7.5/ Results of the Cyclic Load Tests Performed on the Model Bridge

OHBDC serviceability loads for 3×10^6 cycles is considered adequate. In timber-steel composite structures, the concern is for the performance of the bulkhead shear connector and the integrity of the laminated deck. The girder fatigue characteristics are of minor importance. The bulkheads remained intact and the laminated deck did not show loosening or local failures common to nail laminated decks.

REFERENCES

[1] Csagoly, P.F., and Taylor, R.J., "A Development Program for Highway Bridges," 79-SRR-7, Ministry of Transportation and Communications (MTC), Downsview, Ontario, Canada, 1979.

[2] Taylor, R.J., and Csagoly, P.F., "Transverse Post-Tensioning of Longitudinally Laminated Timber Bridge Decks," RR220, MTC, Downsview, Ontario, June, 1979.

[3] Taylor, R.J., "Rehabilitation of Wood Highway Bridges in Ontario," 82-SRR-2, MTC., Downsview, Ontario, 1982.

[4] Ontario Highway Bridge Design Code, MTC, Downsview, Ontario, Canada, 1983.

[5] Bakht, B., "Statistical Analysis of Timber Bridges," ASCE Journal of the Structural Division, Vol 103, No. 8, pp 1761-1779, Aug 1983.

[6] Goodman, J.R., and Bodig, J., "Orthotropic Elastic Properties of Wood" Journal of the Structural Division, ASCE Nov 1970 pp 2301-2319.

[7] Csagoly, P.F. and Taylor, R.J., Tests on Steel-Wood Composite Beams, Unpublished Internal Report, MTC, 1980.

[8] Csagoly, P.F. and Taylor, R.J., "A Structural Wood System for Highway Bridges," International Association for Bridge and Structural Engineering Proceeding P-35/80, IABSE, Vienna, Austria, 1980.

[9] Slutter, R.G., and Driscell, G.C.,"Flexural Strength of Steel-Concrete Composite Beams," ASCE Journal in the Structural Division, 1965, pp 71-99.

[10] King, D.C., Slutter, R.G., Driscell, G.C., "Fatigue Strength of 1/2" Diameter Shed Sheer Connectors," HRB Record 103, pp 78-106, 1965.

[11] McGaraagh J.B., and Baldwin, J.W., "Lightweight Concrete-on-Steel Composite Beams," AISC Engineering Journal, pp 90 - 98, July, 1971.

[12] Chapman, J.C., "Composite Construction in Steel and Concrete -- The Behavior of Composite Beams," The Structural Engineer, April 1964, No. 4, Volume 42.

[13] Sen, R., "Program for the Grillage Analysis of Slab or Pseudo Slab Bridge Decks," Highway Engineering Computer Branch, HECB/B/9-Grids, Department Enviroment, London, England, 1975.

APPENDIX A

DESIGN OF MODEL BRIDGE

Theory of Models

Notation:

p - prototype	P - load
m - model	L - length, width, etc.
ε - strain	σ, f - stress
E - elastic modulus	

Prototype-to-model compatibility is achieved by keeping:

$$\varepsilon_p = \varepsilon_m \tag{1}$$

If the scale down factor is S_ℓ

$$L_p = S_\ell \cdot L_m \tag{2}$$

In this particular design, elastic modulus of the prototype and model are assumed to be the same,

Therefore:

$$\begin{aligned} E_p &= E_m \\ G_p &= G_m \\ S_f &= 1.0 \end{aligned} \tag{3}$$

The relationship between the applied loading between prototype and model is given by,

$$\frac{E_p L_p^2}{P_p} = \frac{E_m L_m^2}{P_m}$$

$$P_p = S_f \cdot S_\ell^2 P_m \tag{4}$$

Using $S_f = 1.0$, $S_L = {}^1/_2$ (for half scale model)

$$P_p = 4\ P_m \text{ or } P_m = {}^1/_4\ P_p \qquad (5)$$

The truck load is the critical case for the prototype bridge of span 12.0 m. The model is designed with ${}^1/_4$ OHBDC truck loads with axle spacing reduced by the scale factor of ${}^1/_2$.

Model Bridge Design

The prototype bridge is to have a span of 12.0 m and deck width of 6.0 m. The half scale model of the bridge is shown below.

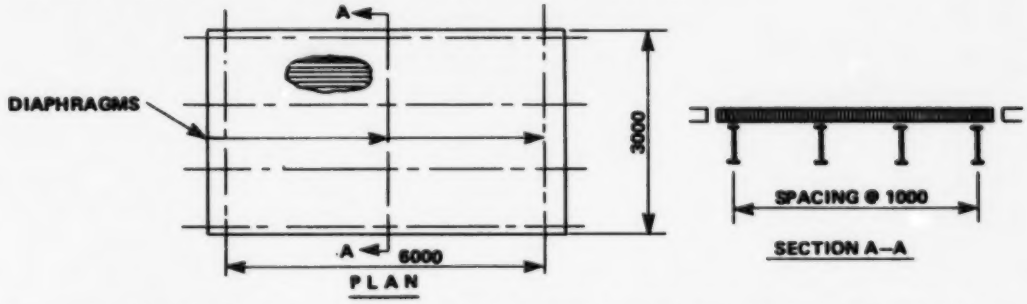

An approximate design procedure is adopted and the design details are given below:

Deck:

The deck is designed as a plain longitudinal laminated deck spanning the diaphragm supports.

Midspan Moment = 15.5 kNm/line of OHBDC wheels

Support Moment = 10.9 kNm/line of OHBDC wheels

Ultimate Moment 1.40 x 1.20 x 15.5 = 26.2 kNm/line of OHBDC wheels

Using approximate D_d value given in Table 3.7.1.2.1 of OHBDC:

$$S/D_d = \frac{1}{1.8} = 0.56$$

Therefore, ultimate moment 26.2 x 0.56 = 14.7 kNm/1000 mm decks.
Using 50 x 100 mm laminates,

Deck strength = $0.9 \times 13 \times (1000 \times {}^{3}/_{4}) \times \frac{100^2}{6} \times 1.5 \times 1.3 = 28.5$ kNm

where $k_d = 1.0$, $k_l = 1.0$, $k_m = 1.5$, $k_s = 1.3$, $f_c = 13$ MPa

Therefore, 50 x 100 mm laminates can be used.

Steel Girder:

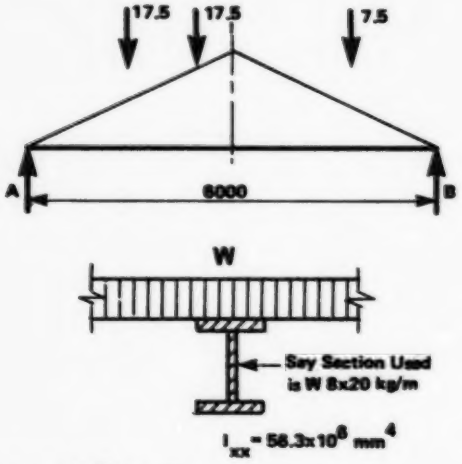

$$D_x = \frac{56.3 \times 10^6}{1000} = \frac{E_s}{E_c} E_L$$

$$D_y = \frac{100^3}{12} E_T$$

$$D_{xy} = \frac{100^3}{6} \times G_{LT} = D_{yx}$$

$G_{LT} = 585$ MPa $\qquad E_T = 450$ MPc

$D_x = 1.12 \times 10^{10}$ N.mm $\qquad D_y = 37.5 \times 10^6$ N.mm

$D_{xy} = D_{yx} = 97.5 \times 10^6$ N.mm $\qquad D_1 = D_2 = 0$

$$\alpha = \frac{2 \times 97.5 \times 10^6}{(2 \times 1.12 \times 10^{10} \times 37.5 \times 10^6)^{0;5}} = 0.15$$

$$\theta = \frac{3.2}{6.0} (1.12 \times 10^{10} / 37.5 \times 10^6)^{0;25} = 2.21$$

D = 1.90 External $\qquad$ say $D_d = 1.50$

= 1.48 Internal

$$\therefore \frac{S}{D_d} = \frac{1}{1.5} = 0.667$$

$$R_B = \frac{7.5(4.84) + (3.03 + 2.44)17.5}{6} = 22.0 \text{ kN}$$

Maximum Moment = 22 x 3.04 - 7.5 x 1.8 = 5.34 kNm

Ultimate Moment = 0.667 x 1.4 x 1.21 x 53.4 = 60.4 kNm/Girder

Non composite section capacity of W8 x 20 beam is given by,

$$M_r = 0.9 \times 335 \times 10^3 \times \frac{300}{10^6} = 90.4 \text{ kNm} \qquad >> 60.4$$

Shear Connector:

Maximum shear $17.5 \times 1 + 17.5 \times \frac{5.4}{6} + \frac{7.5 \times 3.6}{6} = 37.8$ kN/beam

Section Properties

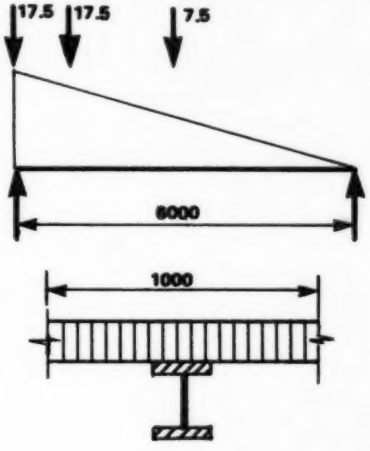

$E_{Timber} = 9000$ MPa $\quad E_{st} = 200{,}000$ MPa

$\frac{E_s}{E_T} = 22.2 \qquad B_{eqi} = 45$ mm

$\bar{y} = 84.5$ mm $\qquad I_{xx} = 56.3 \times 10^6 \text{mm}^4$

$Q = 1.54 \times 10^5 \text{ mm}^3$

$V_r = 1.4 \times 1.21 \times 37.8 = 64.0$ kN

$$S_r = 64 \times \frac{1.54 \times 10^5}{56.3 \times 10^6} = 0.175 \text{ kN/mm}$$

Total Shear Force $0.175 \times 3000 = 525$ kN

Shear resistance provided by 6 bulkheads

$6 \times 3 \times 35 = 630$ kN

Ultimate compressive strength of deck $1000 \times 100 \times 20 \times 10^{-3} = 2000$ kN

> 630 kN

Therefore, the girder will fail first by shear connection failure.

Prestressing:

Maximum stress value at Jacking (N_i) = 0.25 F_{q1}

F_{q1} for spruce/pine/fir = 3.3 MPa

N_i = 0.825 MPa

Minimum final value N_f = 0.5 N_i or 0.35

0.5 x 0.825 = 0.413 < 0.35

Design Prestress = 0.825 Mpa

Bearing resistance of timber = ϕ f_{q1} A_b

ϕ = 1.0 f_{q1} = 3.3

A_b = 100 x (2 x 4 x 25.4) = 20320 mm^2

Therefore, allowable bearing load = 67.0 kN

Prestress force required 0.825 x 30500 x 10^{-3} = 25 kN < 67.0

Use prestressing @ 305 CRS

Anchorage slip 5%

N_i = 52.9 kN

= 53 kN

Diaphragm Design:

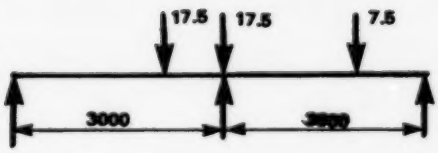

Maximum shear force

$$17.5 + 17.5 \times \frac{2.4}{3.0} + 7.5 \times \frac{1.2}{3} = 34.5$$

Ultimate shear load

1.4 x 1.21 x 34.5 x 0.667 S/Dd = 37.9 kN

Moment on diaphragm beam (assuming the load as uniformly distributed)

$$\frac{37.9 \times 1.0}{8} = 4.74 \text{ kNm}$$

Try channel C 130 x 10

$$fy = \frac{4.74 \times 10^6}{0.9 \times 48.6 \times 10^3} = 108.4 \text{ MPa} < 300 \text{ MPa}$$

APPENDIX B

Evaluation of Applied Moments Using the Measured Stresses

This describes the development of the computer program to calculate the induced moments from the measured stresses in a section.

The figure below shows the typical stress distribution observed on the wood-steel composite beam during the failure test.

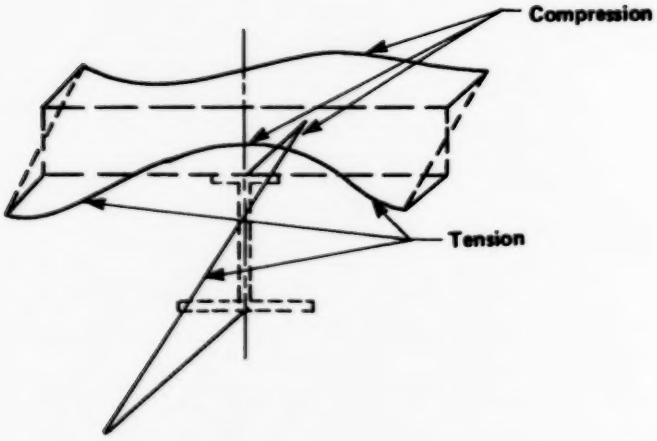

STRESS DIAGRAM

The program is codified to do the following:

1) The deck is divided into specified subdivisions. The average neutral axis of the deck is calculated. The resultant moments and the axial force of the section is calculated for each of the subdivisions.

2) The neutral axis of the steel beam is evaluated. The resultant moment and axial force of the section is calculated.

3) The moment induced on the section is calculated by totalling the individual deck and girder moments and that resulting from the average axial force times the lever arm.

The program listing, a sample input and the output is given below:

```
**** ISO FOREGROUND HARDCOPY ****
DSNAME=TCER.MOMENT.FORT

C                                                                       00000100
CC   PROGRAM TO CALCULATE THE BENDING MOMENT AT A SECTION               00000200
C                                                                       00000300
      DIMENSION SCURVE(10,2),BCURVE(10,2),XT(10),XB(10),TITLE(16),      00000400
     1       YSLAB(10),BMST(10),ZBEAM(10),YBEAM(10),CURVE(10,2),        00000500
     2       XBS(10),XTS(10),BMSTS(10)                                  00000501
      REAL MOMS,MOMB,MOMTOT                                             00000510
      INTEGER TITLE                                                     00000511
      READ(5,*) NPROB                                                   00000512
      NDONE=0                                                           00000513
    1 IF(NDONE.EQ.NPROB) GOTO 9000                                      00000521
      NDONE=NDONE+1                                                     00000522
      MOMS=0.                                                           00000523
      MOMB=0.                                                           00000524
      AXFS=0.                                                           00000525
      AXFB=0.                                                           00000526
      WRITE(6,800)                                                      00000527
      READ(5,3) TITLE                                                   00000530
    3 FORMAT(16A4)                                                      00000540
      READ(5,*) NSLAB,ZSLAB,NBEAM,ZNA,NPNTS                             00000600
      READ(5,*) (YSLAB(I),I=1,NSLAB)                                    00000700
      NSLAB2=NSLAB+1                                                    00000710
      READ(5,*) (XB(I),I=1,NSLAB2)                                      00000800
      READ(5,*) (XT(I),I=1,NSLAB2)                                      00000900
      READ(5,*) (ZBEAM(I),I=1,NBEAM)                                    00001000
      READ(5,*) (YBEAM(I),I=1,NBEAM)                                    00001100
      NBEAM2=NBEAM+1                                                    00001110
      READ(5,*) (BMST(I),I=1,NBEAM2)                                    00001200
      READ(5,*) (SCURVE(I,1),I=1,NPNTS)                                 00001300
      READ(5,*) (SCURVE(I,2),I=1,NPNTS)                                 00001400
      READ(5,*) (BCURVE(I,1),I=1,NPNTS)                                 00001500
      READ(5,*) (BCURVE(I,2),I=1,NPNTS)                                 00001600
C                                                                       00001601
CC   CONVERT THE STRAINS INTO STRESSES                                  00001602
C                                                                       00001603
      DO 40 I=1,NSLAB2                                                  00001604
      SIGN=1.                                                           00001605
      IF(XB(I).LT.0.) SIGN=-1.                                          00001606
      STRAIN=ABS(XB(I))                                                 00001607
      CALL CNVRT(STRAIN,SCURVE,STRESS,NPNTS)                            00001608
      XBS(I)=STRESS*SIGN                                                00001609
      SIGN=1.                                                           00001610
      IF(XT(I).LT.0.) SIGN=-1.                                          00001611
      STRAIN=ABS(XT(I))                                                 00001612
      CALL CNVRT(STRAIN,SCURVE,STRESS,NPNTS)                            00001613
   40 XTS(I)=STRESS*SIGN                                                00001614
      DO 50 I=1,NBEAM2                                                  00001615
      SIGN=1.                                                           00001616
      IF(BMST(I).LT.0.) SIGN=-1.                                        00001617
      STRAIN=ABS(BMST(I))                                               00001618
      CALL CNVRT(STRAIN,BCURVE,STRESS,NPNTS)                            00001619
   50 BMSTS(I)=STRESS*SIGN                                              00001620
C                                                                       00001621
CC   PRINT THE INPUT DATA                                               00001622
C                                                                       00001623
      WRITE(6,100) TITLE                                                00001624
      DO 8 I=1,NSLAB                                                    00001625
      WRITE(6,200) I,ZSLAB,YSLAB(I),XB(I),XB(I+1),XT(I),XT(I+1)         00001626
    8 WRITE(6,425) XBS(I),XBS(I+1),XTS(I),XTS(I+1)                      00001627
      WRITE(6,300)                                                      00001628
      DO 9 I=1,NBEAM                                                    00001630
      WRITE(6,400) I,ZBEAM(I),YBEAM(I),BMST(I),BMST(I+1)                00001640
    9 WRITE(6,250) BMSTS(I),BMSTS(I+1)                                  00001641
      WRITE(6,450) ZNA                                                  00001642
      WRITE(6,600)                                                      00001643
      DO 13 I=1,NPNTS                                                   00001644
   13 WRITE(6,700) SCURVE(I,1),SCURVE(I,2),BCURVE(I,1),BCURVE(I,2)      00001650
C                                                                       00001660
CC   BEGIN CALCULATIONS                                                 00001670
C                                                                       00001680
      DO 10 I=1,NSLAB                                                   00001700
      XTAVG=(XTS(I)+XTS(I+1))/2.                                        00001710
      XBAVG=(XBS(I)+XBS(I+1))/2.                                        00001770
      PROD=XTAVG*XBAVG                                                  00001795
      IF(PROD.LT.0.) GOTO 20                                            00001796
      CALL FSTCSE(XTAVG,XBAVG,ZSLAB,YSLAB,I,MOMS,AXFS)                  00001797
      GOTO 10                                                           00001799
   20 CALL SCDCSE(XTAVG,XBAVG,ZSLAB,YSLAB,I,MOMS,AXFS)                  00001800
   10 CONTINUE                                                          00001900
      DO 15 J=1,NBEAM                                                   00002500
   15 CALL BMCSE(BMSTS,J,STRAIN,BCURVE,STRESS,NPNTS,ZBEAM,YBEAM,ZNA,    00002600
     * MOMB,AXFB)                                                       00002700
      MOMTOT=MOMB+MOMS-(AXFB-AXFS)*(ZSLAB/2.+ZNA)/2.                    00002800
      MOMTOT=MOMTOT/1.0E6*(-1.)                                         00002400
      WRITE(6,500) MOMTOT                                               00003300
      GOTO 1                                                            00003310
```

```
  100 FORMAT(1X,68('*'),/,1X,'* ',16A4,' *',/,1X,68('*'),///,                00003400
     1 1X,'SLAB INPUT DATA',//,                                              00003410
     2 1X,'SECTION',5X,'HEIGHT',5X,'WIDTH',6X,'SB(I)',5X,'SB(I+1)',          00003500
     3 5X,'ST(I)',5X,'ST(I+1)',/)                                            00003510
  200 FORMAT(3X,I2,7X,F6.0,5X,F6.0,5X,F6.0,5X,F6.0,5X,F6.0,5X,F6.0)          00003600
  250 FORMAT(33X,'(',F6.1,')',4X,'(',F6.1,')',/)                             00003610
  300 FORMAT(//,1X,'BEAM INPUT DATA',//,1X,'SECTION',5X,'HEIGHT',5X,         00003700
     *'WIDTH',5X,'BMST(I)',4X,'BMST(I+1)',/)                                 00003800
  400 FORMAT(3X,I2,7X,F6.0,5X,F6.0,5X,F6.0,6X,F6.0)                          00003900
  425 FORMAT(33X,'(',F6.2,')',3X,'(',F6.2,')',3X,                            00003901
     1 '(',F6.2,')',3X,'(',F6.2,')',/)                                       00003902
  450 FORMAT(/,1X,'THE NEUTRAL AXIS IS ',F7.1,' FROM TOP OF BEAM')           00003910
  500 FORMAT(///,1X,46('*'),/,1X,'*  THE TOTAL APPLIED MOMENT IS ',          00004000
     1 F9.3,' KNM *',/,1X,46('*'))                                           00004001
  600 FORMAT(///,6X,'SLAB CURVE',20X,'BEAM CURVE',//,2X,'STRAIN',7X,         00004010
     1 'STRESS',11X,'STRAIN',7X,'STRESS')                                    00004011
  700 FORMAT(1X,F6.0,5X,F9.0,10X,F6.0,5X,F9.0)                               00004020
  800 FORMAT(1H1)                                                            00004030
 1000 FORMAT(1X,2F10.0)                                                      00004040
 9000 STOP                                                                   00004100
      END                                                                    00004200
C                                                                            00004201
C  SUBROUTINE TO CALCULATE AXFS ANB MOMS IF (PROD.GT.0.)                     00004210
C                                                                            00004220
      SUBROUTINE FSTCSE(XTAVG,XBAVG,ZSLAB,YSLAB,I,MOMS,AXFS)                 00004300
      DIMENSION YSLAB(10)                                                    00004400
      REAL MOMS                                                              00004410
      SIGN=1.                                                                00004501
      IF(XTAVG.LT.0.) SIGN=-1.                                               00004502
      XTRI=SIGN*ABS(XTAVG-XBAVG)                                             00005300
      IF(ABS(XBAVG).GT.ABS(XTAVG)) GOTO 10                                   00005500
      XRECT=XBAVG                                                            00005501
      ARM=ZSLAB/6.                                                           00005510
      GOTO 20                                                                00005600
   10 XRECT=XTAVG                                                            00005700
      ARM=-ZSLAB/6.                                                          00005800
   20 VTRI=XTRI*ZSLAB*YSLAB(I)/2.                                            00005900
      MOMS=MOMS+VTRI*ARM                                                     00006000
      AXFS=AXFS+VTRI+XRECT*ZSLAB*YSLAB(I)                                    00006010
      RETURN                                                                 00006100
      END                                                                    00006200
C                                                                            00006210
C  SUBROUTINE TO CALCULATE AXFS AND MOMS IF (PROD.LT.0.)                     00006220
C                                                                            00006230
      SUBROUTINE SCDCSE(XTAVG,XBAVG,ZSLAB,YSLAB,I,MOMS,AXFS)                 00006300
      DIMENSION YSLAB(10)                                                    00006310
      REAL MOMS                                                              00006320
      ZN=ZSLAB*XBAVG/ABS(XTAVG-XBAVG)                                        00006400
      VOL=XTAVG*(ZSLAB-ZN)/2.*YSLAB(I)                                       00006410
      MOMS=MOMS+VOL*(ZN/3.+ZSLAB/6.)                                         00006411
      AXFS=AXFS+VOL                                                          00006412
      VOL=XBAVG*ZN/2.*YSLAB(I)                                               00006420
      MOMS=MOMS+VOL*(ZN/3.-ZSLAB/2.)                                         00006500
      AXFS=AXFS+VOL                                                          00006600
      RETURN                                                                 00006700
      END                                                                    00006800
C                                                                            00007701
C  SUBROUTINE TO CALCULATE AXFB AND MOMB FOR THE BEAM                        00007710
C                                                                            00007720
      SUBROUTINE BMCSE(BMSTS,J,STRAIN,BCURVE,STRESS,NPNTS,ZBEAM,YBEAM,       00007800
     * ZNA,MOMB,AXFB)                                                        00007801
      DIMENSION BMSTS(10),ZBEAM(10),YBEAM(10),BCURVE(10,2)                   00007810
      REAL MOMB                                                              00007820
      SAVG=(BMSTS(J)+BMSTS(J+1))/2.                                          00007900
      ARM=0.                                                                 00008300
      IF(J.EQ.1) GOTO 10                                                     00008400
      J2=J-1                                                                 00008410
      DO 20 K=1,J2                                                           00008500
   20 ARM=ARM+ZBEAM(K)                                                       00008600
   10 ARM=ARM+ZBEAM(J)/2.                                                    00008700
      VOL=SAVG*ZBEAM(J)*YBEAM(J)                                             00008800
      ARM=ZNA-ARM                                                            00008810
      MOMB=MOMB+VOL*ARM                                                      00008820
      AXFB=AXFB+VOL                                                          00008830
      RETURN                                                                 00008900
      END                                                                    00009000
C                                                                            00009010
C  SUBROUTINE TO CONVERT STRAIN TO STRESS                                    00009020
C                                                                            00009030
      SUBROUTINE CNVRT(STRAIN,CURVE,STRESS,NPNTS)                            00009100
      DIMENSION CURVE(10,2)                                                  00009200
      DO 10 I=1,NPNTS                                                        00009300
      IF(STRAIN.EQ.CURVE(I,1)) GOTO 20                                       00009400
      IF(STRAIN.GT.CURVE(I,1)) GOTO 10                                       00009500
      GOTO 30                                                                00009501
   10 CONTINUE                                                               00009502
   20 STRESS=CURVE(I,2)                                                      00009503
      GOTO 40                                                                00009504
   30 I2=I-1                                                                 00009510
      STRESS=((CURVE(I,2)-CURVE(I2,2))*(STRAIN-CURVE(I2,1))/                 00009600
     1 (CURVE(I,1)-CURVE(I2,1)))+CURVE(I2,2)                                 00009700
   40 RETURN                                                                 00009800
      END                                                                    00009900
```

```
**********************************************************************
*        EXAMPLE 6 : BENDING MOMENT AT A SECTION                     *
**********************************************************************
```

SLAB INPUT DATA

SECTION	HEIGHT	WIDTH	SB(I)	SB(I+1)	ST(I)	ST(I+1)
1	100.	175.	515. (6.18)	311. (3.73)	-712. (-8.54)	-710. (-8.52)
2	100.	175.	311. (3.73)	15. (0.18)	-710. (-8.52)	-556. (-6.67)
3	100.	175.	15. (0.18)	283. (3.40)	-556. (-6.67)	-665. (-7.98)
4	100.	175.	283. (3.40)	435. (5.22)	-665. (-7.98)	-869. (-10.43)

BEAM INPUT DATA

SECTION	HEIGHT	WIDTH	BMST(I)	BMST(I+1)
1	10.	100.	-935. (-187.0)	-808. (-161.6)
2	60.	6.	-808. (-161.6)	-175. (-35.0)
3	60.	6.	-175. (-35.0)	414. (82.8)
4	60.	6.	414. (82.8)	1031. (206.2)
5	10.	165.	1031. (206.2)	1154. (230.8)

THE NEUTRAL AXIS IS 116.500 FROM TOP OF BEAM

SLAB CURVE		BEAM CURVE	
STRAIN	STRESS	STRAIN	STRESS
0.	0.	0.	0.
1000.	12.	1500.	300.
2000.	24.	3000.	300.

```
*********************************************
*  THE TOTAL APPLIED MOMENT IS    88.155 KNM *
*********************************************
```